



A11103 935979

NIST
PUBLICATIONS



United States Department of Commerce
Technology Administration
National Institute of Standards and Technology

NISTIR 5027

SUPERCONDUCTOR CRITICAL CURRENT STANDARDS FOR FUSION APPLICATIONS

L.F. Goodrich
J.A. Wiejaczka
A.N. Srivastava
T.C. Stauffer

QC
100
.U56
NO. 5027
1994

NISTIR 5027

SUPERCONDUCTOR CRITICAL CURRENT STANDARDS FOR FUSION APPLICATIONS

L.F. Goodrich
J.A. Wiejaczka
A.N. Srivastava
T.C. Stauffer

Electromagnetic Technology Division
Electronics and Electrical Engineering Laboratory
National Institute of Standards and Technology
Boulder, Colorado 80303

Prepared for
Office of Fusion Energy
Department of Energy
Washington, DC 20545
and
Plasma Fusion Center
Massachusetts Institute of Technology
NW16-164
Cambridge, MA 02139

November 1994



U.S. DEPARTMENT OF COMMERCE, Ronald H. Brown, Secretary
TECHNOLOGY ADMINISTRATION, Mary L. Good, Under Secretary for Technology
NATIONAL INSTITUTE OF STANDARDS AND TECHNOLOGY, Arati Prabhakar, Director

FOREWORD

This is the final progress report for the nine month period from October 1993 to July 1994. We were asked to help design, participate in, perform research studies on, and report on the first International Thermonuclear Experimental Reactor (ITER) interlaboratory comparison of Nb₃Sn critical current measurements. This report contains: a comparison of results from the U.S. laboratories, a comparison of results from a number of international laboratories, a homogeneity study of one Nb₃Sn wire, observations on the standard specimen mandrel design, a commentary on the future possibility of creating a Nb₃Sn Reference Wire, and a compilation of Data Format Sheets from U.S. Laboratories.

The authors extend their thanks to M. Takayasu (Massachusetts Institute of Technology, MIT) for his contribution in the design of the common mandrel, J. Minervini (MIT) for his organization of the interlaboratory comparison, U.S. ITER Home Team for their cooperation, W.P. Dubé for assisting with experiment design, and L.T. Medina for assisting with this work. This work was supported by the U.S. Department of Energy Office of Fusion Energy and the MIT Plasma Fusion Center.

Contents

	Page
FOREWORD	ii
1. COMPARISON OF CRITICAL CURRENT MEASUREMENTS FROM U.S. LABORATORIES	2
1.1 Introduction	2
1.2 Standardized Mandrels and Attachment Procedure	3
1.3 Experimental Results	4
1.4 Recommendations	6
1.5 Reference	7
2. COMPARISON OF CRITICAL CURRENT MEASUREMENTS FROM INTERNATIONAL LABORATORIES	21
2.1 Introduction	21
2.2 Experimental Results	21
2.3 Discussion	22
3. CRITICAL CURRENT HOMOGENEITY OF A Nb ₃ Sn WIRE	30
3.1 Experimental Details of the Homogeneity Study	30
3.2 Experimental Results	31
3.3 Discussion of Experimental Results	33
3.4 References	34
4. OBSERVATIONS AND RECOMMENDATIONS ON THE CRITICAL CURRENT MEASUREMENT PROCEDURE	51
4.1 Critical Current Measurement Apparatus	51
4.2 Current Contacts	52
4.3 Electrolytic Method for Removing Cr Plating from Reacted Nb ₃ Sn Wires . .	53
4.4 Superconductivity of the Ti-6Al-4V Measurement Mandrel	53
4.5 Critical Current Measurements on the Nb-Ti Wire SRM-1457	55
4.6 Observations on the Standard Specimen Mandrel	55
4.7 References	57

5.	COMMENTARY ON A Nb ₃ Sn REFERENCE WIRE	65
5.1	Introduction	65
5.2	Advantages	65
5.3	Disadvantages	66
5.4	Recommendation	67
	Appendix A. STANDARDIZED LABORATORY REPORTING SHEETS	68
	Appendix B. A SIMPLE AND REPEATABLE TECHNIQUE FOR MEASURING THE CRITICAL CURRENT OF Nb ₃ Sn WIRES.	92

SUPERCONDUCTOR CRITICAL CURRENT STANDARDS FOR FUSION APPLICATIONS

October 1993-July 1994

L.F. Goodrich, J.A. Wiejaczka, A.N. Srivastava, and T.C. Stauffer
Electromagnetic Technology Division
Electronics and Electrical Engineering Laboratory
National Institute of Standards and Technology
Boulder, CO 80303

This report describes research conducted to help establish a standard critical current measurement technique for the Nb₃Sn superconducting wires that may be used in fusion applications. The main part of this report is a detailed presentation of results from the first ITER international interlaboratory comparison of Nb₃Sn critical current measurements. A common procedure and a common reaction and measurement mandrel were used by U.S. laboratories in this comparison, whereas no common procedure was followed by the international laboratories. The largest difference in I_c measurements of two laboratories that did not use a common procedure was 23%. The largest difference in I_c measurements of two laboratories that did use a common procedure was 6.5%. There may still be room for improvement, but this indicates the strong need for a common detailed procedure. Results on the homogeneity of one of the Nb₃Sn wires used in this study and a commentary on creating a Nb₃Sn Reference Wire are also presented.

Key words: critical current; homogeneity; interlaboratory comparison; Nb₃Sn; Nb-Ti; n-value; standard mandrel; standards

1. COMPARISON OF CRITICAL CURRENT MEASUREMENTS FROM U.S. LABORATORIES

An interlaboratory comparison of critical current measurements was made on Nb₃Sn strand wires for the ITER application. The results for the United States (U.S.), Japan (JA), Russian Federation (RF), and European Community (EC) samples are shown as measured by six U.S. laboratories. The laboratories are listed in the text as Lab A through F to avoid directly identifying data with the laboratory that obtained them. Likewise the samples will be listed as W, X, Y, and Z. This is a brief presentation of these results.

1.1 Introduction

The data presented here are critical current I_c and n-value measurements made during an interlaboratory comparison in which a common mandrel with standardized design was used for reaction and measurement. Titanium alloy (Ti-6Al-4V; composition is in mass percent) mandrels were chosen because they can be used for both reaction and measurement, thus eliminating the need to transfer the delicate sample from the reaction to the measurement mandrel. This reduced a major source of variability. The Ti alloy mandrels have other advantages: they are inexpensive and nonmagnetic, and have low thermal expansion, high electrical resistivity, and low resistivity ratio.

The thermal contraction of this Ti alloy is 0.17% from 295 to 4 K. Differential thermal contraction causes the Nb₃Sn wire to tighten onto the mandrel as it cools to the measurement temperature. This tightened state reduces sample motion and the need for a binding agent to hold the sample, as long as the Lorentz force is directed into the mandrel. Differential contraction also puts the wire into hoop strain, and creates a transverse stress gradient and slight bending strain. We think that the hoop strain is the most significant strain effect. Tensile hoop strain will slightly increase the I_c from the intrinsic value.

Incoloy was not selected for the mandrel material, even though it would have less differential contraction with the Nb₃Sn wire, because of the complicating issues of the magnetism of Incoloy, its limited availability, and higher cost.

The low temperature electrical resistivity of this Ti alloy is 147 $\mu\Omega\text{cm}$, which is quite high compared to Incoloy or stainless steel (approximately 53 $\mu\Omega\text{cm}$). This high resistivity reduces the effect of current sharing in the measurement mandrel that would affect the determination of I_c and n-value.

We conducted preliminary measurements to test the conductivity of the Ti mandrel and discovered that this mandrel is superconducting at 4.2 K and magnetic fields below 2 T. Thus, reliable I_c measurements can be obtained only at fields higher than 2 T at 4.2 K with this mandrel material.

The superconducting properties of this alloy depend on the annealing and machining of the mandrel.

All Nb₃Sn I_c measurements reported here were made at magnetic fields of 6 T and above, where the Ti alloy mandrel is a normal metal and will not have a significant current-sharing effect. The normal state resistance of the machined (not annealed) mandrel is about 460 μΩ between the current contacts.

Winding and reacting processes were conducted at MIT. The specimens were subsequently distributed to six U.S. laboratories. The laboratories that participated were: Teledyne Wah Chang Albany, MIT Francis Bitter National Magnet Laboratory, MIT Plasma Fusion Center, University of Wisconsin Applied Superconductivity Center, Brookhaven National Laboratory, and the National Institute of Standards and Technology. The laboratories are listed in the text as Laboratory A through F to avoid directly identifying data with the laboratory that obtained it. Likewise the samples will be listed as W, X, Y, and Z.

1.2 Standardized Mandrels and Attachment Procedure

The procedure for mounting the sample to the mandrel and mounting the mandrel to the test fixture is given below.

The reaction mandrel consists of three Ti alloy parts: a main tube (barrel), and two removable end rings. The main tube has a threaded groove (8 threads/in, 3.15 threads/cm) with a groove angle of 90°. The end rings are held onto the main tube with a stainless steel wire (spring clip) through mating holes in the main tube and end cap. The end rings are not threaded; their outer diameter was machined to hold the sample at the same coil diameter as when seated in the grooves of the main tube. A small diameter retaining wire is used to tie the specimen to each end ring and thus hold the wire coil on the reaction mandrel.

After reaction, the end rings are removed and Cu current contact rings are put on and held in place with stainless steel wire. It is important that the Cu ring fit correctly on the main Ti tube so that the sample is not strained in the transition region between the Cu ring and the Ti tube. If there is a Cr coating on the Nb₃Sn wire, it is removed from the region of the current contacts and voltage taps. One end of the sample is clamped and the sample is seated into a groove starting from the clamp end and proceeding along the wire to the far end which is then clamped. The sample is then soldered to the Cu current contact rings, and voltage tap wires are soldered to the sample. At this stage, the sample is a fully instrumented and self-contained unit, which we will call an instrumented sample.

Other laboratories prepared its own specimens and followed a procedure similar to that described here. There are still some differences, such as the geometry of the Cu current contact rings. These details and procedures may be further standardized in the future. No bonding material was

used to hold the specimen on the measurement mandrel. The I_c measurements were made with the Lorentz force directed into the mandrel.

We also standardized the way the instrumented sample is attached to the test fixture. In all cases, the current contact to the instrumented sample was made by pressure contacts to each end (each Cu ring). The pressure contact mechanism must be designed so that it does not torque the instrumented sample when the pressure is applied. This makes the instrumented samples self-contained and interchangeable; this will allow interlaboratory comparisons to be made in a classical round-robin where each sample is measured by each laboratory. This approach would reduce variability due to sample inhomogeneity and handling, thus allowing more precise interlaboratory comparisons. The classical round robin approach in combination with each laboratory instrumenting samples could be used to identify and separate mounting effects from sample inhomogeneity and measurement conditions.

1.3 Experimental Results

The test results given in this section are in the form of tables and figures. Raw data from each laboratory for each sample are given in the tables as well as statistical summaries of the results of the intercomparison. Extra digits are provided for precise interpolation. The figures illustrate trends for each sample and each laboratory.

The Nb₃Sn samples measured here were not intended to meet a given specification; in fact, they had different wire diameters.

Table 1-1 is a summary of critical current measurements on Nb₃Sn strand Sample W at 10 μ V/m (0.1 μ V/cm) and 12 T. The table indicates the raw critical current (as measured), the temperature at which the measurement was made, and the critical current at a temperature of 4.2 K. The data for each laboratory were corrected to a temperature of 4.20 K using the temperature dependence measured at Laboratory C. The temperature correction equation used was:

$$I_c(B, T) = I_{cr}(B, T_r) [(T_c^*(B) - T) / (T_c^*(B) - T_r)], \text{ where}$$

$$T_c^* \text{ is defined by } I_c(B, T) = I_{c0}(B) [1 - T/T_c^*(B)].$$

T_c^* is the effective transition temperature, and I_{cr} is the measured critical current at a reference temperature T_r . The n-values are also shown for each laboratory and each specimen. Average critical currents at 4.2 K are also shown. A few extreme outliers (see footnotes) were omitted from the calculated averages and standard deviations.

Tables 1-2 to 1-4 have the same format as Table 1-1, except that they are for Samples X, Y, and Z, respectively. Figure 1-1 illustrates the critical current measurements from each laboratory for each sample; the average critical current for each sample is shown by a horizontal line.

Table 1-5 shows statistics on the critical current and n-value determined for each of the four samples using data from all six laboratories. The coefficient of variation is the standard deviation divided by the average expressed in percent. The statistics for Sample W used 11 measurements of I_c and 10 measurements of n. The statistics for the other samples used 12 measurements of I_c and n. These statistics are illustrated in Figures 1-4 to 1-7. Figure 1-4 shows the percent difference of the measured critical current for each laboratory from the overall average for each sample, as a function of sample. Figure 1-5 is the same as Figure 1-4 with a more sensitive scale; Sample W had two extreme outliers that are off scale. Figure 1-6 illustrates the percent difference of the determined value of n for each laboratory from the average n-value for each sample, as a function of sample. Figure 1-7 is the same as Figure 1-6 but on a more sensitive scale. The sample which had extreme outliers for the I_c measurements also had three outlying n-values which are off scale in Figure 1-7.

Table 1-6 shows measurement statistics for each laboratory that participated in the intercomparison. These measurement statistics are relative to the average value for each of the four samples. For this table, the percentage differences between the results of a laboratory's measurements on a given sample and the overall average for that sample are calculated. The range of these percent differences in I_c for all samples is shown in the row of the table labeled I_c Range (%). The average of these percent differences for a given laboratory and all samples is shown in the row of the table labeled I_c Average Bias (%). Thus, the average bias of I_c indicates the average position of a laboratory's results relative to the overall averages, and the I_c range indicates the variability of a laboratory's results for two specimens of each of four samples. These measurement statistics are best illustrated in Figures 1-2 and 1-3. Figure 1-2 shows the variation in I_c measurements made by a given laboratory for each sample. There were outlying measurements made by Laboratories A and B. We suspect that Laboratory A's outlier is due to a damaged sample, while Laboratory B's outlier is due to a short circuit in the cryostat. Laboratory A remeasured this suspect specimen using two pairs of voltage taps and found that nearly all of the voltage drop was coming from part of the specimen, which is consistent with sample damage. Laboratory B's suspect specimen was remeasured, and the measured value of I_c fell by about 30%. The other laboratories values were clustered around 0. Figure 1-3 is the same as Figure 1-2 but on a more sensitive scale excluding these outliers. The statistics on the n-value measurements were done in the same way and are illustrated in Figures 1-8 and 1-9, with Figure 1-9 having a more sensitive scale. This analysis was used to attempt to quantify the results from each laboratory, and it is not an independent evaluation because the overall averages were used.

Table 1-7 shows the I_c coefficients of variation for various laboratory subsets. These subsets were selected to illustrate the influence of some measured values on the overall statistics. There might be an indication of a significant effect for Sample X, whose coefficient of variation increases by a factor of 2 in going from four to six laboratories. Most of the changes for the other samples were not unusual. However, there is an indication that some of the laboratories had problems measuring some samples.

Table 1-8 shows Laboratory C's critical current and n-value measurements versus magnetic field at 4.2 K and the approximate temperature-dependent coefficients T_c^* for two specimens of each of the four wires. These data are provided to allow comparisons at other fields, temperatures, and electric field criteria.

1.4 Recommendations

Based on these results, we recommend the following methods for enhancing the quality of the critical current measurements:

1. For critical current measurements, we recommend that *critical currents*, as opposed to *critical current densities*, be reported by all laboratories participating in the interlaboratory comparison. The critical current density reports have a higher uncertainty since they are composed of uncertainties due to the critical current measurement and uncertainties due to the measurement of the conductor's cross-sectional area.
2. Standardize the test procedure, the test fixtures, and the analysis methods. Also, select a method that does not require the sample to be transferred from reaction to measurement mandrel. A standard procedure for making the critical-current measurements was proposed by L.F. Goodrich during the Versailles Project on Advanced Materials and Standards (VAMAS) interlaboratory comparisons of critical currents [1]. That experiment showed that the variability in the measurement could be significantly reduced by adopting a standardized system. Due to the scale of the ITER project, the test procedure must be scalable so that a large number of samples can be accommodated. This has to be balanced with high data reliability which can be achieved with the no-transfer method and Ti alloy mandrel described here. We think that the approach presented here is viable for ITER.
3. Control the tension of the conductor before reaction and before measurement. A standard tension will aid in reducing the variability of the measurement between laboratories. This is expected to be the case for all types of reaction and measurement mandrel materials unless a rigid bonding material is used. Rigid bonding materials for measurement mandrels, such as solder or epoxy, have other negative side effects. A paper on the effects of conductor tension on the measurement mandrel is included as Appendix B.
4. Use standardized reporting sheets (see Section 6). The experimenter can use these sheets to document the conditions under which the I_c measurements were made.
5. Avoid soldering more than about 0.8 turn of the specimen onto the current contact. A multiple-turn contact can carry a current induced by a changing background magnetic field. This current will oppose the change in the background magnetic field. This current will decay slowly with time, creating a time-varying magnetic field on the sample; this leads to time dependent I_c measurements.

6. Avoid making I_c measurements with the Lorentz force directed outward, since this can strain the specimen and alter subsequent measurements. If measurements with the Lorentz force directed outward are useful for diagnostic purposes, they should be done after all measurements with the Lorentz force directed inward are completed.

7. Instrument the sample with a pair of voltage taps spanning the entire length of the sample and the current contacts. The pressure current contact in this design should also be included between these voltage taps. A single measurement of the voltage-current characteristic of this tap pair will contain information on the contact resistance and performance of the entire sample length. This information will indicate the total amount of sample heating and possible limiting sections of the sample that are outside the main voltage tap pair. Likewise, multiple voltage tap pairs along the sample can be useful to indicate the local homogeneity of the specimen.

1.6 Reference

[1] Wada, H.; Itoh, K. *Cryogenics* 32 ICMC Supplement. p.557; 1992.

Table 1-1. Summary of critical current measurements on Nb₃Sn strand.
Sample W: 10 μV/m, 12 T

Lab	Specimen number		Raw critical current (A)		Temperature (K)		Critical current (A)		n-value	
							@ 4.20 K ^a			
A	W 2-5	W 4-6	72.8	120.4	4.23-4.24		73.29	121.22	9.1	28.6
B	W 2-3	W 4-4	119	154 (125) ^b	4.229	4.229 (4.205)	119.67	154.87 (125.12)	32	17 (59)
C	W 2-2	W 4-1	115.67	117.15	4.200	4.200	115.67	117.15	30.1	30.4
D	W 2-6	W 4-2	116.5	118	4.200	4.200	116.5	118	21	28
E	W 2-1	W 4-3	110	116	4.187	4.187	109.45	115.71	32	30
F	W 2-4	W 4-5	120.4	120.9	4.213	4.224	120.70	121.46	30.0	29.3
Aver.							118.24 ^{b,c}		29.14 ^{b,c}	

^a T_c * used for correction was 9.39 K.

^b Sample was remeasured and the second value (125.12 A) was used to compute the average value.

^c Averages do not include Lab A's measurement of W 2-5, or Lab B's n-values for W 4-4.

Table 1-2. Summary of critical current measurements on Nb₃Sn strand.
Sample X: 10 μV/m, 12 T

Lab	Specimen number		Raw critical current (A)		Temperature (K)		Critical current(A)		n-value	
							@ 4.20 K ^a			
A	X 2-5	X 4-3	212.3	202.7	4.23-4.24		213.47	203.82	27.0	25.9
B	X 2-2	X 4-6	208	207	4.205	4.205	208.16	207.16	28	26
F	X 2-3	X 4-5	210.40	215.08	4.200	4.200	210.40	215.08	28.3	28.9
D	X 2-4	X 4-4	222	223	4.200	4.200	222	223	36	29
F	X 2-6	X 4-2	213	213	4.187	4.187	212.57	212.57	32	31
F	X 2-1	X 4-4	205.0	229.1	4.216	4.220	205.52	229.82	26.6	27.3
Aver.							213.63		28.83	

^a T_c * used for correction was 10.57 K.

Table 1-3. Summary of critical current measurements on Nb₃Sn strand.
Sample Y: 10 μ V/m, 12 T

Lab	Specimen number		Raw critical current (A)		Temperature (K)		Critical current (A)		n-value	
							@ 4.20 K ^a			
A	Y 2-6	Y 4-2	141.7	145.8	4.23-4.24		142.70	146.83	29.2	30.2
B	Y 2-3	Y 4-1	135	142	4.229	4.229	135.79	142.83	27	24
C	Y 2-2	Y 4-6	138.08	136.03	4.200	4.200	138.08	136.03	28.9	29.1
D	Y 2-1	Y 4-3	156.5	141.5	4.200	4.200	156.5	141.5	-----	24.4
E	Y 2-4	Y 4-5	136	139	4.187	4.187	135.72	138.72	30	27
E	Y 2-5	Y 4-4	137.0	136.7	4.224	4.226	137.66	137.42	29.5	27.6
Aver.							140.82		27.90	

^a T_c * used for correction was 9.18 K.

Table 1-4. Summary of critical current measurements on Nb₃Sn strand.
Sample Z: 10 μ V/m, 12 T

Lab	Specimen number		Raw critical current (A)		Temperature (K)		Critical current (A)		n-value	
							@ 4.20 K ^a			
A	Z 2-4	Z 4-5	83.3	83.9	4.23-4.24		83.70	84.31	14.0	14.1
B	Z 2-5	Z 4-3	83	84	4.205	4.205	83.06	84.06	14	15
C	Z 2-6	Z 4-1	83.69	84.35	4.200	4.200	83.69	84.35	14.2	14.2
D	Z 2-3	Z 4-2	88.25	87.75	4.200	4.200	88.25	87.75	15.7	15
E	Z 2-1	Z 4-6	82	79	4.187	4.187	81.85	78.86	17	16
F	Z 2-2	Z 4-3	83.6	84.8	4.222	4.220	83.85	85.03	17.0	17.1
Aver.							84.06		15.28	

^a T_c * used for correction was 11.48 K.

Table 1-5. Summary statistics for each sample measured by six laboratories at 4.2 K and 12 T.

	Sample W	Sample X	Sample Y	Sample Z
I_c average (A)	118.24	213.63	140.82	84.06
I_c standard deviation (A)	4.11	7.80	6.01	2.44
I_c coefficient of variation (%)	3.48	3.65	4.27	2.90
n-value average	29.14	28.83	27.90	15.28
n-value standard deviation	3.13	2.93	2.13	1.25
n-value coefficient of variation (%)	10.74	10.16	7.63	8.18

Table 1-6. Statistical summary of laboratory measurements of critical currents and n-values relative to the average value for each of the four samples at 4.2 K and 12 T.

	Lab A	Lab B	Lab C	Lab D	Lab E	Lab F
I_c average bias (%)	0.47	-0.24	-1.17	3.45	-3.06	0.60
I_c range (%)	8.86	9.39	4.08	12.61	6.93	11.38
n-value average bias (%)	-3.07	-4.32	-0.02	-2.57	6.45	2.29
n-value range (%)	18.41	23.79	11.36	52.79	14.52	19.70

Table 1-7. I_c coefficients of variation at 4.2 K and 12 T for various laboratory subsets.

I_c coefficient of variation (%)	Sample W	Sample X	Sample Y	Sample Z
Labs A,B,C,E	4.23	1.79	2.94	2.24
Labs A,B,C,E,F	3.84	3.45	2.67	2.13
Labs A,B,C,D,E	3.67	2.86	4.55	3.19
Labs A,B,C,D,E,F	3.48	3.65	4.27	2.90

Table 1-8. Laboratory C's critical current and n-value measurements versus field and the temperature dependence of the critical current.

$\mu_0 H, T$	Sample Y				Sample X			
	I_c, A (2-2)	I_c, A (4-1)	T_c^*, K (avg)	$n@4.2 K$ (avg)	I_c, A (2-3)	I_c, A (4-5)	T_c^*, K (avg)	$n@4.2 K$ (avg)
8	374.33	377.34	13.242	41.39				
7	308.93	311.32	12.617	39.79				
8	255.78	257.89	11.874	38.04	431.51	438.59	13.244	32.68
8	211.78	213.69	11.295	36.26	363.18	369.64	12.589	31.66
10	174.64	176.39	10.600	34.37	304.76	310.50	11.900	30.90
11	142.95	144.58	10.020	32.43	254.30	259.51	11.217	29.87
12	115.67	117.15	9.385	30.21	210.40	215.08	10.574	28.57

$\mu_0 H, T$	Sample Y				Sample Z			
	I_c, A (2-2)	I_c, A (4-6)	T_c^*, K (avg)	$n@4.2 K$ (avg)	I_c, A (2-6)	I_c, A (4-1)	T_c^*, K (avg)	$n@4.2 K$ (avg)
6	515.40	511.20	13.940	50.55	217.37	219.98	16.334	12.05
7	421.33	417.64	13.080	46.42	185.05	187.10	15.595	12.44
8	343.90	340.67	12.252	42.27	158.19	159.86	14.682	12.83
9	279.18	276.30	11.482	38.77	135.50	136.82	13.972	13.20
10	224.45	221.87	10.669	35.53	115.92	116.97	13.202	13.55
11	177.84	175.51	9.881	32.22	98.80	99.71	12.436	13.91
12	138.08	136.03	9.132	28.98	83.69	84.35	11.479	14.19

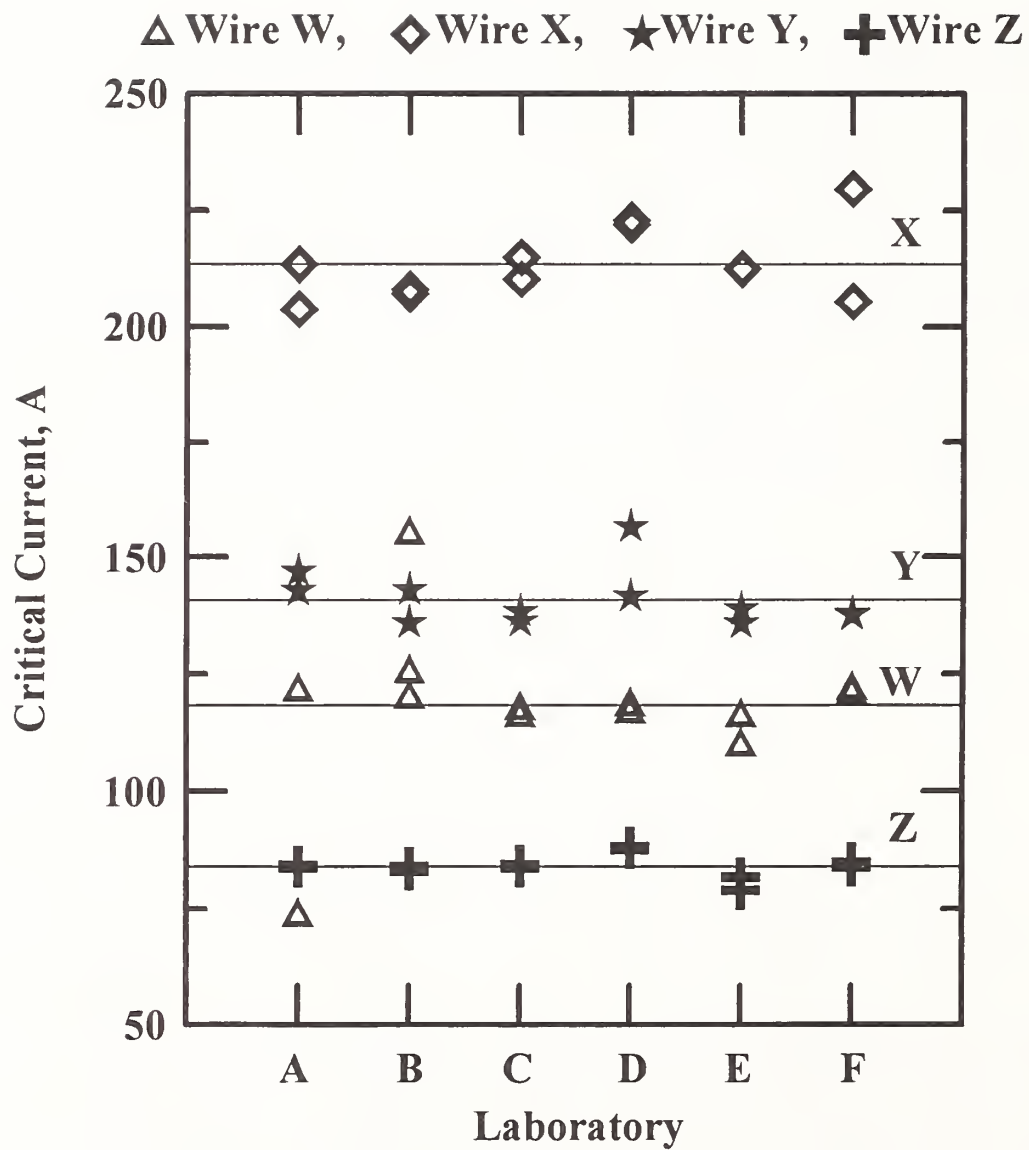


Figure 1-1. Critical current versus laboratory for each of the four samples. The horizontal lines show the average I_c for each sample.

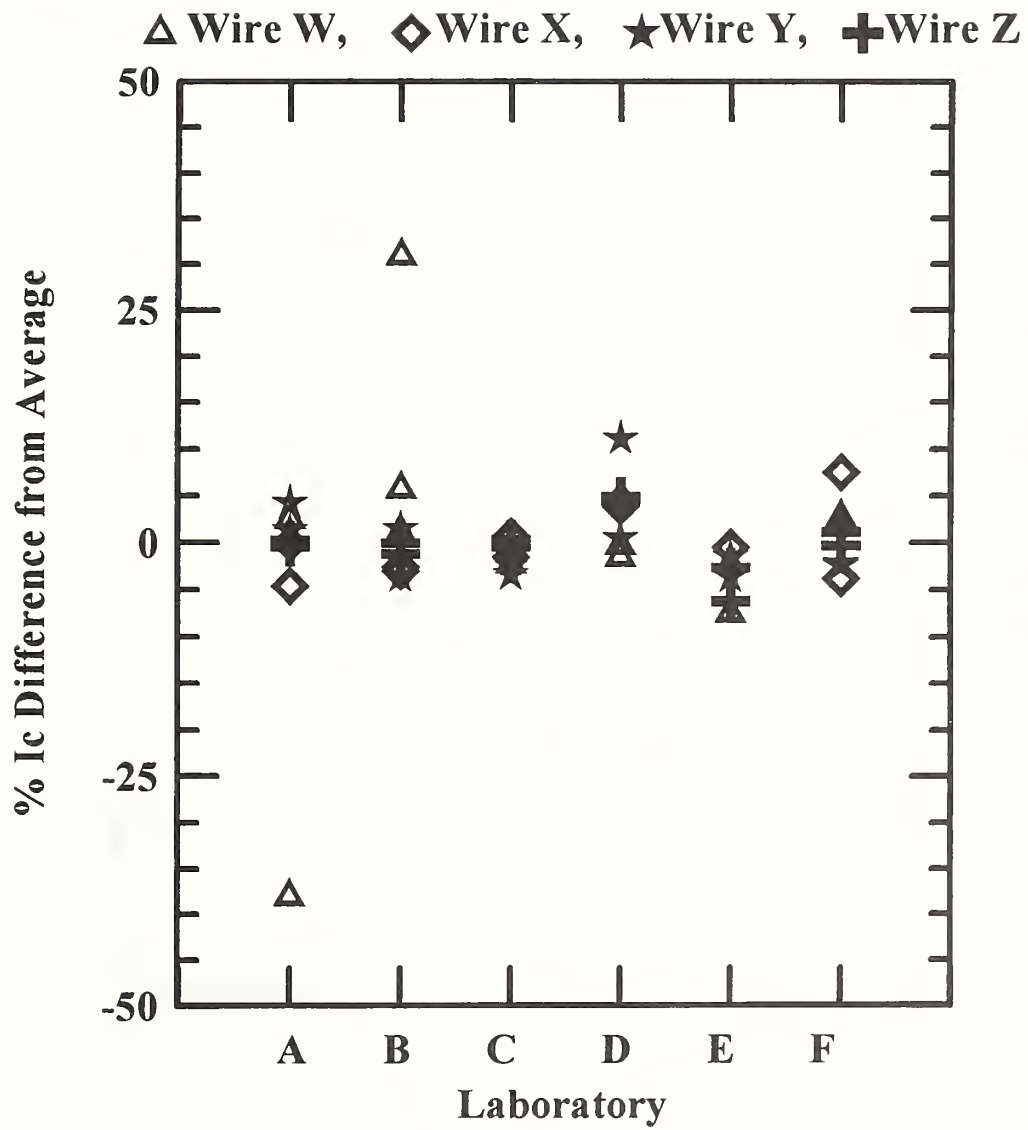


Figure 1-2. Percent difference of critical current versus laboratory for each sample measured.

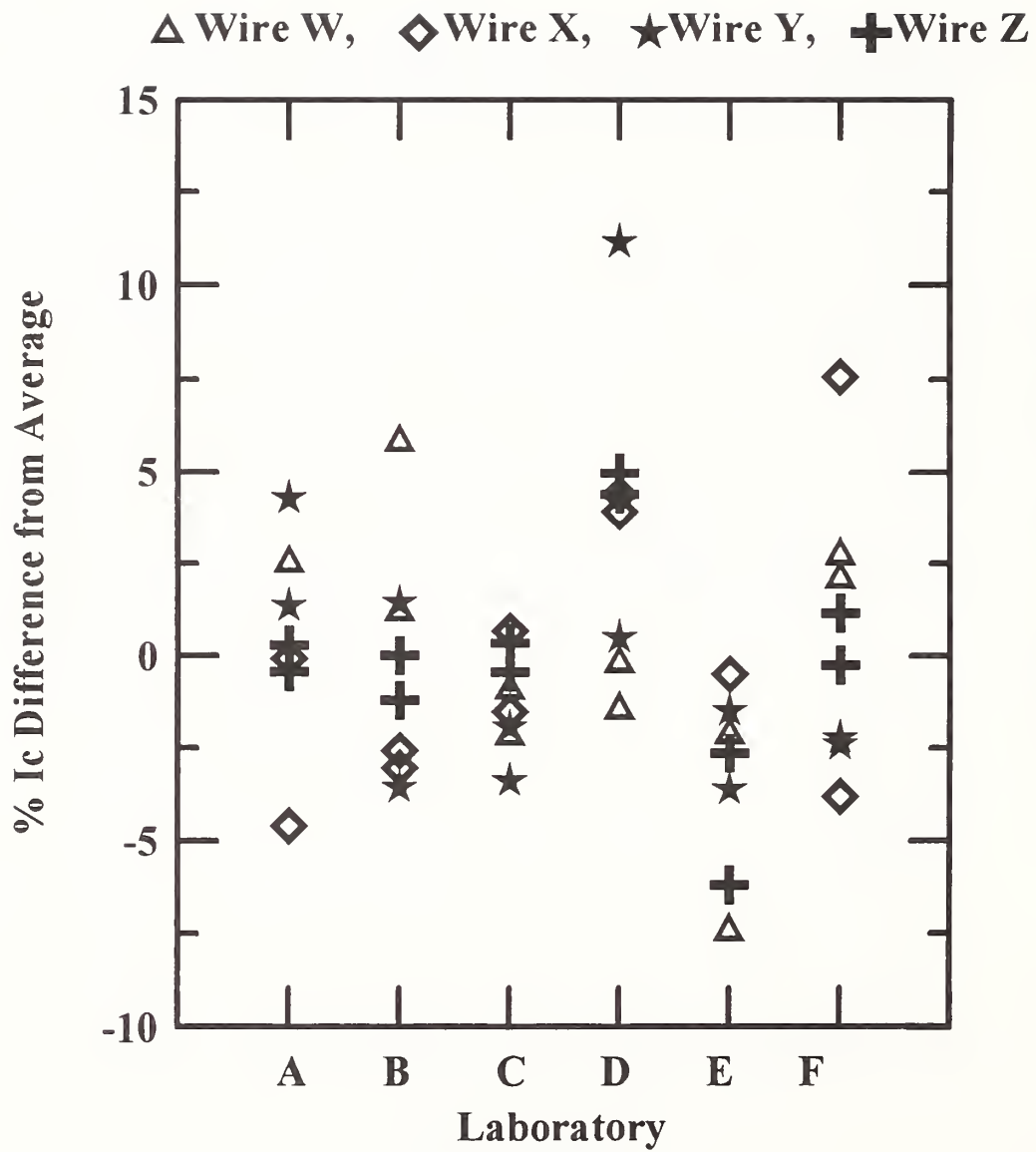


Figure 1-3. Percent difference of critical current versus laboratory for each sample measured. This plot is the same as Figure 1-2 except on a more sensitive scale excluding two outliers.

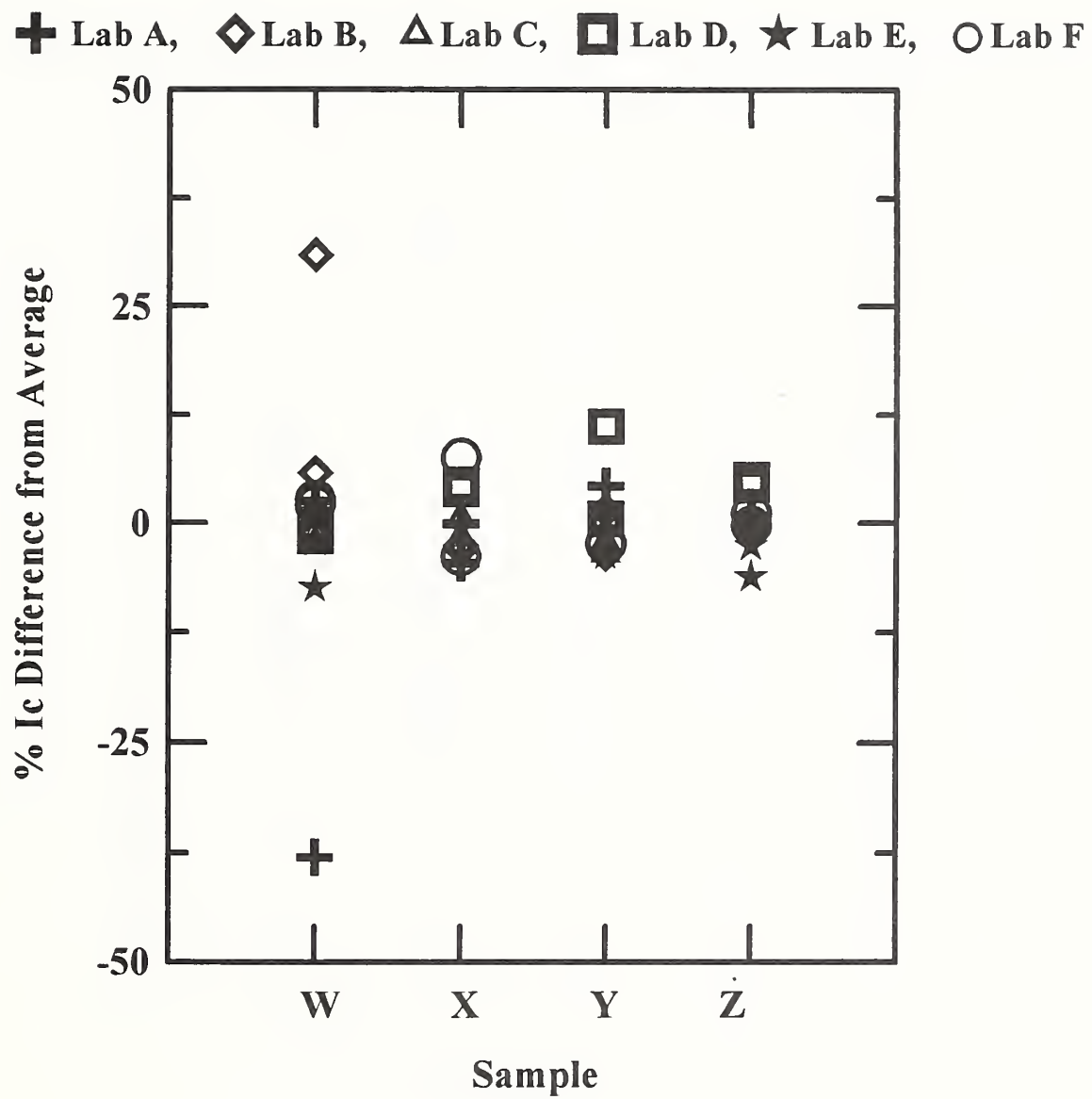


Figure 1-4. Percent difference of critical current versus sample for each laboratory.

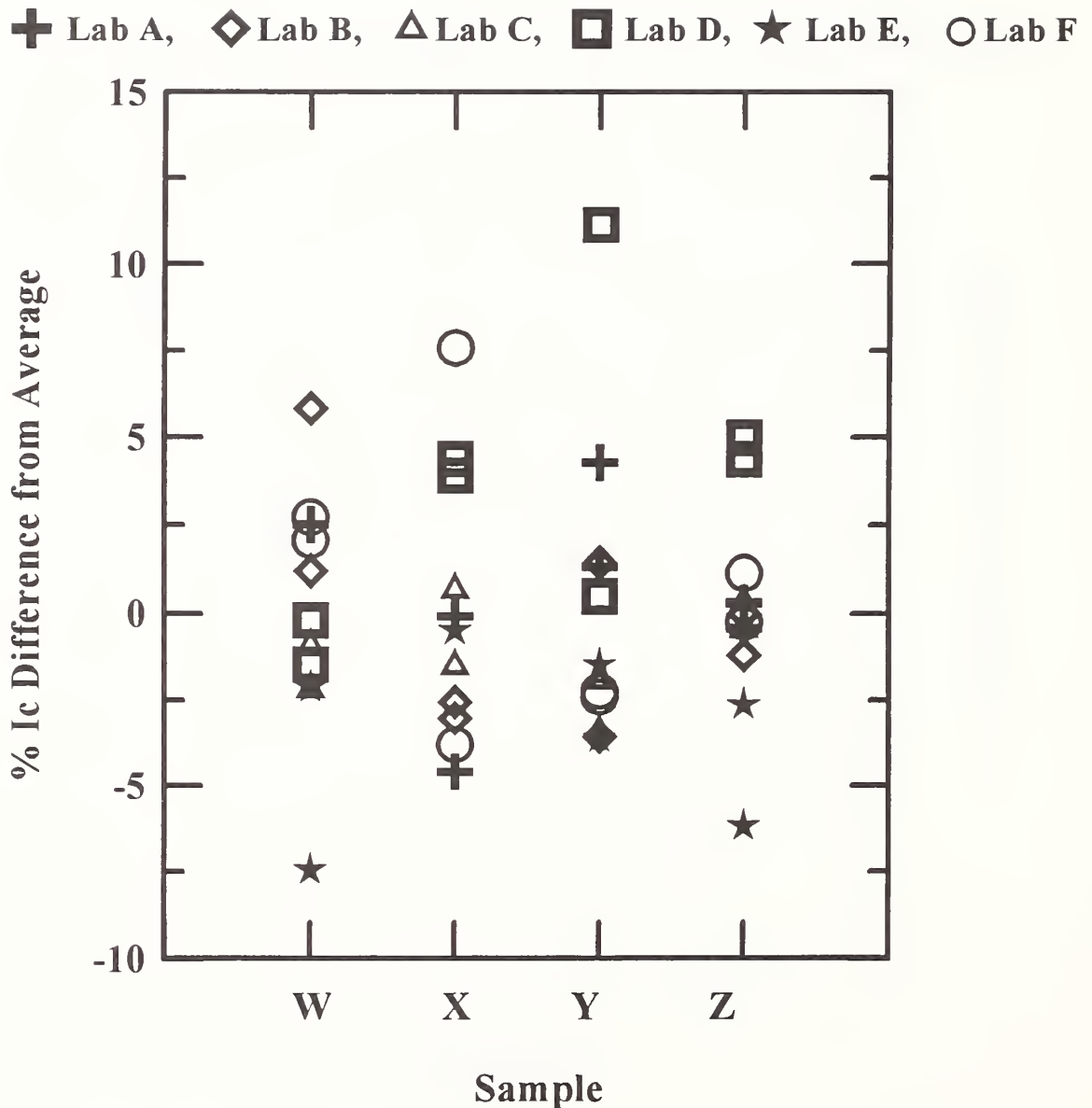


Figure 1-5. Percent difference of critical current versus sample for each laboratory. This plot is the same as Figure 1-4 except on a more sensitive scale excluding two outliers.

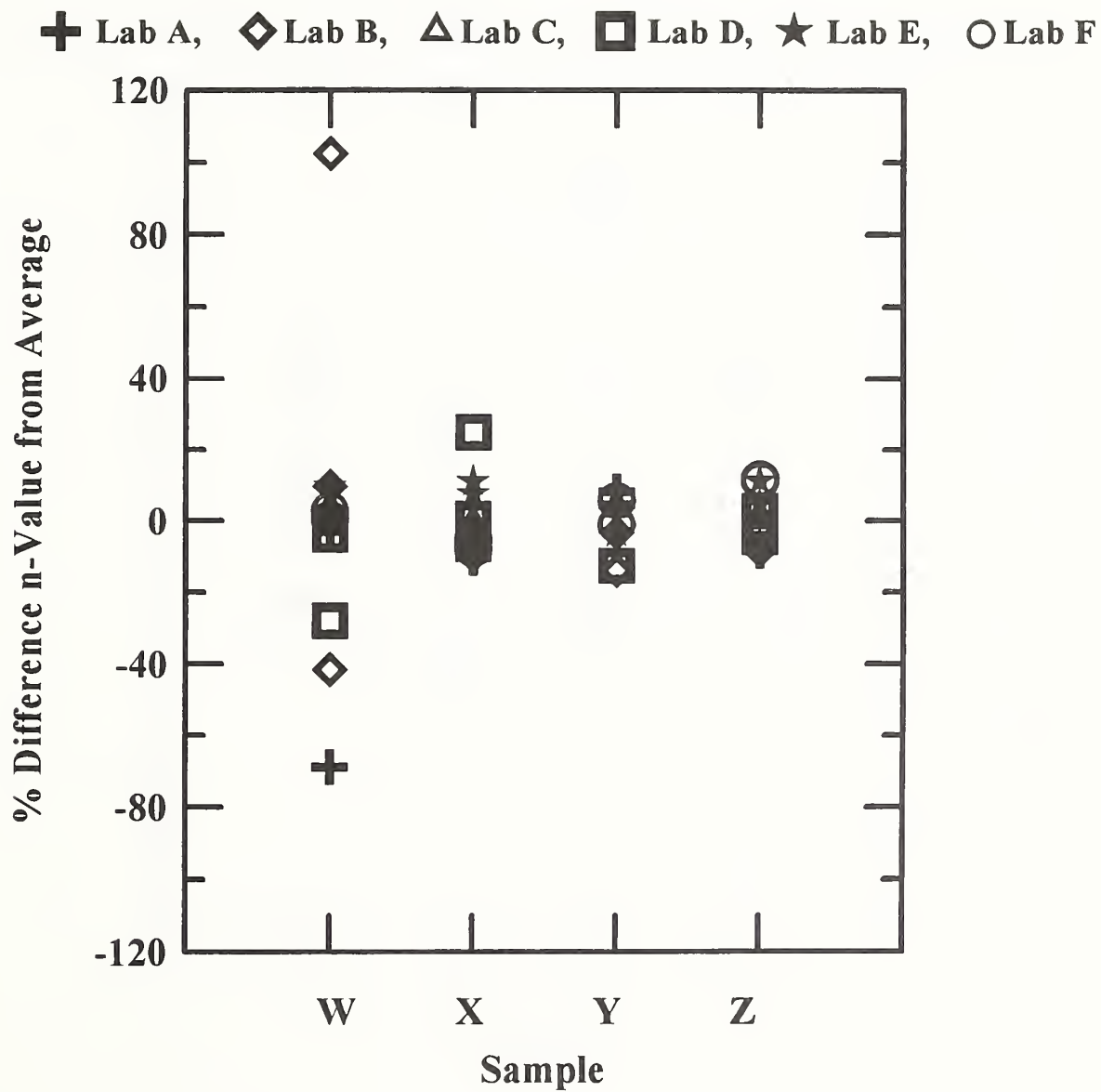


Figure 1-6. Percent difference of n-value versus sample for each laboratory.

+ Lab A, ◊ Lab B, △ Lab C, ◻ Lab D, ★ Lab E, ○ Lab F

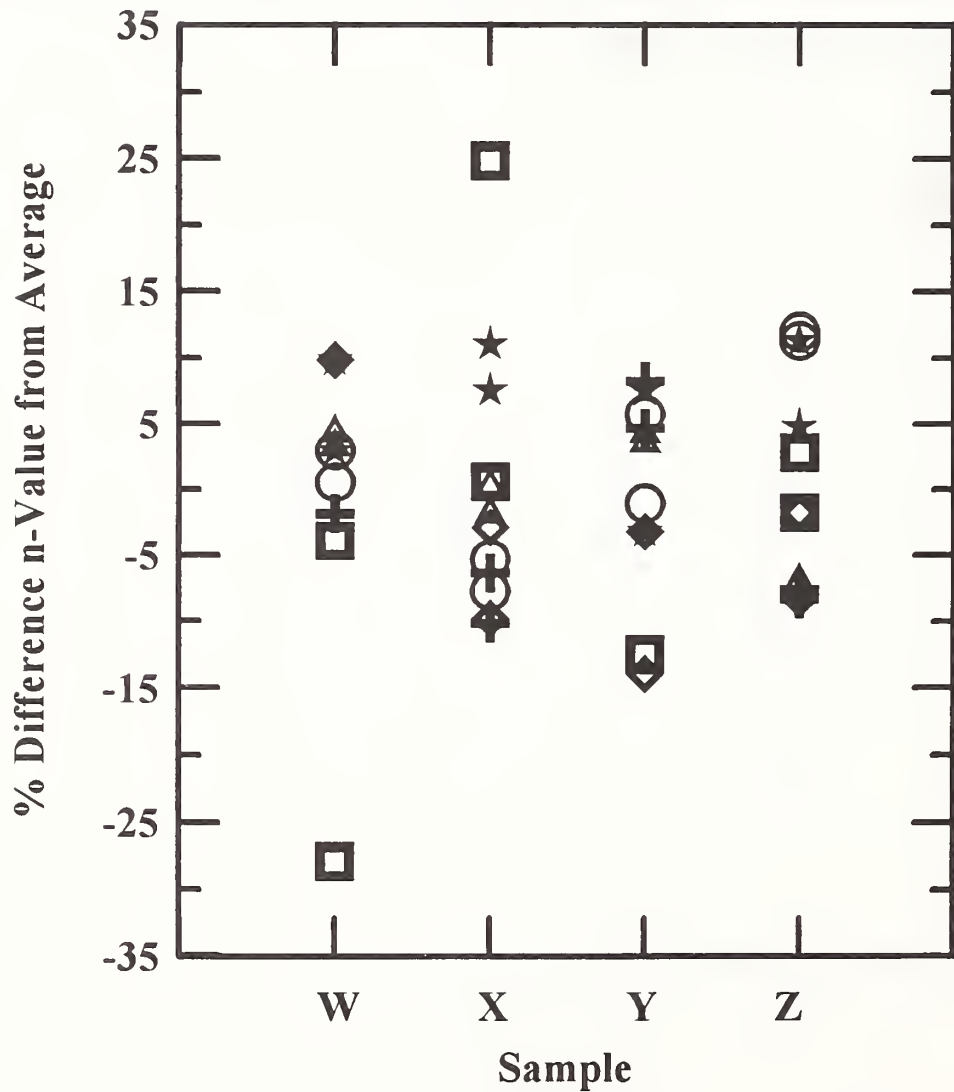


Figure 1-7. Percent difference of n-value versus sample for each laboratory. This plot is the same as Figure 1-6 except on a more sensitive scale excluding three outliers.

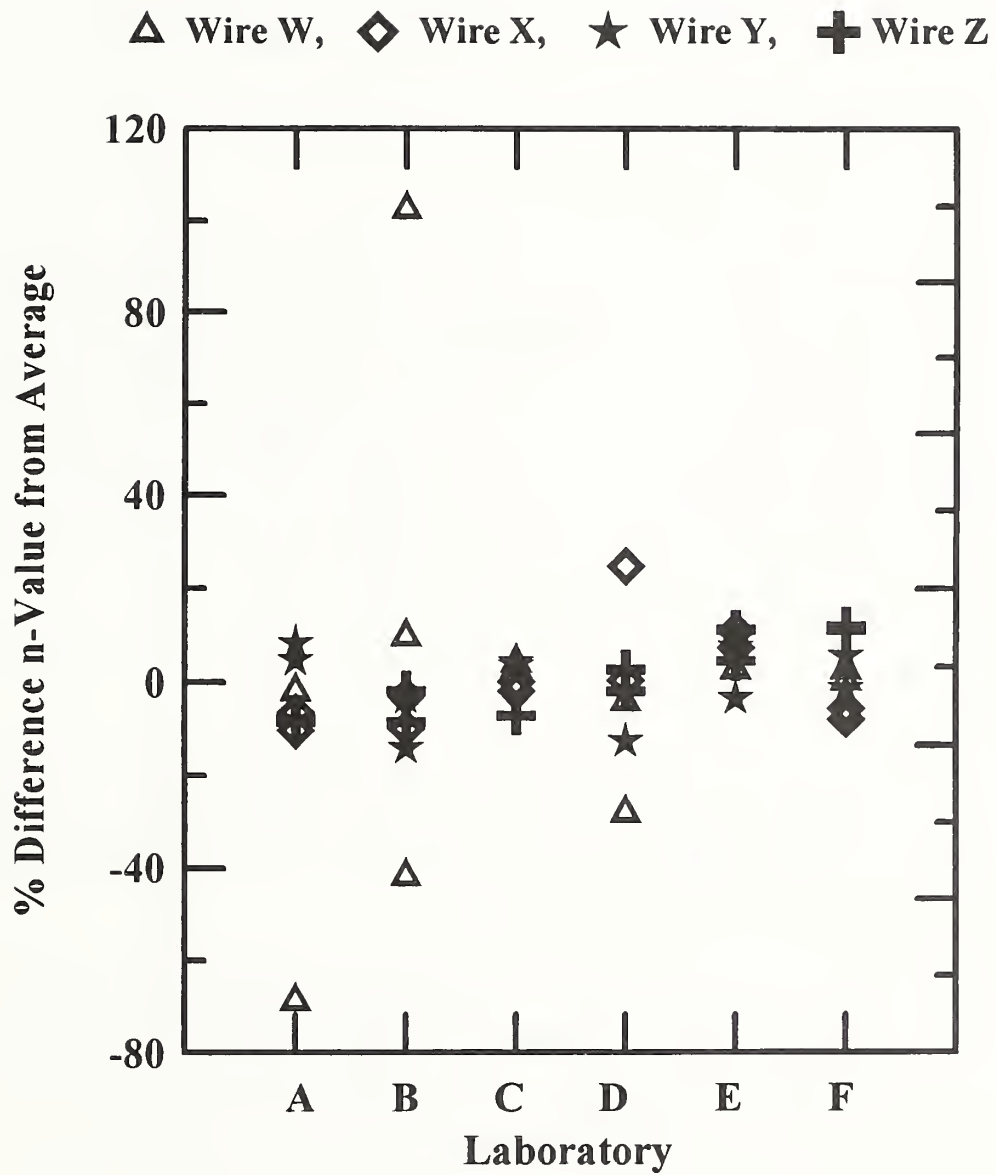


Figure 1-8. Percent difference of n-value versus laboratory for each sample measured.

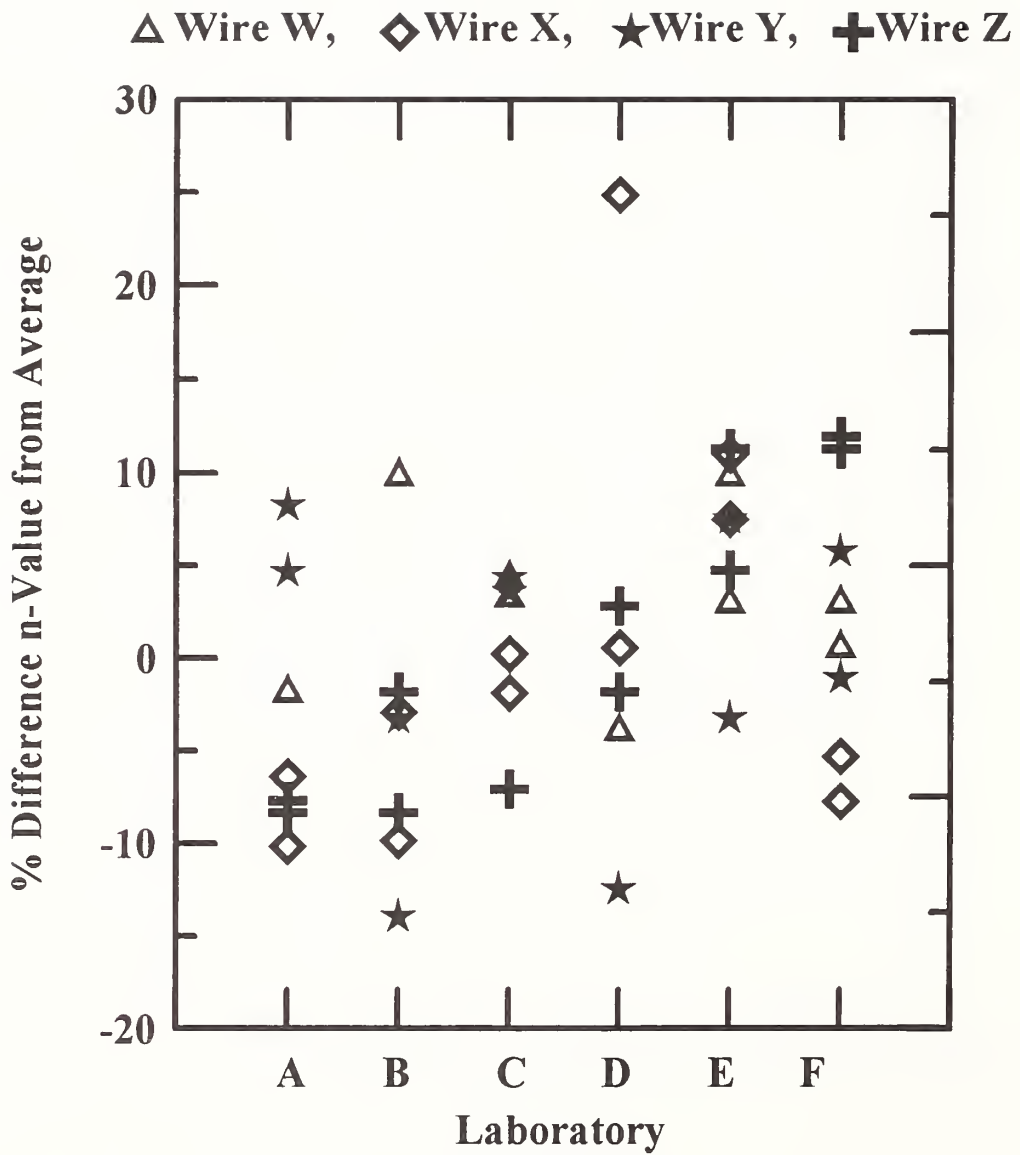


Figure 1-9. Percent difference of n-value versus laboratory for each sample measured. This plot is the same as Figure 1-8 except on a more sensitive scale excluding three outliers.

2. COMPARISON OF CRITICAL CURRENT MEASUREMENTS FROM INTERNATIONAL LABORATORIES

A second data comparison was compiled using data from five international laboratories to determine the present agreement among the international laboratories that make critical current measurements. A five laboratory subset, including one U.S. laboratory and all of the non-U.S. laboratories, was selected to represent a cross section of laboratories that did not use a standardized measurement procedure. These laboratories were labeled C, G, H, J, and K. The samples used are labeled W, X, Y, and Z. This is a brief presentation of these results.

2.1 Introduction

The analytical approach to comparing the results among these five laboratories was similar to the previous approach used for the six U.S. laboratories. Each laboratory contributed data for critical current and n-value measurements for each of four samples, labeled W, X, Y, and Z (Laboratory G did not measure Sample X and Laboratory H measured only Sample W). Because some of the laboratories contributed different numbers of measurements for each sample, a weighted average was calculated with equal weight given to each laboratory. Each laboratory's data was averaged for each sample, and these laboratory averages were used to compute an overall average for each sample which we define as the weighted average. The statistics shown in Tables II-1 to II-3 and Figures 2-1 to 2-5 are relative to this weighted average.

2.2 Experimental Results

Table 2-1 is a summary of each of the five laboratories' measurements of critical current and n-values for each of four samples at $10 \mu\text{V/m}$, 12 T, and 4.2 K. The weighted average for I_c and n-value for each sample is given at the bottom of the table. Figure 2-1 illustrates the critical current measurements from each laboratory for each sample; the weighted average is shown by a horizontal line.

Table 2-2 gives the statistical summary of I_c and n-value measurements for each sample using data from all five international laboratories. The coefficient of variation is the standard deviation divided by the weighted average, expressed in percent. The statistics for Sample W used 8 measurements, Sample X used 6 measurements, Sample Y used 12 measurements and Sample Z used 11 measurements. These statistics are illustrated in Figures 2-3 and 2-4. Figure 2-3 shows the percent difference of the measured critical current for each laboratory from the overall weighted average for each sample, as a function of sample. Figure 2-4 shows the percent difference in a similar manner for the n-values of each sample.

Table 2-3 shows measurement statistics for each laboratory that participated in the intercomparison. These measurement statistics are relative to the weighted average value for each of the four samples. For this table, the percentage differences between the results of a laboratory's measurements on a given sample and the overall average for that sample are calculated. The range of these percent differences in I_c for all samples is shown in the row of the table labeled I_c Range (%). The average of these percent differences for a given laboratory and all samples is shown in the row of the table labeled I_c Average Bias (%). These measurement statistics are best illustrated in Figure 2-2. This figure shows the variation in I_c measurements made by a given laboratory for each sample. Thus, the average bias of I_c indicates the average position of a laboratory's results relative to the overall weighted averages and the I_c range indicated the variability of a laboratory's results for two specimens of each of four samples. The statistics on the n-value measurements were done in the same way and are illustrated in Figure 2-5. This analysis was used to attempt to quantify the results from each laboratory and it is not an independent evaluation because the overall weighted averages were used.

2.3 Discussion

It is informative to contrast the results from this international comparison to the comparison among U.S. laboratories. The average critical current values in the international comparison were lower than the U.S. laboratory comparison for all four samples. The coefficient of variations for the international comparison ranged from 9.6% to 14.2% compared to 2.9% to 4.3% for the U.S. laboratories. Also, the biases for each international laboratory were more pronounced than for the U.S. laboratories. The lack of a standard measurement mandrel material for all laboratories may have caused this increase in variation and bias. Another factor affecting variability may be that some laboratories transferred samples between reaction and measurement mandrels.

Table 2-1. International laboratories and one U.S. laboratory: Summary of critical current and n-value measurements on Nb₃Sn strand: 10 μV/m, 12 T, and 4.2 K.

Laboratory	Wire W		Wire X		Wire Y		Wire Z	
	I _c (A)	n-value						
C	117	32	210	29	138	29	84	11
	116	32	215	29	136	29	84	11
G	95	27			105	25	86	26
	97	24			110	26	72	12
					106	26	77	20
					115	31	67	12
					120	28	68	12
							67	13
H	110	37						
J	102	30	174	28	123	25	70	17
K	126	24	233	33	151	33	79	11
	127	26	232	31	151	32	80	12
			241	31	150	35		
					150	34		
Weighted average	110.20	29.90	207.28	29.56	130.43	28.68	76.58	13.83

Table 2-2. International laboratories and one U.S. laboratory: Summary statistics for each sample measured at 4.2 K and 12 T.

	Sample W	Sample X	Sample Y	Sample Z
I_c average (A)	110.20	207.28	130.43	76.58
I_c standard deviation (A)	12.5	26.8	18.5	7.3
I_c coefficient of variation (%)	11.3	12.9	14.2	9.6
n-value average	29.90	29.56	28.68	13.83
n-value standard deviation	4.7	2.0	3.6	4.8
n-value coefficient of variation (%)	15.6	6.6	12.7	35.0

Table 2-3. International laboratories and one U.S. laboratory: Statistical summary of laboratory measurements of critical current and n-value at 4.2 K and 12 T.

	Lab C	Lab G	Lab H	Lab J	Lab K
I_c average bias (%)	5.7	-9.9	-0.2	-9.4	12.7
I_c range (%)	11.0	31.8	0.0 ^a	10.4	13.1
n-value average bias (%)	-3.5	2.4	23.7	1.3	2.0
n-value range (%)	27.5	107.7	0.0 ^a	35.7	42.5

^a Lab H only measured one specimen of one sample therefore their range was zero.

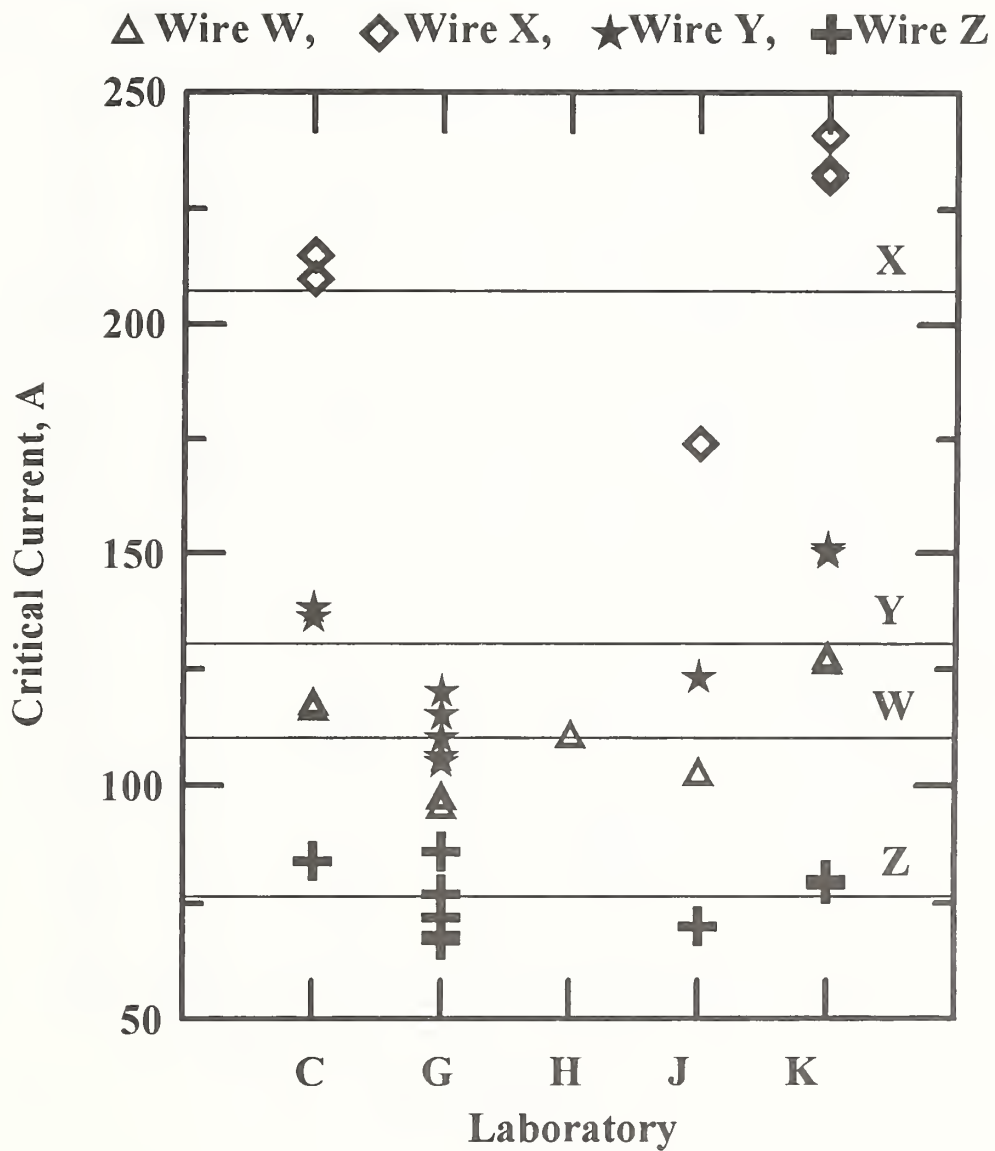


Figure 2-1. Critical current versus laboratory for each of the four samples. The horizontal lines show the weighted average I_c for each sample.

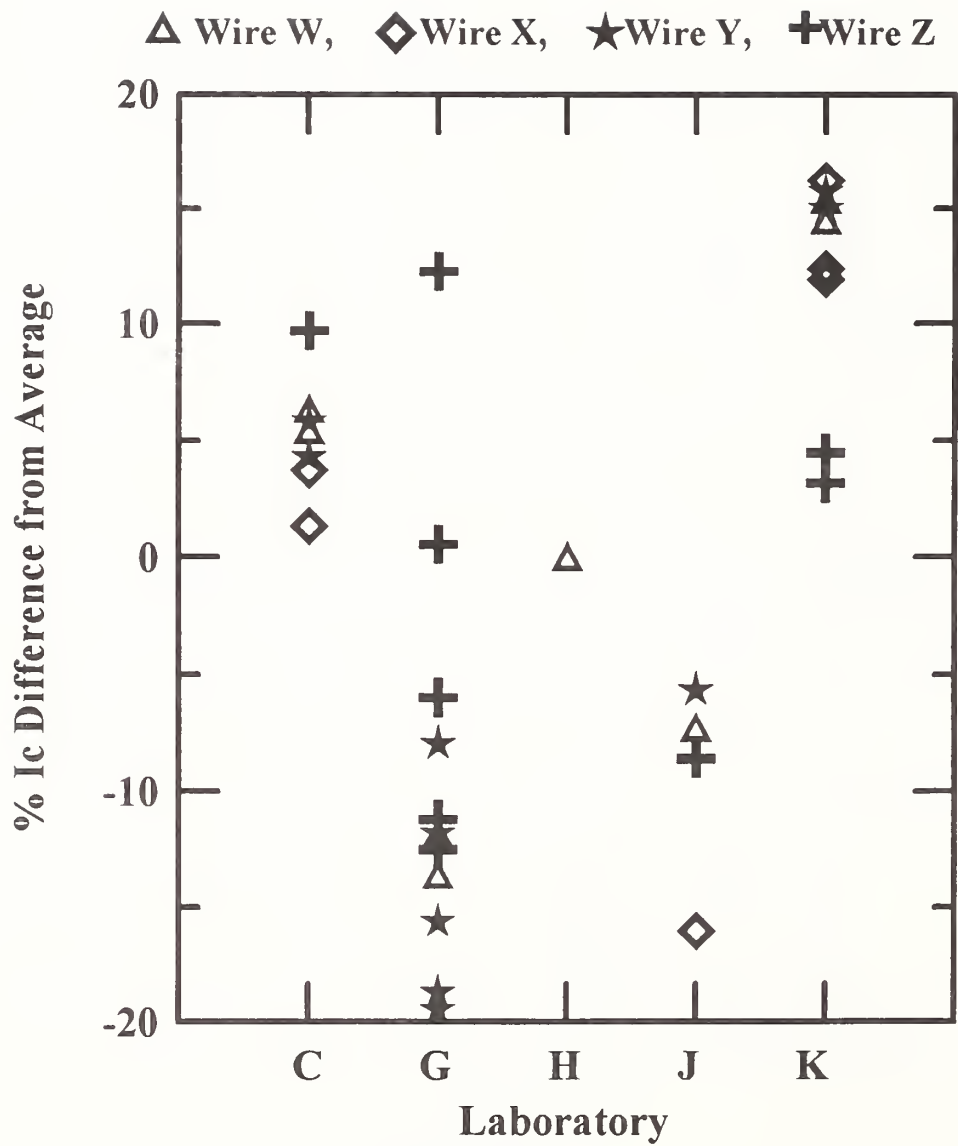


Figure 2-2. Percent difference of critical current versus laboratory for each sample measured.

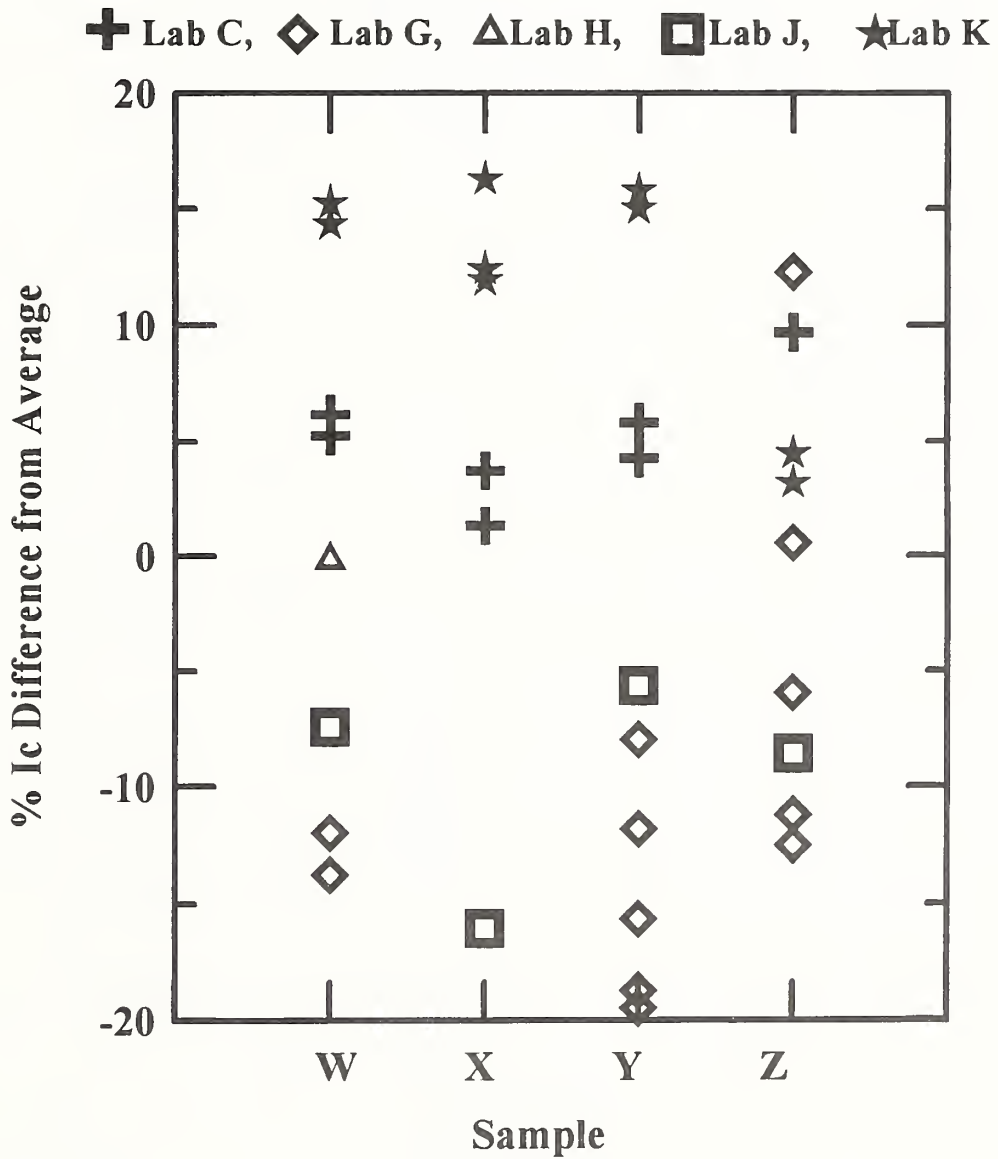


Figure 2-3. Percent difference of critical current versus sample for each laboratory.

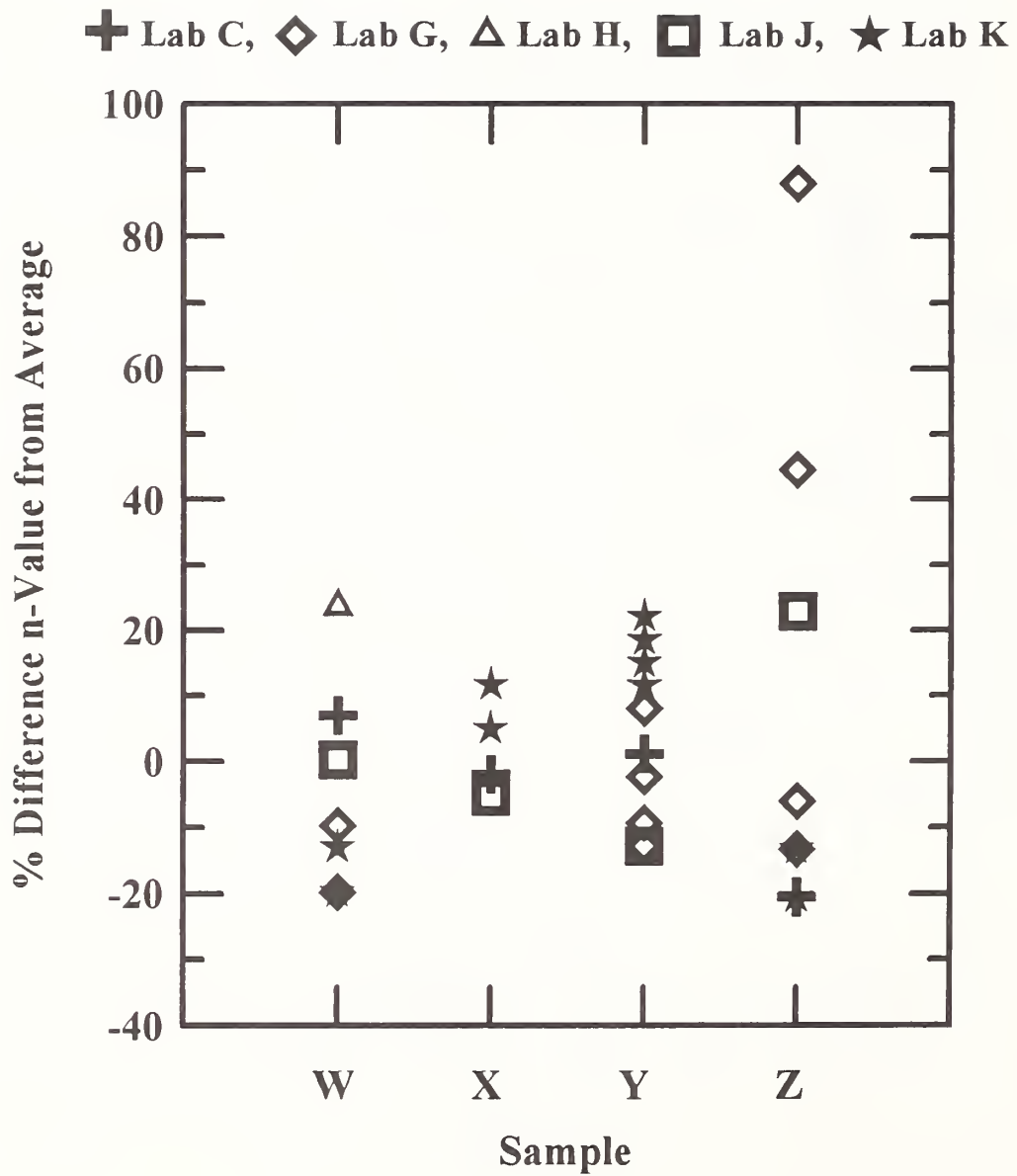


Figure 2-4. Percent difference of n-value versus sample for each laboratory.

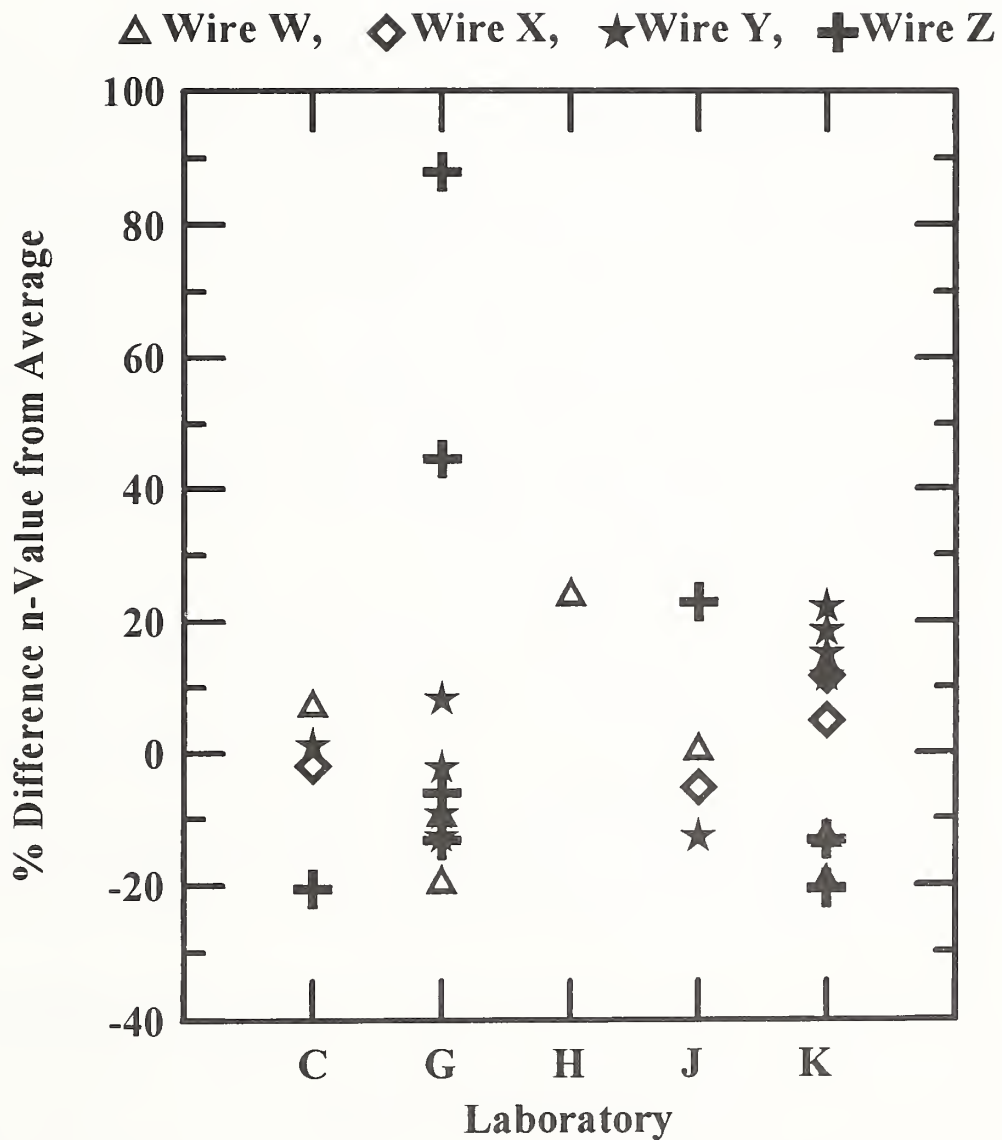


Figure 2-5. Percent difference of n-value versus laboratory for each sample measured.

3. CRITICAL CURRENT HOMOGENEITY OF A Nb₃Sn WIRE

This chapter discusses the results of critical current homogeneity studies that were carried out on one of the Nb₃Sn wires that was used in an ITER interlaboratory comparison. The data included here are a summary of critical current measurements made at seven magnetic fields and two temperatures, and for three repeat determinations at each setting on ten specimens.

3.1 Experimental Details of the Homogeneity Study

This study was conducted to verify the critical current I_c homogeneity of one of the Nb₃Sn conductors used in the ITER Benchmarking Test (interlaboratory comparison). The part of the wire used in the interlaboratory comparison started as a continuous piece that was about 450 m long. This length was divided into nine pieces which were identified with codes that started with numbers 1 through 9 in the same sequence that they had in the continuous length. The pieces with odd number codes were 10 m long. Those with even number codes were 100 m long.

A number of specimens were cut from the 10 m pieces. These specimens were used to perform homogeneity studies on the following parameters: I_c , ac losses, Cu to non-Cu ratio, and residual resistivity ratio. These parameters were studied in the interlaboratory comparison. The 100 m pieces were distributed to the four ITER parties to be measured by a number of laboratories. This sampling pattern allowed for testing of the homogeneity over the whole length including specimens on each side of the four 100 m lengths.

Two specimens from each of five 10 m lengths were used in the I_c homogeneity study for a total of ten specimens. The two specimens within each 10 m length were identified either as a tail (t) or point (p) specimen, depending on the specimen's location within the 10 m length. Thus, the ten specimens in the I_c homogeneity study were identified as: 1t, 1p, 3t, 3p, 5t, 5p, 7t, 7p, 9t, and 9p. Specimens 1t and 1p were separated by less than 10 m in the original continuous length of wire. Specimens 1p and 3t were separated by a little more than 100 m. Each specimen was instrumented with three pairs of adjacent voltage taps, with each pair separated by 25 cm. The voltage taps are identified as tap 1 (center), 2 (bottom), and 3 (top). The separation between the current contacts and the nearest voltage tap was more than 7 cm.

The ten specimens were measured at magnetic fields of 6 to 12 T and at temperatures of approximately 4.02 and 4.2 K. At each setting of field and temperature, the voltage-current (V-I) characteristics of the three voltage tap pairs were simultaneously measured. This was repeated three times, yielding a total of 126 V-I curves on each specimen.

Each V-I curve was analyzed to determine the I_c at an electric field criterion of 10 $\mu\text{V}/\text{m}$. Thus, we obtained three determinations of I_c for each voltage tap pair at each setting. To correct for

magnetic field profile in each tap region, we performed a first-order correction to the measured I_c . This correction was about 0.4% at 12 T (maximal case).

Figure 3-1 shows the repeatability of the I_c measurement as a function of temperature at a magnetic field of 12 T. There were three determinations of I_c on each tap at each of three temperatures. The extra data at the middle temperature were taken on this specimen to demonstrate the linearity of the temperature dependence of I_c over this field and temperature range. This specimen was from the same 450 m sample as the homogeneity specimens. The dependence of I_c on temperature is very nearly linear: typical standard deviations from the least-squares fit line are less than 0.03%. The temperature intercept of this fit is defined as T_c^* and its physical interpretation is the effective transition temperature at a given magnetic field. The T_c^* equations are:

$$I_c(B, T) = I_{cr}(B, T_r) [(T_c^*(B) - T) / (T_c^*(B) - T_r)], \text{ where}$$
$$T_c^* \text{ is defined by } I_c(B, T) = I_{c0}(B) [1 - T / T_c^*(B)]$$

T_c^* is the effective transition temperature and I_{cr} is the measured critical current at a reference temperature T_r . The first equation can be used to estimate I_c at any temperature using I_{cr} , T_r , and T_c^* .

The estimated uncertainty of these I_c measurements is $\pm 2\%$ for Nb_3Sn wires. The estimated precision is $\pm 1\%$. Extra digits are provided in data tables for precise interpolation. The estimated uncertainty of the n-value measurements is $\pm 10\%$ with a precision of $\pm 2\%$. The effective transition temperature, T_c^* , is just an expression of the measured temperature dependence of I_c at each magnetic field.

3.2 Experimental Results

Figures 3-2a and 3-3a show the critical current homogeneity of the Nb_3Sn conductor at a temperature of 4.2 K and magnetic fields of 6 and 12 T, respectively. Figures 3-2b and 3-3b show the corresponding n-values. The solid symbols indicate the measurements made on the tail, while the open symbols indicate measurements made on the point. The circle, square, and triangles correspond to voltage taps 1 (center), 2 (bottom), and 3 (top), respectively. A summary of the statistics for I_c , n-value, and T_c^* are given in Table 3-1.

The I_c measurements at 6 T shown in Figure 3-2a have a 7.9% range (maximum to minimum), although most of the data fall within half of this range. These data suggest that there may be an 'end effect' on this wire as indicated by the higher I_c on specimens 1t and 1p which originated on one end of the wire. This effect, however, is not as evident at 12 T; therefore there may not be an end effect.

The I_c measurements at 12 T shown in Figure 3-3a have a 10.9% range. Although the 5t-tap-3 data point at 12 T might seem like an outlier, it is not inconsistent with the distribution of the rest of the data points. The I_c 's of 3p are less than 2% different from this point. Also, the I_c of 5t-tap-3 at 6 T was not an extreme data point.

The range of critical currents shown in Figures 3-2a and 3-3a shows that the critical current is somewhat inhomogeneous along the length of the conductor. By observing the range of values obtained on the three pairs of voltage taps on each specimen, we can get an indication of the local inhomogeneity of the wire. Six specimens had a small range of values (less than 1.3%) for the three pairs. Four specimens had a large range: 3.4, 3.5, 3.6, and 7.6%. This suggests that the wire can exhibit significant local inhomogeneity, which may be of concern in the application of these wires. These results may give insight to the source of this inhomogeneity.

The coefficient of variation ($\sigma/\text{average}$) is about 2.6% at 12 T, a temperature of 4.2 K, and an electric field criterion of $10 \mu\text{V}/\text{m}$. For comparison to other Nb_3Sn wires, the homogeneity of two wires used in the first VAMAS interlaboratory comparison are 2.4% at 10 T for Sample A and 1.3% at fields of 7 to 15 T for Sample B [1].

Figure 3-2b shows a 24.5% range and 7.9% coefficient of variation in the measured values of n at 6 T. Figure 3-3b shows a 31.2% range and 6.3% coefficient of variation at 12 T. The lowest n -value at 12 T was obtained on 5t-tap-3 which also had the lowest I_c . Variation in n -value is not as critical an issue as variation in I_c , and the present variation in n may be acceptable.

I_c measurements at magnetic fields between 6 and 12 T and the systematic trends with magnetic field are illustrated in Figures 3-4 to 3-9 and Tables 3-2 to 3-5. Figure 3-4 shows I_c as a function of magnetic field for ten samples with three taps at integer magnetic fields between 6 and 12 T at a temperature of 4.2 K. Figure 3-5 shows the percent difference of the measured critical current from the average measurement at a given field. The lines connect the data points for a given tap on a given specimen. These lines are fairly smooth across magnetic field, which indicates a systematic trend with respect to the average and a self consistency of the measurements. Most of the lines diverge from the average with increasing magnetic field. The trend for 5t-tap-3 is somewhat exaggerated, which is consistent with the observations made on Figure 3-2a and Figure 3-3a. All measurements fell within $\pm 6\%$ of the average, and the percentage range is relatively constant with magnetic field.

Figure 3-6 shows the n -value at 4.2 K for each I_c measurement given above. Figure 3-7 shows the difference in the determined n -values from the average n -value at each field. Notice that the y-axis in Figure 3-7 is not in percent. Again, there are systematic trends with magnetic field for each tap and self consistency of the measurements. The curve with the lowest n -value at 12 T is from 5t-tap-3.

Figure 3-8 shows the values of T_c^* for each critical current measurement given above. Figure 3-9 shows the difference in the determined T_c^* from the average T_c^* at each field. Notice that

the y-axis in Figure 3-9 is not in percent. We analyzed the effect of using the values of T_c^* computed, including and excluding the outliers on Sample 7t. We suspect that these outliers were caused by a lack of thermal equilibrium between the liquid helium and the ullage pressure in the Dewar. Our measurement procedure for the elevated temperature is to: raise the pressure and heat the liquid helium to get it in equilibrium with a pressure higher than the target point, let it soak for a few minutes, then drop the pressure to the target point. This was apparently not done correctly in this case. The liquid will asymptotically approach equilibrium with the gas pressure. This fact and the sequence of I_c measurements starting at 6 T and ending at 12 T explains the shape of the 7t curve with field, that is the largest error at 6 T and the smallest error at 12 T. We calculated the error in I_c that resulted from this error in T_c^* when the I_c was corrected from 4.02 K to 4.2 K. The maximum error was 0.45% at 6 T, which is small compared to the observed inhomogeneity. The error in I_c was 0.14% at 12 T. The errors in I_c without these outliers, using the data points furthest from the average T_c^* were -0.08% at 6 T and -0.17% at 12 T. The majority of the T_c^* determinations were within ± 0.2 K, indicating high repeatability.

3.3 Discussion of Experimental Results

The variations seen in the critical current as a function of specimen indicate inhomogeneity along the length of the conductor. There are a number of possible sources of inhomogeneity; the following is a partial list of sources:

1. Intrinsic sample variations: The intrinsic properties may vary along the length of the conductor, thus leading to the nonuniform critical current measurements.
2. Variation due to nonuniform precompression: Nonuniform precompression along the length of the conductor could be another source of variation [2].
3. Variation in tension: The wire tension for each specimen and variation in wire tension along a specimen would cause a variation in the measured I_c . Variation in tension along the wire on a given specimen does not seem likely since both the wire and its holding groove are smooth. Moreover, the tension is applied uniformly along the wire. This, coupled with the fact that significant inhomogeneity was observed in some specimens suggests that variation in tension cannot explain all of the observed variation.
4. Variation in mechanical properties of the sample: The sample could have mechanical instabilities along its length. For example, a weak section in the conductor might focus all the strain, thus leading to nonuniform strain along the conductor and nonuniform critical currents. The differential contraction between the sample and the mandrel puts a mechanical load on the whole 1 m length of wire. This situation has not been studied before in the U.S.. A typical sample length for testing I_c as a function of strain is 3 cm. If mechanical variations are present in the conductor, they may be observed in this coil- I_c measurement. If these variations cause problems in the test, they may also affect the magnet application.

5. Accidental damage to the samples: This may be possible but unlikely because of the design of the sample mandrel. There is very little handling of the portion of the sample between the voltage taps.

This list is not exhaustive: there could be a host of other possibilities for the measured inhomogeneity. The most pronounced evidence of the problem is the observed variation among the three voltage taps.

3.4 References

[1] Tachikawa, K.; Itoh, K.; Wada, H.; Gould, D.; Jones, H.; Walters, C. R.; Goodrich, L.F.; et. al. "VAMAS intercomparison of critical current measurement in Nb₃Sn Wires," IEEE Trans. Magn., Vol. 25, No. 3, p. 2368; 1989.

[2] Ekin, J.W. NIST/Boulder, Personal communication, 1994.

Table 3-1. Summary statistics of I_c , n-values and T_c^* .

I_c @ 4.2 K							
	6 T	7 T	8 T	9 T	10 T	11 T	12 T
# pts.	30	30	30	30	30	30	30
Average, A	383.47	316.68	262.71	218.04	180.37	148.21	120.52
Std. dev., A	7.85	6.60	5.62	4.84	4.19	3.65	3.19
Min, A	370.08	305.37	253.08	209.80	172.79	141.02	113.72
Max, A	400.52	330.93	274.74	228.24	189.04	155.60	126.81
Range, A	30.44	25.56	21.66	18.44	16.25	14.58	13.09
Coeff., %	2.05	2.09	1.99	2.22	2.32	2.46	2.65
n-value @ 4.2 K							
	6 T	7 T	8 T	9 T	10 T	11 T	12 T
# pts.	30	30	30	30	30	30	30
Average	43.24	41.44	39.80	38.10	36.25	34.29	32.13
Std. dev.	3.40	2.97	2.72	2.46	2.30	2.17	2.03
Min	37.56	36.55	34.61	32.37	30.30	27.95	25.53
Max	48.16	46.33	44.91	41.94	41.00	38.58	35.54
Range	10.60	9.78	10.30	9.56	10.70	10.63	10.01
Coeff., %	7.87	7.16	6.83	6.47	6.35	6.33	6.33
T_c^* with outliers							
	6 T	7 T	8 T	9 T	10 T	11 T	12 T
# pts.	30	30	30	30	30	30	30
Average, K	13.596	12.772	12.013	11.369	10.727	10.101	9.498
Std. dev., K	0.665	0.333	0.127	0.115	0.096	0.097	0.093
Min, K	13.041	12.464	11.803	11.156	10.499	9.838	9.254
Max, K	15.791	13.820	12.384	11.698	10.988	10.339	9.686
Range, K	2.751	1.356	0.581	0.541	0.489	0.501	0.432
Coeff., %	4.891	2.606	1.058	1.009	0.892	0.962	0.984
T_c^* w/o outliers							
	6 T	7 T	8 T	9 T	10 T	11 T	12 T
# pts.	27	27	27	27	27	27	27
Average, K	13.382	12.666	11.980	11.342	10.704	10.080	9.484
Std. dev., K	0.118	0.079	0.080	0.079	0.068	0.078	0.086
Min, K	13.041	12.464	11.803	11.156	10.499	9.839	9.254
Max, K	13.568	12.800	12.086	11.461	10.787	10.175	9.604
Range, K	0.527	0.336	0.283	0.305	0.288	0.337	0.350
Coeff., %	0.878	0.613	0.665	0.698	0.634	0.747	0.904

Table 3-2. Summary of I_c measurements at $10 \mu\text{V/m}$, 4.20 K, and 6 T to 12 T.

Field	Tap#	1t	1p	3t	3p	5t	5p	7t	7p	9t	9p
6	1	397.70	392.00	381.33	370.99	384.42	379.94	382.87	385.27	384.49	376.00
6	2	396.68	393.07	382.18	373.52	388.56	379.50	388.31	377.01	386.27	381.01
6	3	400.52	394.30	379.92	370.08	373.65	375.36	378.38	383.30	384.08	383.44
7	1	328.45	323.46	314.81	306.07	317.27	313.80	316.56	318.27	317.66	310.01
7	2	327.93	324.46	315.76	308.26	320.98	313.40	321.15	311.02	319.25	314.83
7	3	330.93	325.45	313.78	305.37	307.54	310.20	312.77	316.82	317.30	316.75
8	1	272.54	268.21	261.08	253.59	263.05	260.40	262.86	264.06	263.65	256.70
8	2	272.34	269.08	262.06	255.52	266.46	259.99	266.84	257.68	265.10	261.32
8	3	274.74	269.90	260.35	253.08	254.19	257.60	259.66	263.09	263.35	262.86
9	1	226.24	222.55	216.63	210.13	218.13	216.14	218.36	219.22	218.95	212.58
9	2	226.30	223.28	217.59	211.86	221.35	215.70	221.87	213.51	220.29	217.02
9	3	228.24	224.01	216.08	209.80	210.02	214.00	215.69	218.59	218.68	218.27
10	1	187.22	184.11	179.13	173.48	180.27	178.84	180.79	181.43	181.25	175.41
10	2	187.49	184.71	180.06	175.06	183.31	178.37	183.92	176.28	182.52	179.66
10	3	189.04	185.35	178.74	173.30	172.79	177.23	178.56	181.08	180.99	180.72
11	1	153.87	151.31	147.14	142.16	147.95	147.00	148.70	149.21	149.07	143.68
11	2	154.33	151.78	148.01	143.59	150.86	146.49	151.54	144.51	150.25	147.77
11	3	155.60	152.37	146.85	142.09	141.02	145.82	146.87	149.08	148.84	148.64
12	1	125.18	123.09	119.61	115.21	120.10	119.58	121.02	121.34	121.39	116.37
12	2	125.78	123.44	120.45	116.54	122.91	119.03	123.61	117.05	122.49	120.27
12	3	126.81	123.97	119.40	115.23	113.72	118.75	119.54	121.38	121.18	121.03

Table 3-3. Summary of I_c measurements at $10 \mu\text{V/m}$, 4.02 K , and 6 T to 12 T .

Field	Tap#	1t	1p	3t	3p	5t	5p	7t	7p	9t	9p
6	1	405.50	399.64	388.68	378.36	391.98	387.37	388.82	392.83	392.04	383.45
6	2	404.52	400.80	389.56	380.89	396.12	386.97	394.48	384.45	393.79	388.34
6	3	408.36	402.01	387.27	377.54	381.26	382.69	384.55	390.76	391.59	390.84
7	1	335.44	330.33	321.43	312.66	324.08	320.45	322.48	324.99	324.39	316.68
7	2	334.87	331.38	322.41	314.87	327.82	320.08	327.20	317.69	326.01	321.46
7	3	337.94	332.36	320.41	311.97	314.24	316.78	318.77	323.45	324.04	323.42
8	1	278.86	274.42	267.04	259.54	269.16	266.37	268.71	270.15	269.74	262.74
8	2	278.60	275.35	268.05	261.50	272.61	265.99	272.71	263.70	271.22	267.32
8	3	281.07	276.16	266.29	259.04	260.21	263.51	265.45	269.10	269.44	268.89
9	1	231.93	228.18	222.02	215.52	223.65	221.56	223.67	224.70	224.44	218.03
9	2	231.96	228.96	223.01	217.27	226.90	221.18	227.20	218.95	225.80	222.44
9	3	233.94	229.66	221.44	215.18	215.45	219.36	220.96	224.04	224.16	223.73
10	1	192.38	189.19	184.07	178.36	185.29	183.75	185.63	186.43	186.23	180.35
10	2	192.63	189.84	185.03	179.94	188.38	183.33	188.80	181.21	187.50	184.59
10	3	194.24	190.46	183.66	178.17	177.73	182.09	183.37	186.05	185.99	185.67
11	1	158.58	155.92	151.63	146.58	152.50	151.46	153.11	153.73	153.61	148.18
11	2	159.02	156.45	152.52	148.04	155.44	150.96	155.98	149.00	154.81	152.27
11	3	160.31	157.00	151.32	146.52	145.53	150.22	151.24	153.58	153.39	153.15
12	1	129.41	127.27	123.65	119.19	124.23	123.63	125.05	125.52	125.46	120.46
12	2	130.00	127.63	124.51	120.54	127.05	123.10	127.67	121.17	126.57	124.38
12	3	131.06	128.16	123.44	119.22	117.77	122.75	123.53	125.54	125.24	125.14

Table 3-4. Summary of n-value measurements at 4.20 K at magnetic fields of 6 to 12 T.

Field	Tap#	1t	1p	3t	3p	5t	5p	7t	7p	9t	9p
6	1	44.68	48.02	42.33	40.01	47.05	46.33	41.85	47.58	44.62	43.22
6	2	41.81	45.68	40.12	39.14	45.02	45.71	48.16	40.42	46.78	45.20
6	3	45.07	46.40	40.43	37.97	38.84	37.57	37.56	38.95	45.02	45.68
7	1	41.57	44.80	40.68	38.81	44.58	44.39	41.05	46.33	43.08	41.86
7	2	40.32	43.23	38.86	37.75	42.98	43.15	45.90	38.65	43.81	43.20
7	3	42.75	45.03	39.02	36.86	36.64	36.55	36.97	38.25	42.72	43.54
8	1	40.27	43.27	39.01	37.39	43.20	42.50	39.76	44.91	41.12	39.92
8	2	38.78	41.06	37.65	36.20	40.78	41.11	43.39	37.03	41.60	41.39
8	3	41.16	42.30	37.67	35.42	34.61	35.71	35.85	38.10	41.13	41.66
9	1	38.32	41.35	37.35	35.95	40.76	40.27	38.62	41.94	39.41	38.49
9	2	37.25	38.95	36.39	34.88	39.05	38.64	41.49	35.17	39.82	40.01
9	3	39.75	40.47	36.29	34.24	32.37	34.38	34.95	37.08	39.55	39.81
10	1	36.24	38.73	35.75	34.24	37.85	39.19	36.78	41.00	37.26	36.52
10	2	35.42	37.65	35.15	33.29	37.11	37.07	39.07	33.32	37.74	37.35
10	3	37.02	38.19	35.04	32.49	30.30	33.34	33.63	35.99	37.01	37.89
11	1	33.85	36.23	34.25	32.31	35.35	36.63	34.82	38.58	35.37	34.19
11	2	33.79	35.13	33.46	31.39	35.06	34.55	37.29	31.17	35.81	35.54
11	3	35.12	36.01	33.43	31.12	27.95	31.90	32.23	34.81	35.20	36.05
12	1	31.86	33.57	32.36	30.31	32.48	34.87	32.61	35.54	33.24	32.10
12	2	31.68	32.76	31.73	29.26	32.80	32.33	34.84	29.04	33.74	33.33
12	3	33.43	33.56	31.76	29.38	25.53	30.19	30.65	32.74	33.18	33.00

Table 3-5. Summary of T_c *'s at each magnetic field from 6 T to 12 T.

Field	Tap#	1t	1p	3t	3p	5t	5p	7t	7p	9t	9p
6	1	13.381	13.435	13.535	13.257	13.355	13.403	15.791	13.373	13.370	13.282
6	2	13.308	13.350	13.533	13.316	13.453	13.338	15.523	13.327	13.452	13.568
6	3	13.405	13.403	13.505	13.132	13.041	13.422	15.239	13.448	13.404	13.527
7	1	12.666	12.672	12.762	12.566	12.587	12.688	13.820	12.734	12.687	12.573
7	2	12.708	12.647	12.745	12.596	12.646	12.645	13.761	12.598	12.691	12.751
7	3	12.703	12.681	12.731	12.528	12.464	12.690	13.593	12.800	12.677	12.745
8	1	11.972	11.972	12.085	11.866	11.945	12.045	12.282	12.014	11.986	11.854
8	2	12.034	11.917	12.075	11.887	11.991	12.000	12.384	11.906	12.006	12.029
8	3	12.014	11.969	12.084	11.838	11.803	12.052	12.267	12.086	11.985	12.048
9	1	11.364	11.320	11.432	11.224	11.311	11.373	11.605	11.395	11.387	11.225
9	2	11.402	11.278	11.424	11.239	11.370	11.283	11.698	11.264	11.386	11.405
9	3	11.405	11.346	11.461	11.216	11.156	11.382	11.556	11.408	11.375	11.394
10	1	10.729	10.719	10.726	10.603	10.661	10.751	10.923	10.734	10.743	10.599
10	2	10.774	10.684	10.729	10.646	10.714	10.679	10.988	10.634	10.787	10.767
10	3	10.741	10.739	10.741	10.610	10.499	10.757	10.885	10.755	10.723	10.773
11	1	10.082	10.105	10.092	9.985	10.051	10.135	10.267	10.150	10.111	9.947
11	2	10.112	10.057	10.102	10.011	10.127	10.088	10.339	10.000	10.139	10.116
11	3	10.149	10.121	10.114	9.964	9.839	10.175	10.246	10.171	10.096	10.126
12	1	9.531	9.508	9.538	9.405	9.440	9.508	9.607	9.422	9.567	9.322
12	2	9.568	9.502	9.549	9.443	9.538	9.467	9.686	9.323	9.604	9.476
12	3	9.568	9.533	9.525	9.403	9.254	9.548	9.594	9.450	9.565	9.499

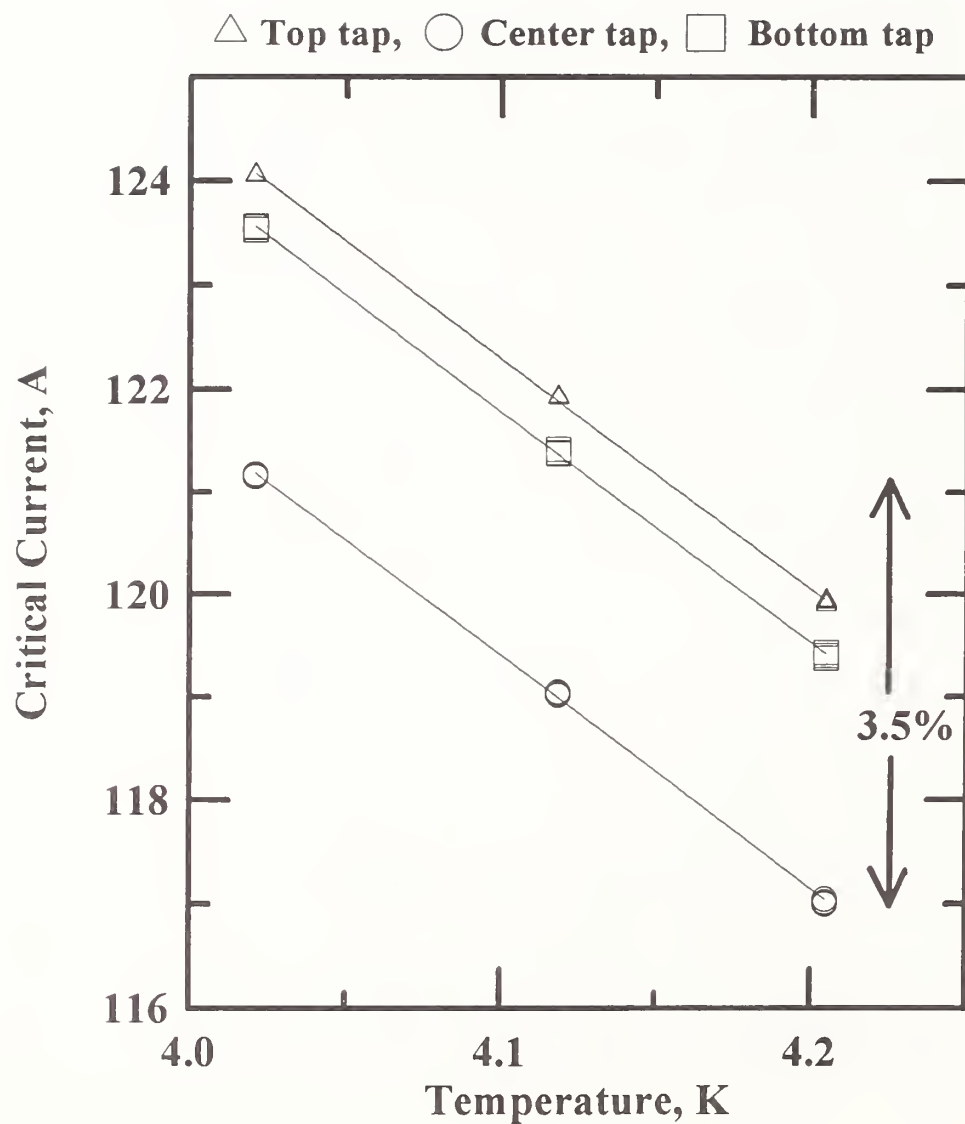


Figure 3-1. Critical current at 12 T versus temperature for three pairs of voltage taps. There are three determinations for each tap at each temperature; however, the three determinations are almost indistinguishable.

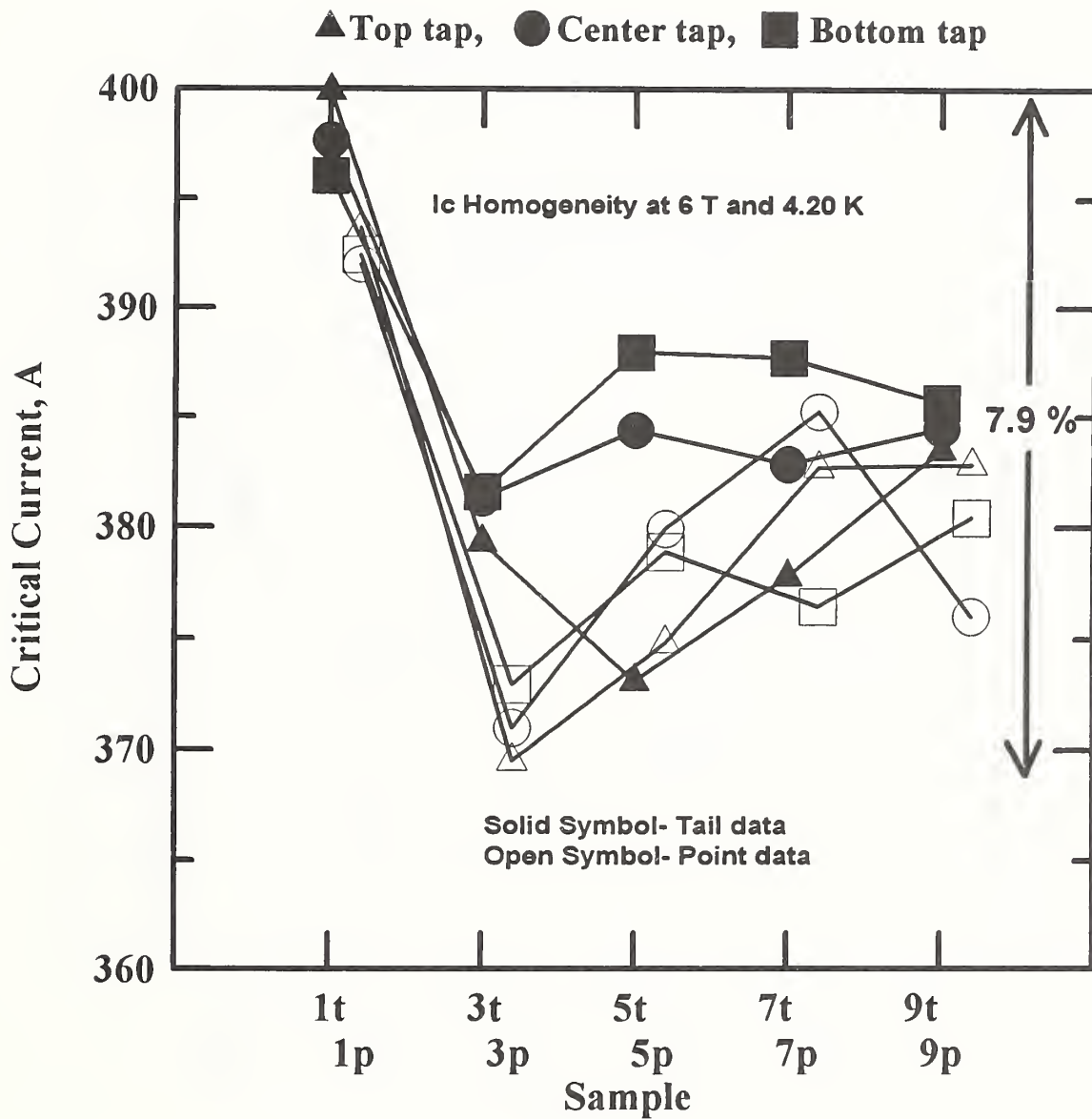


Figure 3-2a. Critical current at 6 T, 4.2 K, and 10 $\mu\text{V}/\text{m}$ versus sample. Each sample had three pairs of voltage taps.

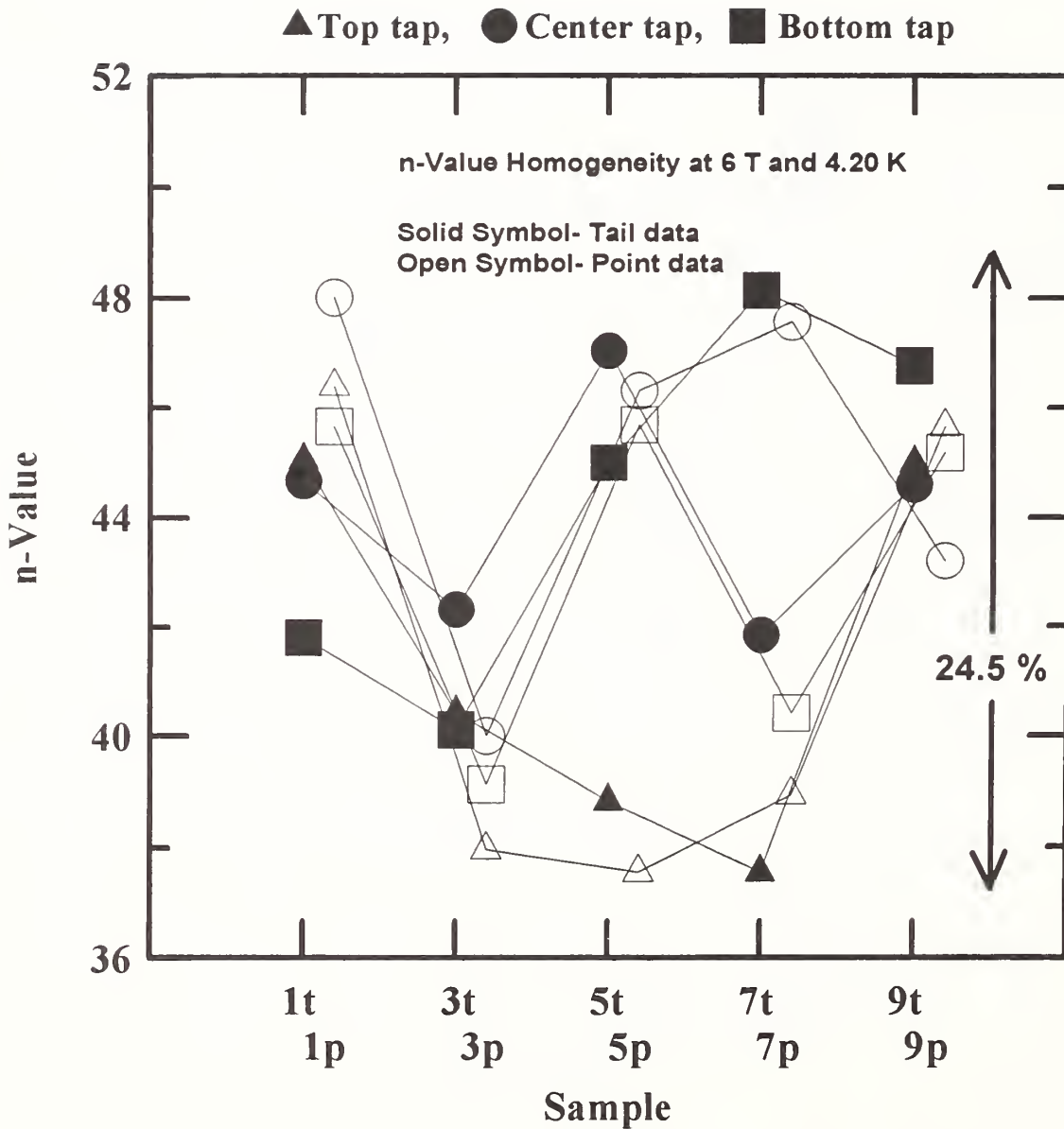


Figure 3-2b. n-values at 6 T, 4.2 K, and $10 \mu\text{V}/\text{m}$ versus sample. Each sample had three pairs of voltage taps.

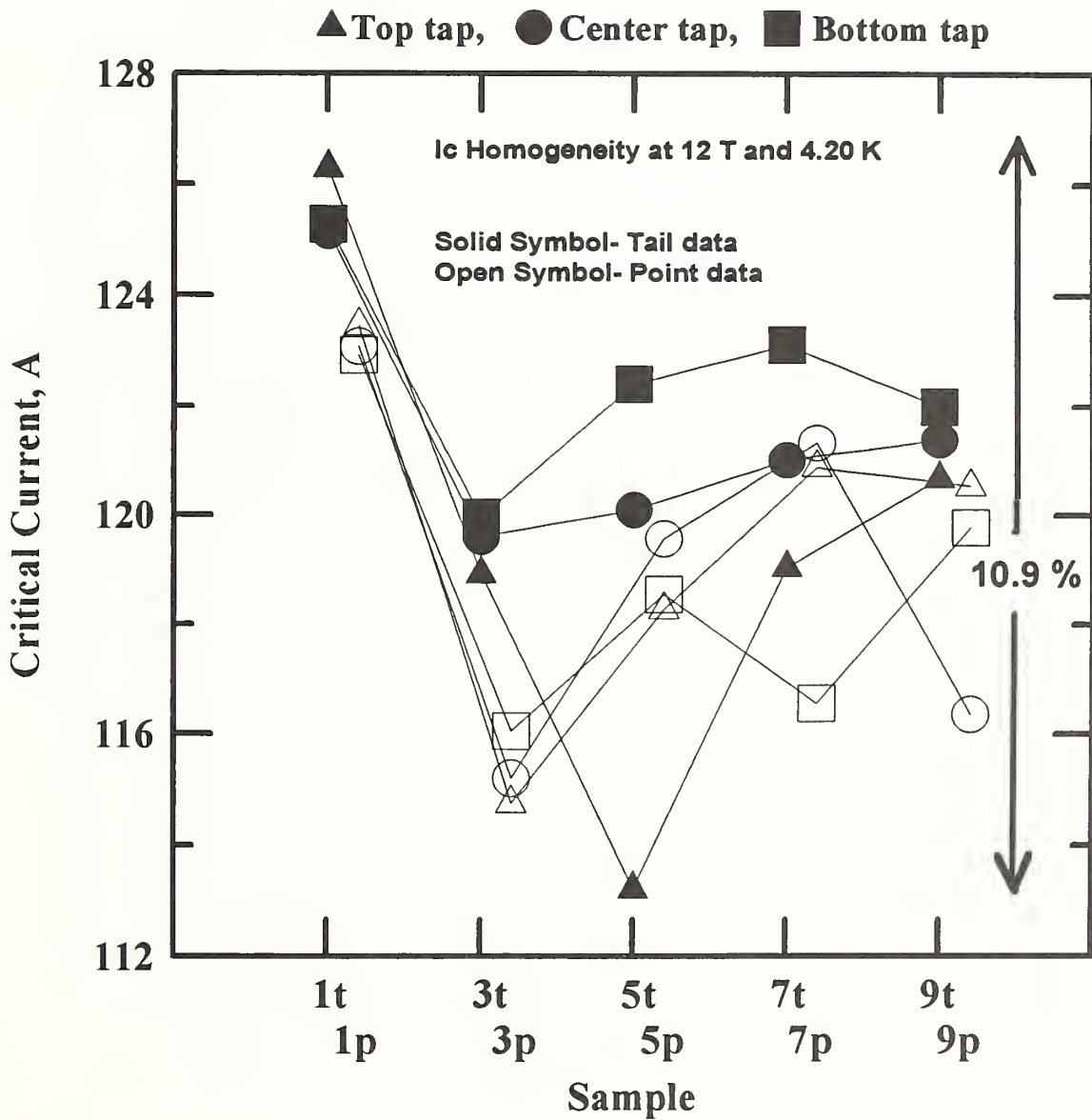


Figure 3-3a. Critical current at 12 T, 4.2 K, and $10 \mu\text{V/m}$ versus sample. Each sample had three pairs of voltage taps.

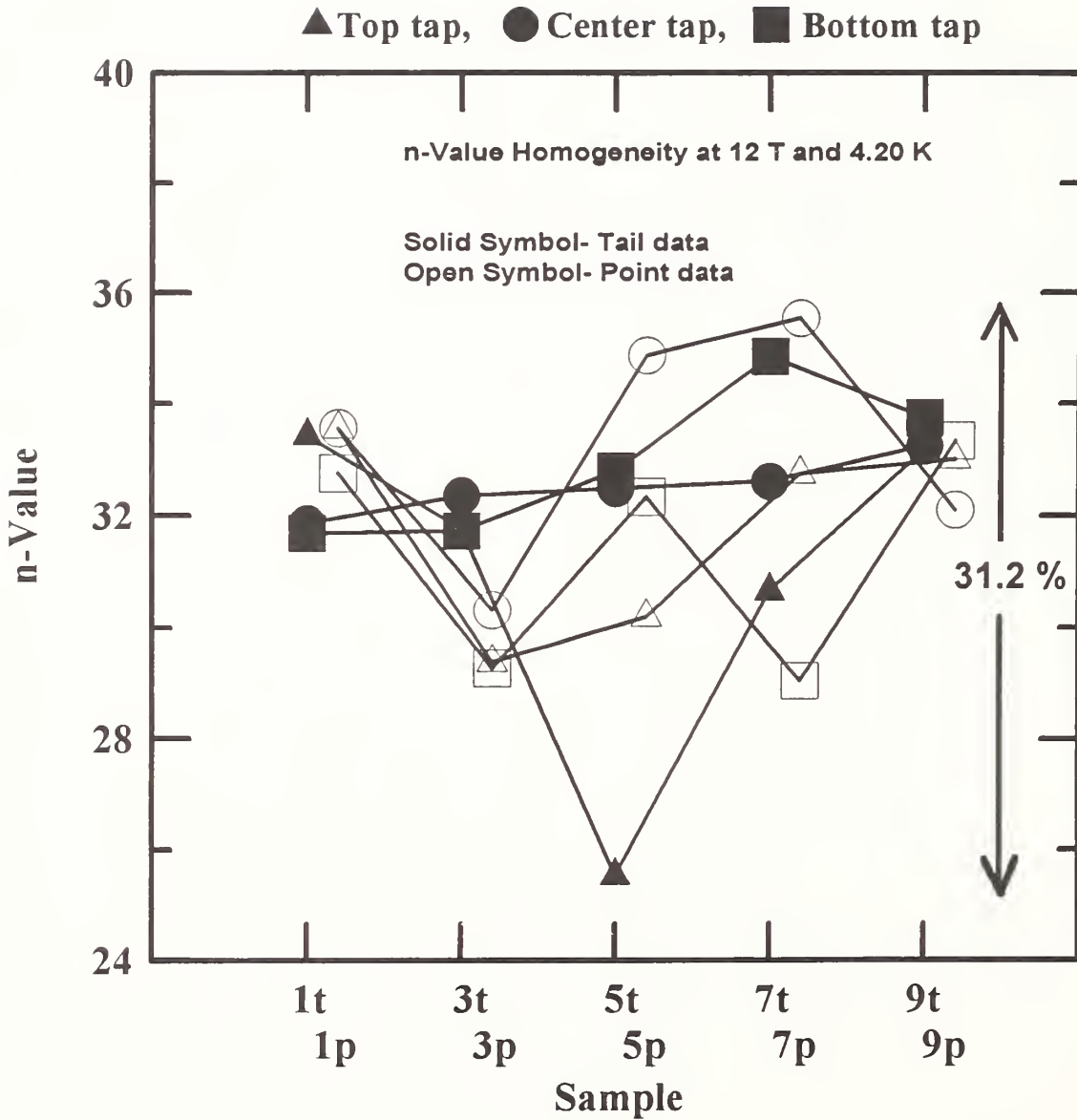


Figure 3-3b. n-values at 12 T, 4.2 K, and 10 $\mu\text{V/m}$ versus sample. Each sample had three pairs of voltage taps.

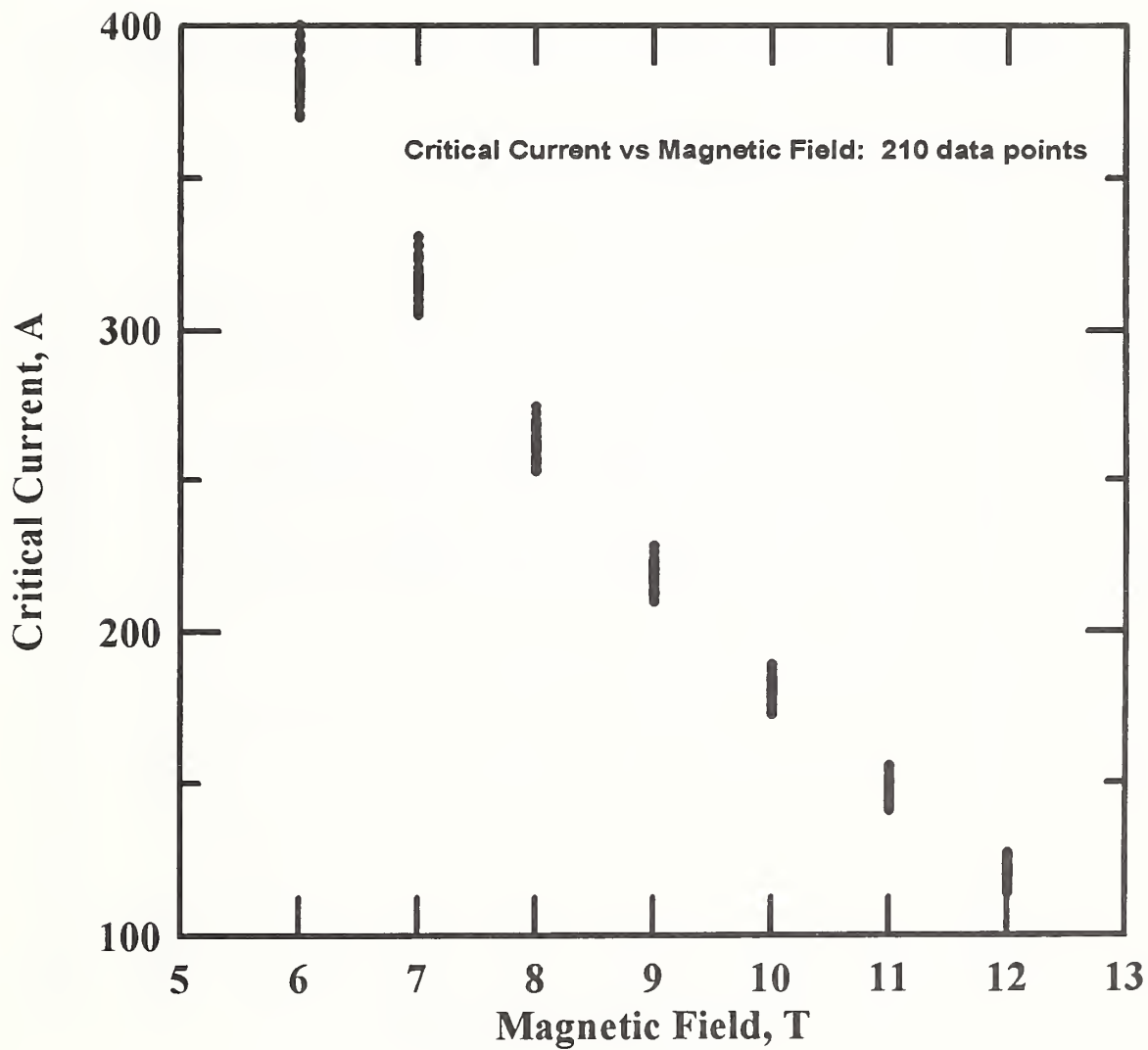


Figure 3-4. Critical current at 4.2 K versus magnetic field for three pairs of voltage taps on each of the ten samples.

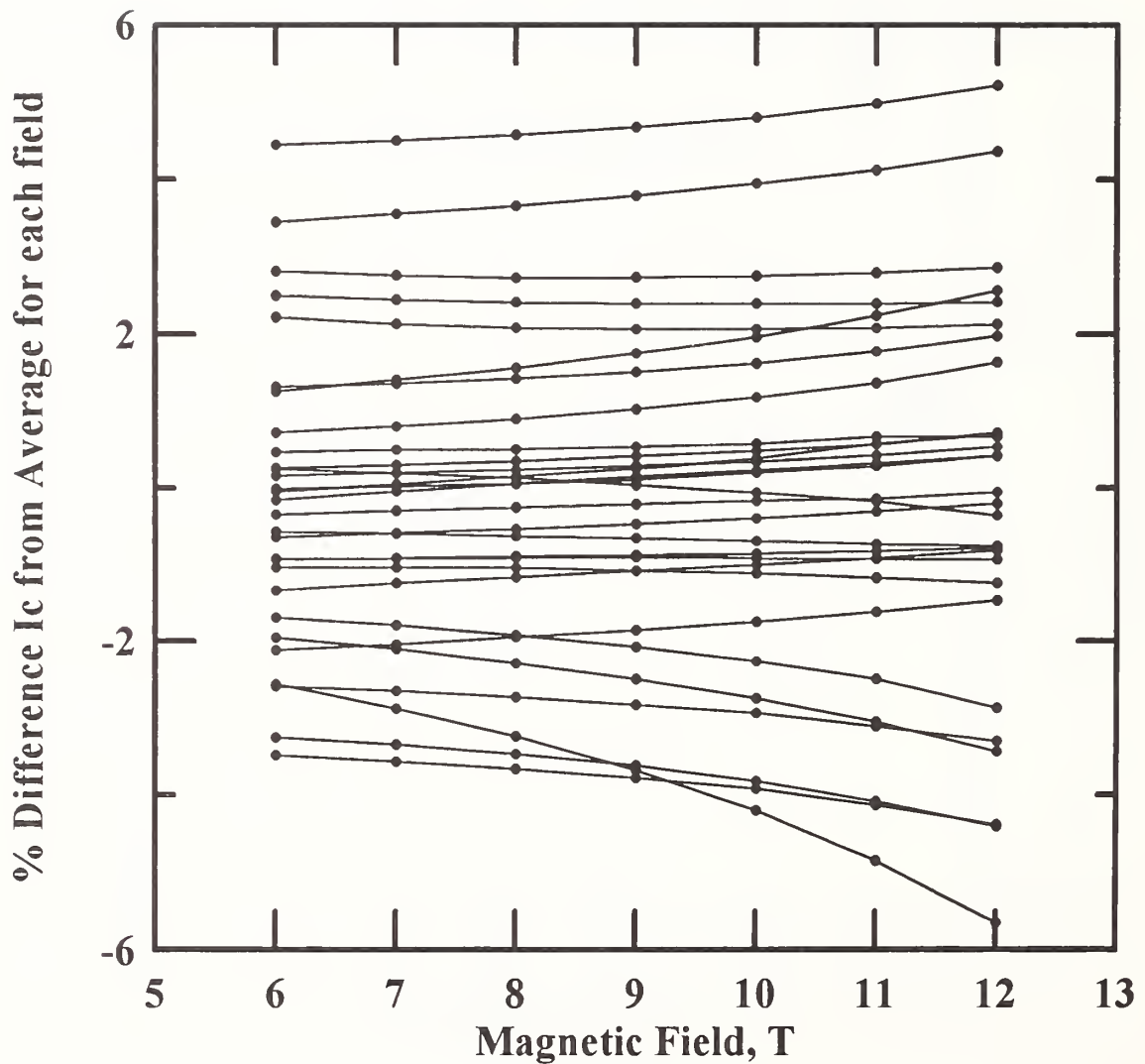


Figure 3-5. Percent difference of critical current at 4.2 K from the average critical current at each field versus magnetic field. The lines connect data points for a given tap on each specimen.

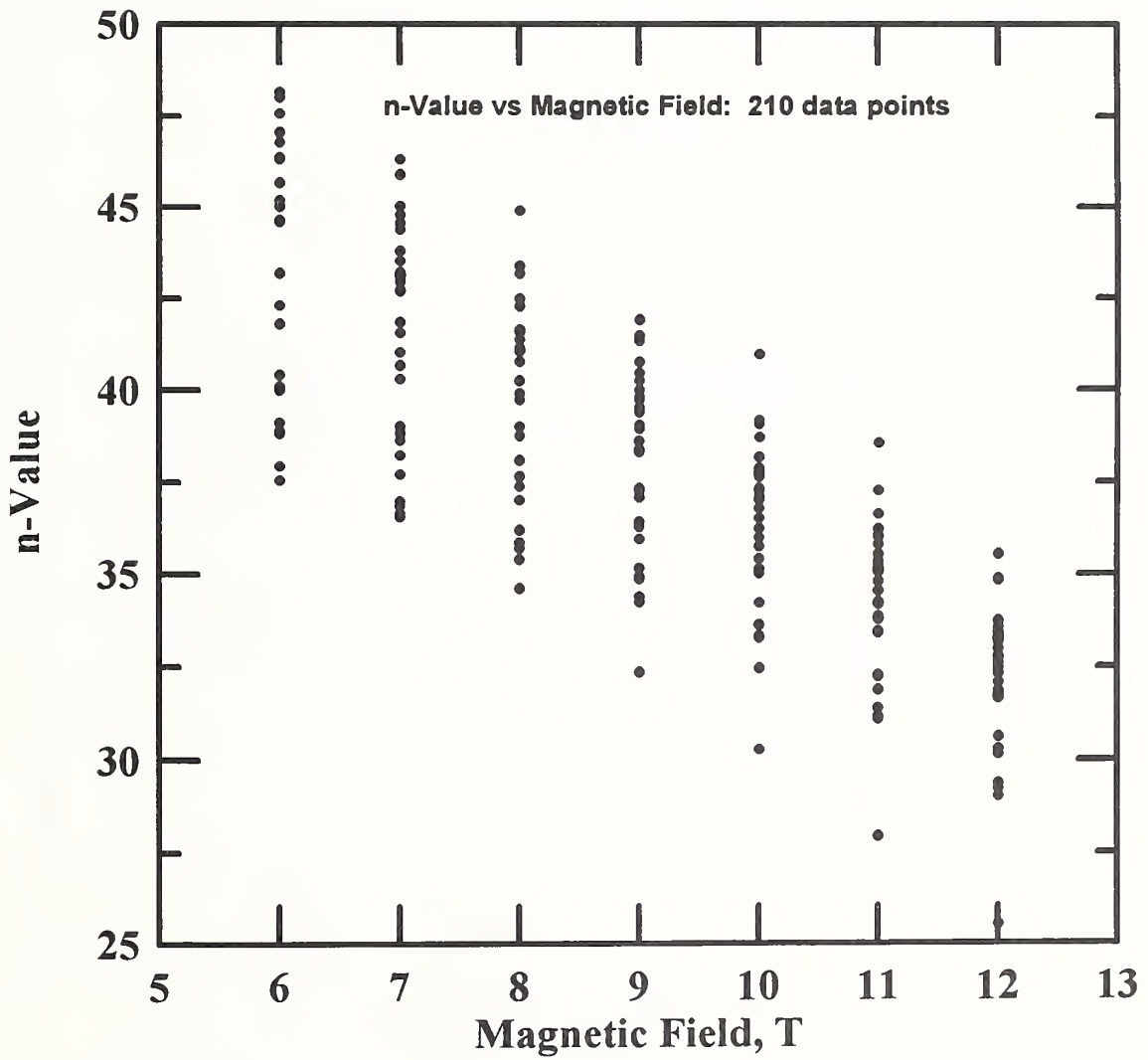


Figure 3-6. n-values at 4.2 K versus magnetic field for three pairs of voltage taps on each of the ten samples.

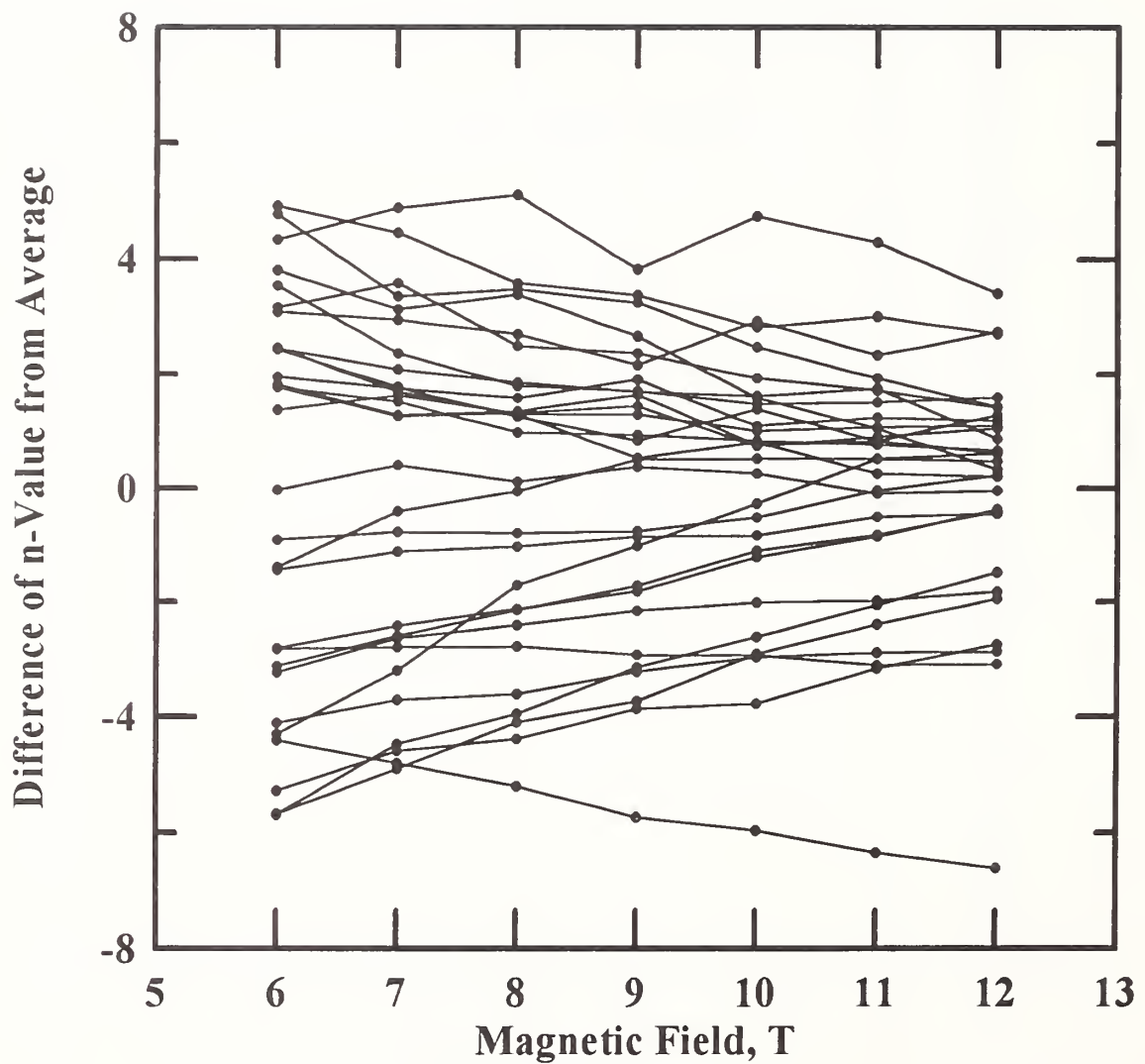


Figure 3-7. Difference of n-value at 4.2 K from the average n-value at each field versus magnetic field. The lines connect data points for a given tap on each specimen.

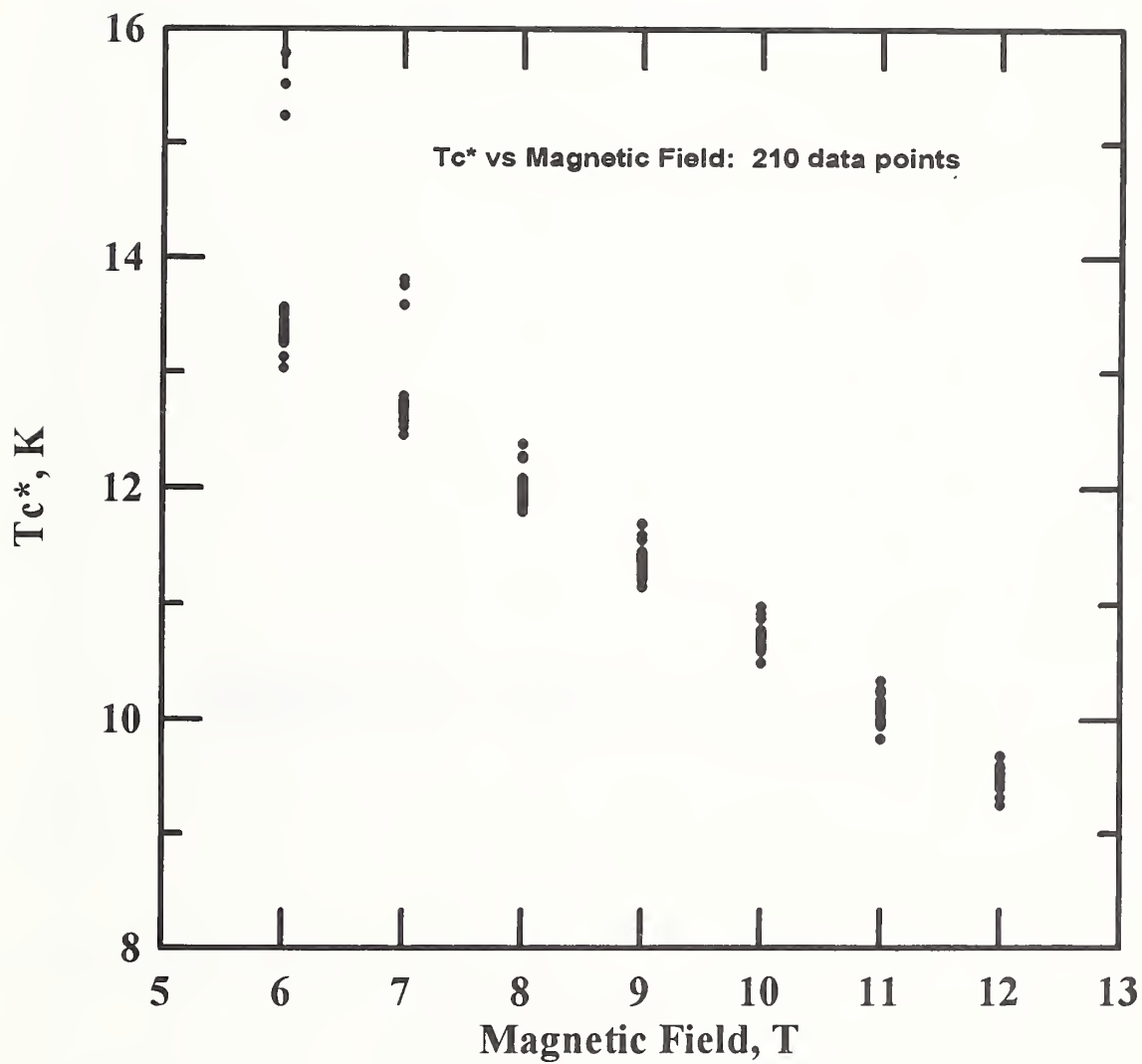


Figure 3-8. T_c^* versus magnetic field for three pairs of voltage taps on each of the ten samples.

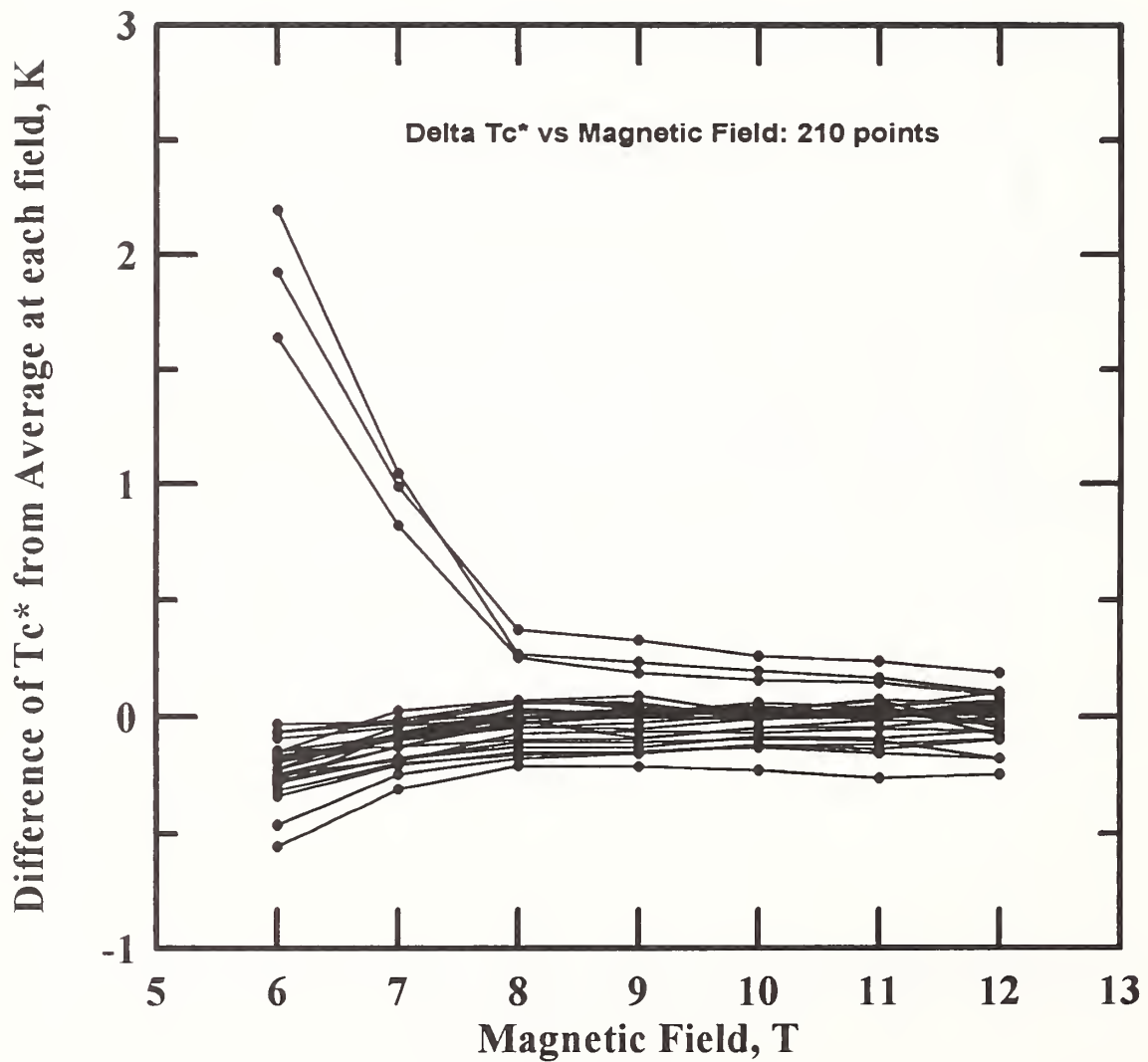


Figure 3-9. Difference of T_c^* from the average T_c^* at each field versus magnetic field. The lines connect data points for a given tap on each specimen. The T_c^* data for three taps on 7t are outliers, possibly due to lack of thermal equilibrium.

4. OBSERVATIONS AND RECOMMENDATIONS ON THE CRITICAL CURRENT MEASUREMENT PROCEDURE

This chapter is a collection of observations and recommendations that we made in our experience using the ITER Standard Critical Current test sample mandrel. This mandrel, adopted by the U.S. ITER Home Team, evolved from the designs used at the University of Wisconsin[1], MIT PFC [2], and Brookhaven National Lab and discussions at U.S. Home Team meetings. The details of the mandrel design and machining drawings were made by Makoto Takayasu (MIT-PFC). A detailed procedure entitled "ITER Critical Current Barrel Assembling" was written by M. Takayasu and R. N. Randall (MIT-PFC). This describes the preparation of the mandrel and sample for reaction and measurement.

4.1 Critical Current Measurement Apparatus

Our measurement apparatus consists of the following parts: G-10 structural tube, 19 mm (3/4 in) brass draw bolt, upper current contact lug, measurement mandrel with copper ring current contacts, lower current contact lug, and a brass nut (see Figure 4-1). The draw bolt is threaded into the G-10 tube and is keyed firmly in position. The G-10 tube also serves as a mounting position for the upper current contact lug and electrically isolates the two current contacts. The brass draw bolt extends through the center of the upper current contact lug, measurement mandrel, and lower current contact lug. An insulating sleeve is placed around the brass draw bolt to keep the stainless steel retaining wire from shorting to the draw bolt. The lower current contact lug is keyed to reduce its rotation about the draw bolt, thus minimizing the transfer of torsional strain to the mandrel or sample when pressure is applied to the system by the brass nut. The lower current contact lug is preloaded by hand with torque in the tight direction to take out the lash in the keyway and reduce the relative motion of the lug and ring when the brass nut is tightened. The lower current contact lug is also held in the tight direction when the brass nut is loosened after the measurements, to again reduce the relative motion of the lug and ring. Using a textbook expression we determined that a 19 mm (3/4 in) diameter bolt torqued to 10.2 N·m (7 ft·lb) produces approximately 2500 N (560 lb) force. We estimate that the differential thermal contraction of the system would produce an additional 156 N (35 lb) of tightening force. The applied force aids in reducing the contact resistance.

Our measurement apparatus also employs two laminated Nb₃Sn and NbTi current leads. One lead is soldered directly to the upper current contact lug of the apparatus. The other lead goes through the center of the draw bolt, the upper current contact lug, measurement mandrel, and lower current contact lug, and is connected to the lower current contact lug with a soldered splice. The splice is necessary for the placement and removal of the lower current contact lug and mounted specimen.

4.2 Current Contacts

Before reaction, the specimen is wound onto the Ti mandrel with approximately 1.5 to 2.5 extra turns around a stainless steel spacer ring on either end of the mandrel. After reaction, in preparation for measurement, the turns at each end are cut so that approximately 3/4 turn of the wire can be soldered with Pb-Sn solder to the Cu current contact ring. This 3/4 turn starts where the wire leaves the end of the grooved mandrel. We use only 3/4 turn to reduce the possibility of persistent current flow in the contact ring.

The total resistance R_c of the current contact needs to be kept low to reduce the ohmic heating of the specimen ends. A significant and variable part of this total resistance is the resistance of the pressure contact between the current lug and the Cu ring. It is important to monitor the total contact resistance as part of the measurement procedure. We used two different techniques for making the pressure contacts.

In one technique, the current contact lugs are tinned with a thin layer of pure In solder; a thick layer of In is soldered onto the specimen's current contact rings and then textured by rolling a knurled tool over it, thus creating a number of well defined ridges. Since the local pressure on these ridges is high, cold welding is promoted. Texturing results in a relatively constant solder thickness. Texturing also breaks up any surface oxide and allows for deformation to accommodate any slight misalignment of the pressure fixture.

The specimen mandrel is then placed onto the measurement apparatus and the draw bolt and nut sandwiches the mandrel with its current contact rings between the current contact lugs of the apparatus. After tightening the mandrel, we allow the In solder to creep for approximately 5 min and then we tighten the nut a second time. Every tightening of this nut is performed with a breakaway torque wrench set at 10.2 N·m (7 ft-lb). Voltage leads from the specimen are then attached to the measurement apparatus. In addition to the three pairs of voltage taps on the specimen, we have a pair with one voltage tap on each Cu ring and a pair with one voltage tap on each lug. Measurements on the lug pair gives the total contact resistance, R_c . Typical values of R_c are 0.5 to 1.5 $\mu\Omega$ (total for both contacts). The power dissipation at 400 A and 1.5 $\mu\Omega$ is 240 mW which is significant; however, this power is not right at the end of the sample, and the copper components will reduce the temperature rise. Typically, the resistance measured on the Cu ring pair is about 0.1 $\mu\Omega$.

In the second technique, the current contact lugs are tinned with a thin layer of pure In solder and the specimen's current contact rings are sanded to a clean Cu surface. This reduces specimen preparation time. The Cu ring is carefully held and the end surface is lapped in a manner to reduce the force and torque on the specimen. This is done with fine-grit paper after the specimen is soldered on. After sanding, the ends of the Cu rings are cleaned with alcohol. Typical values of R_c are 0.5 to 4 $\mu\Omega$. This larger range of values may limit the measurement current to values less than 400 A. Periodic reflowing and cleaning of the In solder on the current lugs may lower

the contact resistance. We did this after every fourth specimen and we observed a trend of increasing R_c with the aging of the In.

The first technique requires careful soldering of the pure In on the end of the Cu ring without unsoldering the Pb-Sn joint that would result in a loss of specimen tension on the mandrel. Reusing the Cu rings can also require that the solders be cleaned off to avoid mixing of the two solders. These complications are avoided in the second technique.

4.3 Electrolytic Method for Removing Cr Plating from Reacted Nb₃Sn Wires

We used an electrolytic oxalic acid bath [3] to etch the Cr coating off of the 3/4 turn current contact region of each end of the wire. The bath was constructed using a stainless steel bath assembly, stainless-steel painted end cap, and a power supply limited at 6 V and 1 A (see Fig. 4-3). The cathode for the electrolytic etch consisted of the bath assembly in electrical contact with the end cap. The anode was the specimen itself; the positive terminal of the power supply was soldered to a small filed spot on the conductor. Lacquer was used to electrically isolate the mandrel from the stainless-steel end cap (cathode) as well as isolating the specimen (anode) from the end cap. The oxalic acid solution was composed of 10 g of oxalic acid and 100 ml of distilled water. The oxalic acid solution was placed in the bath using an eye-dropper to a level that would safely etch the current contact region of the specimen without coming in contact with the Ti mandrel. The mandrel is placed into the end cap, thus allowing the sample to be immersed in the oxalic acid solution. There is no sign of chemical activity until the current is turned on. When the current is applied, a violent fizzing ensues for about 2 min, after which the current drops, indicating that the Cr is fully etched. We think that the acid does not etch the Cu sample appreciably. This process is repeated for the other end of the specimen. The entire specimen and the mandrel are then immersed into a soap bath in an ultrasonic cleaner to remove the Cr etch waste material. In some cases, we etched the specimen again after the cleaning. The sample is then ready for soldering onto the Cu current contact rings.

We have not performed conclusive tests on this process nor studied the relative merits of this process compared to mechanical abrasion or HCl etching. The electrolytic oxalic acid etch removes the Cr effectively with little risk of sample damage and yields a low contact resistance joint.

4.4 Superconductivity of the Ti-6Al-4V Measurement Mandrel

We discovered in this study that the Ti-6Al-4V measurement mandrel itself is superconducting at 4.2 K and at magnetic fields below 2 T. Therefore, reliable I_c measurements can be obtained only at magnetic fields higher than 2 T at 4.2 K with this mandrel material. Each element of this alloy is superconducting at some temperature according to the textbooks (Ti:0.4 K, Al:1.2 K, and V:5.3 K). Vanadium is the element of concern, but it is a minority component of the alloy which makes

the transition temperature of the alloy hard to predict. We ran experiments on annealed and unannealed mandrels to determine the critical current and resistance at magnetic fields of up to 12 T.

Our measurements of critical current and resistance were made on actual machined mandrels that were thought to be more direct than a calculation based on measurements on a more nearly ideal specimen geometry. The more nearly ideal specimen geometry would neglect to account for the deep spiral groove and machining effects. The short cylinder geometry of the mandrel and the fact that contacts could not be soldered to the mandrel severely limited the accuracy of the measured resistance values due to uncertainty in the distribution of the current density. An alternative approach to measuring the resistance may be to take a slice of the mandrel material that is more suitable for resistivity measurements instead of measuring the entire mandrel. This may yield more accurate measurements.

We normalized the measured values of resistance in order to compare the two materials and their transitions. The normalized resistance R_n is the measured resistance divided by the normal state resistance, expressed in percent. The values that we obtained for the normal state resistance of voltage taps separated by 1.27 cm were: 160 $\mu\Omega$ for annealed at 4.0 K and 4.2 K and 95 $\mu\Omega$ for the unannealed at 4.2 K. The difference between these two normal state resistance values is likely due to systematic differences in the current distribution in these two measurements. Tables 4-1 and 4-2 give the critical current and normalized resistance values for an annealed mandrel in fields of 0 to 8 T at 4.0 K and in fields of 0 to 4 T at 4.2 K respectively. Table 4-3 gives the I_c and R_n values for the unannealed mandrel material in fields of 0 to 12 T at 4.2 K. I_c values are listed at two criteria, 1 and 10 $\mu\text{V}/\text{cm}$. R_n values are listed at three current levels: 1, 10, and 50 A. There was negligible change in resistance above 4 T.

Annealing the alloy could change the morphology of the alloy and/or reduce the pinning force; thus lowering the measured critical current significantly. For example, in zero field at 4.2 K, the annealed mandrel had a critical current of 0.56 A while the unannealed mandrel had a critical current of greater than 112 A. The shunt path through the mandrel is much shorter than the spiral path of the superconducting wire, which is why the high criteria of 1 and 10 $\mu\text{V}/\text{cm}$ were selected for these measurements. The n-value of the mandrel is very low, which makes the I_c at 10 $\mu\text{V}/\text{cm}$ much higher than at 1 $\mu\text{V}/\text{cm}$.

Another factor in considering how much current will flow through the mandrel during a measurement of superconductor wire is the contact resistance between the Cu ring and the mandrel. This contact resistance was observed to be as high as 300 $\mu\Omega$ even when the surfaces of the mandrel were cleaned. If superconducting wire was diffusion bonded to the mandrel during the heat treatment, this contact resistance would be much lower.

One possible alternative material is Ti-5Al-2.5Sn. The T_c of Sn is 3.7 K; thus this alloy should not be superconducting at temperatures above 3.7 K. The thermal contraction of this alloy is

about 0.15% from 293 to 4 K. The availability, machinability, oxidation, and high temperature properties would need to be determined.

4.5 Critical Current Measurements on the Nb-Ti Wire SRM-1457

We made I_c measurements on the Nb-Ti wire Standard Reference Material (SRM-1457) which we mounted on the Ti alloy mandrel to compare to previous measurements on a G-10 mandrel. A summary of a number of I_c measurements is given in Table 4-4 and percentage differences from the reference data are plotted in Figure 4-4. The reference data in column 2 of the table are NIST measurement on SRM-1457 mounted on the G-10 mandrel used in the 1990-91 Versailles Project on Advanced Materials and Standards (VAMAS) interlaboratory comparison [4]. The average results of 12 laboratories in VAMAS comparison are within 0.5% of the reference data. The two runs of one specimen on a Ti alloy mandrel are systematically higher, within about 0.6%. The difference between the two runs was less than 0.05% showing the repeatability of the I_c measurements on the Ti mandrel and the potential use of such specimens for precise interlaboratory comparisons. The results on the second specimen on the Ti mandrel were slightly higher, about 0.2%, than the first and had a similar systematic trend with magnetic field. The G-10 mandrel, on which the reference data was taken, had a smaller diameter (25 mm) than the Ti alloy mandrel (32 mm), which could contribute to the observed differences. All of these differences are well within the uncertainty of the measurements and the variability of the SRM.

A summary of the measured n -values corresponding to the above I_c s is given in Table 4-5 and the n -value differences relative to the reference data are shown in Figure 4-5. The n -values measured on the Ti alloy were somewhat lower than the reference data which was obtained on a G-10 mandrel. The significance of this difference is not known because of systematic differences in the data acquisition and the determination of the n -value.

An I_c measurement was made on the SRM at 12 T to determine the possible effect of current sharing between the Nb-Ti sample and the Ti alloy mandrel. The measured I_c was approximately 13 mA at 10 μ V/m, which indicates that there is very little current sharing.

4.6 Observations on the Standard Specimen Mandrel

Some observations were made concerning the design and use of the Ti alloy specimen mandrels. The design of a mandrel that will be used for sample reaction and subsequently for measurement is challenging. Furthermore, there is a trade off between the complexity of the design and the ease of use and fabrication.

The quality of the fit of the current contact ring onto the barrel (main tube) is critical to preventing specimen damage. A stainless steel retaining pin is used to hold the Ti spacer rings in place on

the barrel during reaction as well as holding the copper terminals on the barrel for measurement. The retaining pin goes across the diameter of the barrel and pins the spacer or copper rings at points 180° apart from each other. This pin is shaped like the capital Greek letter omega (Ω). Since the pin cannot be absolutely tight in the pinholes, there is room for the rings to move, either in a rocking motion or a slight rotation. Three situations were observed in which the specimen was damaged because the current contact ring was not fitted correctly.

There was a random phase relation between the pinhole locations and the region where the specimen leaves the barrel and goes onto the contact. If the two are out of phase with each other, a rocking motion might damage the specimen; this situation would be extreme when the phase difference is 90° . We observed specimen damage on a mandrel that had a large rocking latitude on one current contact ring. The damage was between this ring and the nearest voltage tap and this damage limited the measurement current through the specimen. Also, if care is not taken in winding the specimen onto the mandrel before reaction, the rocking motion may cause a small diameter specimen to fall between the end of the grooved barrel and the spacer ring, changing its shape. This has happened, and the reshaping of the specimen may have caused damage.

Another situation arose with a specimen in which the retaining wire had missed the pinhole in the barrel, before the reaction, and only went through the pin hole in the spacer ring. As a result, the spacer ring was tilted, and there was a large gap between the ring and the barrel. The specimen fell into this gap when it was wrapped onto the mandrel and it was reacted to that shape. The current contact could not be put on without moving the specimen from its reacted position to conform to the current contact, which resulted in damage to the specimen.

Another situation occurred because there was a slight rotation between the barrel and copper ring which caused the specimen to loosen itself on the barrel. To counter this effect the copper ring can be preloaded, before soldering, in a manner to remove the rotational slack that otherwise would release specimen tension.

A modification that would reduce the effect of all three of these situations would be to add a second omega-shaped pin 90° out of phase with the first. This may or may not be easy to implement now.

Several specimens bonded to the mandrel during instrumentation. In these cases the specimen was slightly uncoiled to break the bonds to the mandrel. Although great care was taken in breaking the specimen away from the mandrel, the specimen may have experienced some damage. As the mandrels are used repeatedly, their oxidation may become more complete, resulting in less bonding.

4.7 References

- [1] Meingast, C; Larbalestier, D.C. J. Appl. Phys. **66**, p 5971; 1989.
- [2] Takayasu, M.; Gung, C.Y.; Steeves, M.M.; Hoenig, M. O.; Hale, J. R.; Smathers, D. B. IEEE Trans. Mag., **27**, No. 2, p. 1767; 1991.
- [3] Petzow, G. "Metallographic Etching," American Society for Metals, p. 57; 1978.
- [4] Wada, H.; Itoh, K. *Cryogenics ICMC Supplement* **32**, p. 557; 1992.

Table 4-1. Critical current and resistance values of annealed/oxidized Ti-6Al-4V measurement mandrel material @ 4.0 K.

$\mu_0 H$, T	I_c (1 $\mu V/cm$)	I_c (10 $\mu V/cm$)	R/R_n @ 1 A	R/R_n @ 10 A	R/R_n @ 50 A
0	0.56 A	1.91 A	2.5 %	8.8 %	14 %
0.5	0.27 A	1.17 A	6.3 %	14 %	26 %
1	0.18 A	0.89 A	8.8 %	20 %	35 %
1.5	0.13 A	0.69 A	13 %	26 %	47 %
2	0.08 A	0.52 A	18 %	33 %	70 %
2.5	0.028 A	0.26 A	34 %	52 %	93 %
3	0.011 A	0.11 A	74 %	83 %	99 %
4		0.08 A	100 %	100 %	
8			100 %	100 %	

Table 4-2. Critical current and resistance values of annealed/oxidized Ti-6Al-4V measurement mandrel material @ 4.2 K.

$\mu_0 H$, T	I_c (1 $\mu V/cm$)	I_c (10 $\mu V/cm$)	R/R_n @ 1 A	R/R_n @ 10 A	R/R_n @ 50 A
0	0.35 A	1.64 A	3.1 %	10 %	16 %
0.5	0.21 A	1.01 A	7.5 %	17 %	31 %
1	0.13 A	0.74 A	12 %	24 %	46 %
1.5	0.083 A	0.52 A	18 %	34 %	71 %
2	0.024 A	0.24 A	38 %	54 %	93 %
2.5	0.010 A	0.10 A	77 %	86 %	99 %
3	0.0082 A	0.081 A	98 %	99 %	99 %
4	0.0079 A	0.079 A	100 %	100 %	99 %

Table 4-3. Critical current and resistance values of unannealed Ti-6Al-4V measurement mandrel material @ 4.2 K.

$\mu_0 H$, T	I_c (1 $\mu V/cm$)	I_c (10 $\mu V/cm$)	R/R_n @ 1 A	R/R_n @ 10 A	R/R_n @ 50 A
0	>112 A				0.0002 %
0.5	> 80 A	>80 A			0.0002 %
1	40 A	56 A		<0.0005 %	0.11 %
1.5	3.6 A	9.8 A	<1.1 %	1.1 %	74 %
2	0.072 A	0.67 A	20 %	39 %	96 %
2.5	0.017 A	0.17 A	80 %	89 %	99 %
3	0.013 A	0.13 A	97 %	89 %	100 %
3	0.012 A	0.13 A	100 %	100 %	100 %
8	0.015 A	0.13 A	100 %	100 %	100 %
12	0.015 A	0.13 A	100 %	100 %	100 %

Table 4-4. Critical current measurements on SRM-1457.

Field	Reference data	VAMAS average	Specimen 1 run A on Ti	Specimen 1 run B on Ti	Specimen 2 run A on Ti
2	295.84		296.415	296.453	297.123
3	229.8		230.144	230.197	230.491
3	186.88		187.068	187.063	187.335
5	153.17		153.343	153.343	153.579
6	123.34	122.691	123.703	123.721	123.926
7	95.46	95.255	95.857	95.899	96.089
6	68.16	68.107	68.521	68.521	68.741
9	40.9	40.83	41.156	41.171	41.356

Table 4-5. n-Value measurement on SRM-1457.

Field	Reference Data	VAMAS average	Specimen 1 run A on Ti	Specimen 1 run B on Ti	Specimen 2 run A on Ti
2	58		55.95	56.72	55.77
3	58		55.03	55.95	54.63
3	58		53.97	54.65	53.4
5	57		51.85	52.41	51.49
6	53	54.28	48.75	49.37	48.58
7	49	45.62	44.19	43.91	43.64
6	42	40.06	36.78	36.91	36.31
9	30	28.39	26.83	26.32	26.32

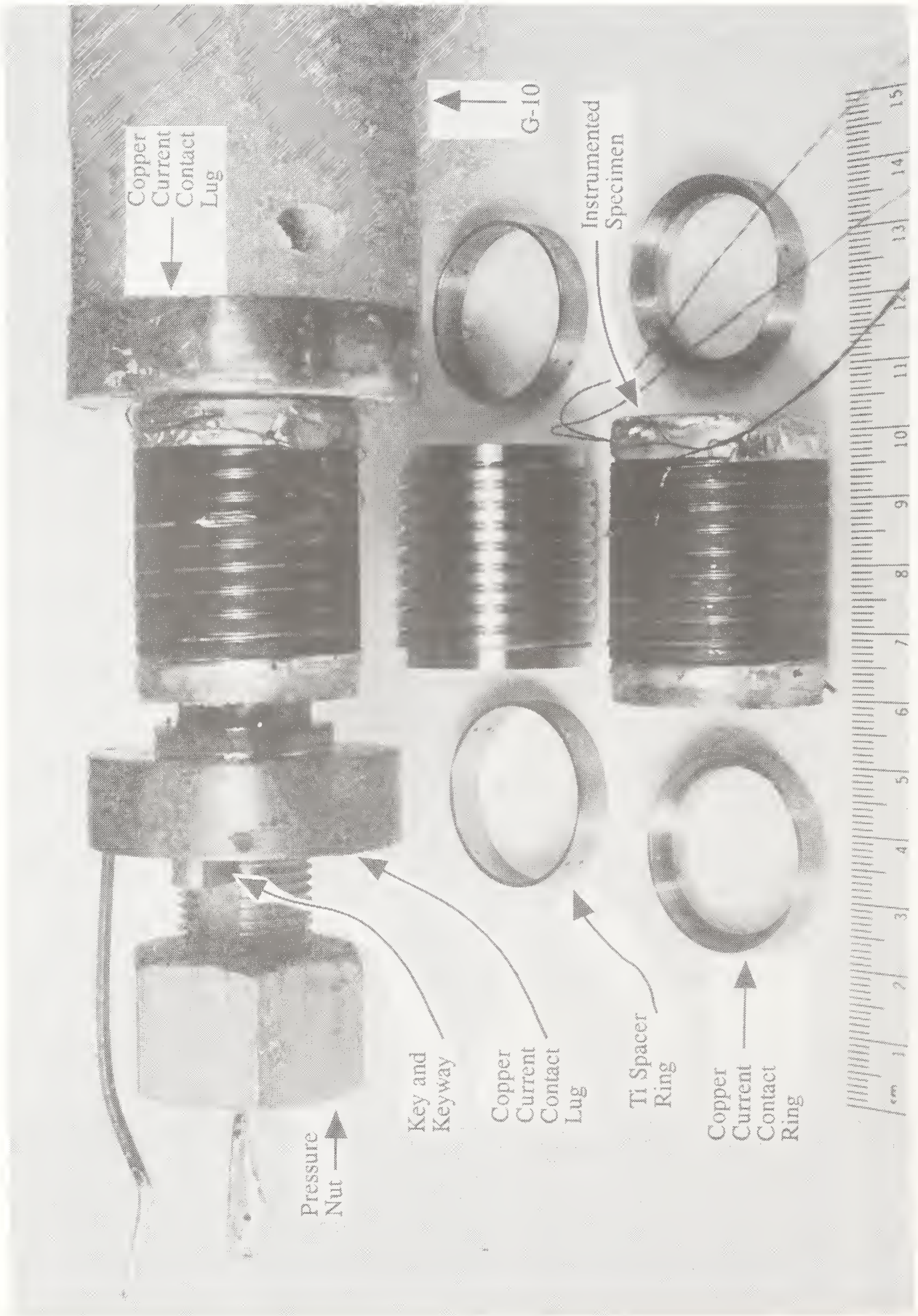


Figure 4-1. Photograph of the test fixture with an exploded view of the mandrel parts. The test fixture is partially assembled to show the key and keyway that reduce the torque transmitted to the instrumented specimen.

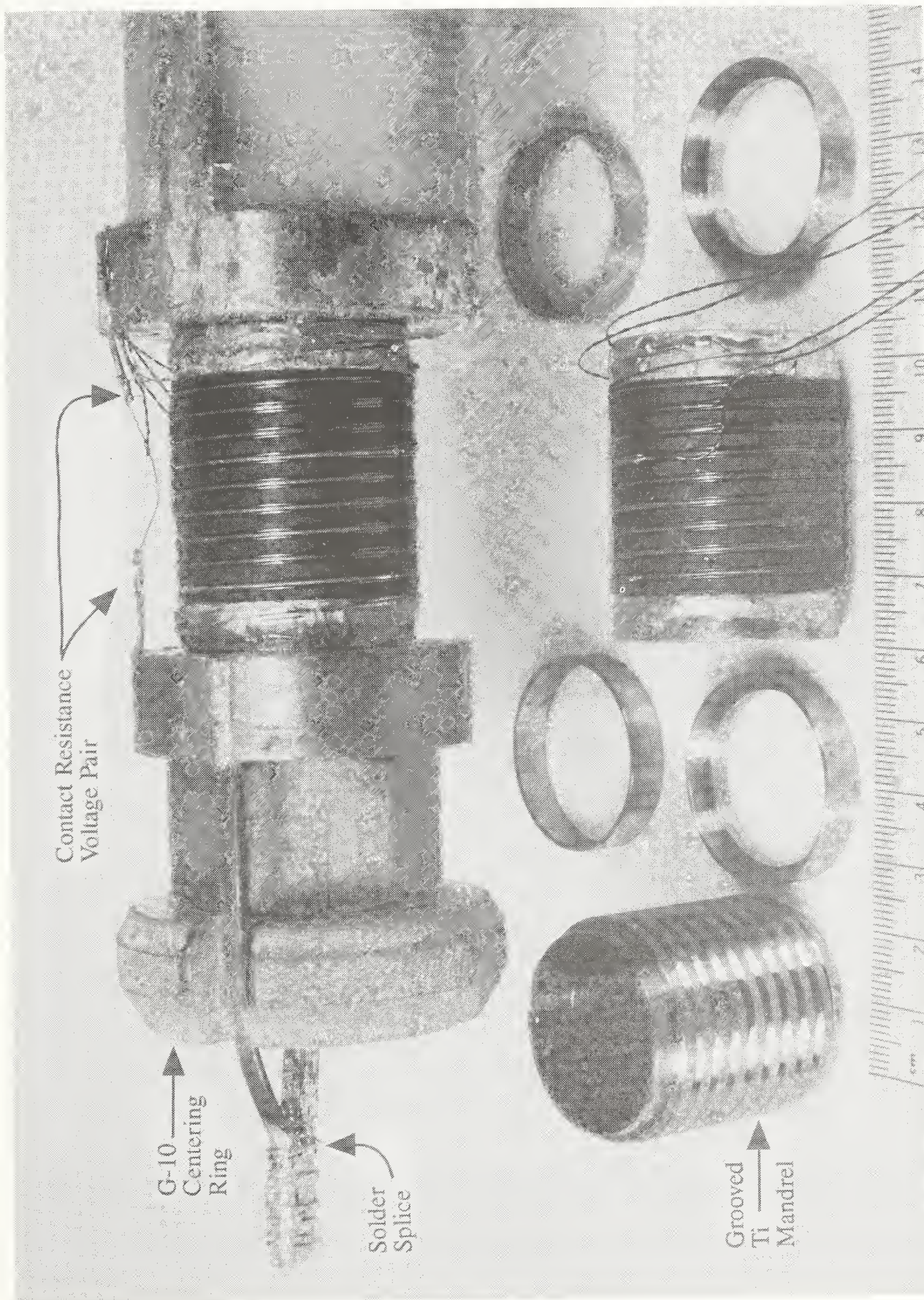


Figure 4-2. Photograph of the fully assembled test fixture with an exploded view of the mandrel parts.

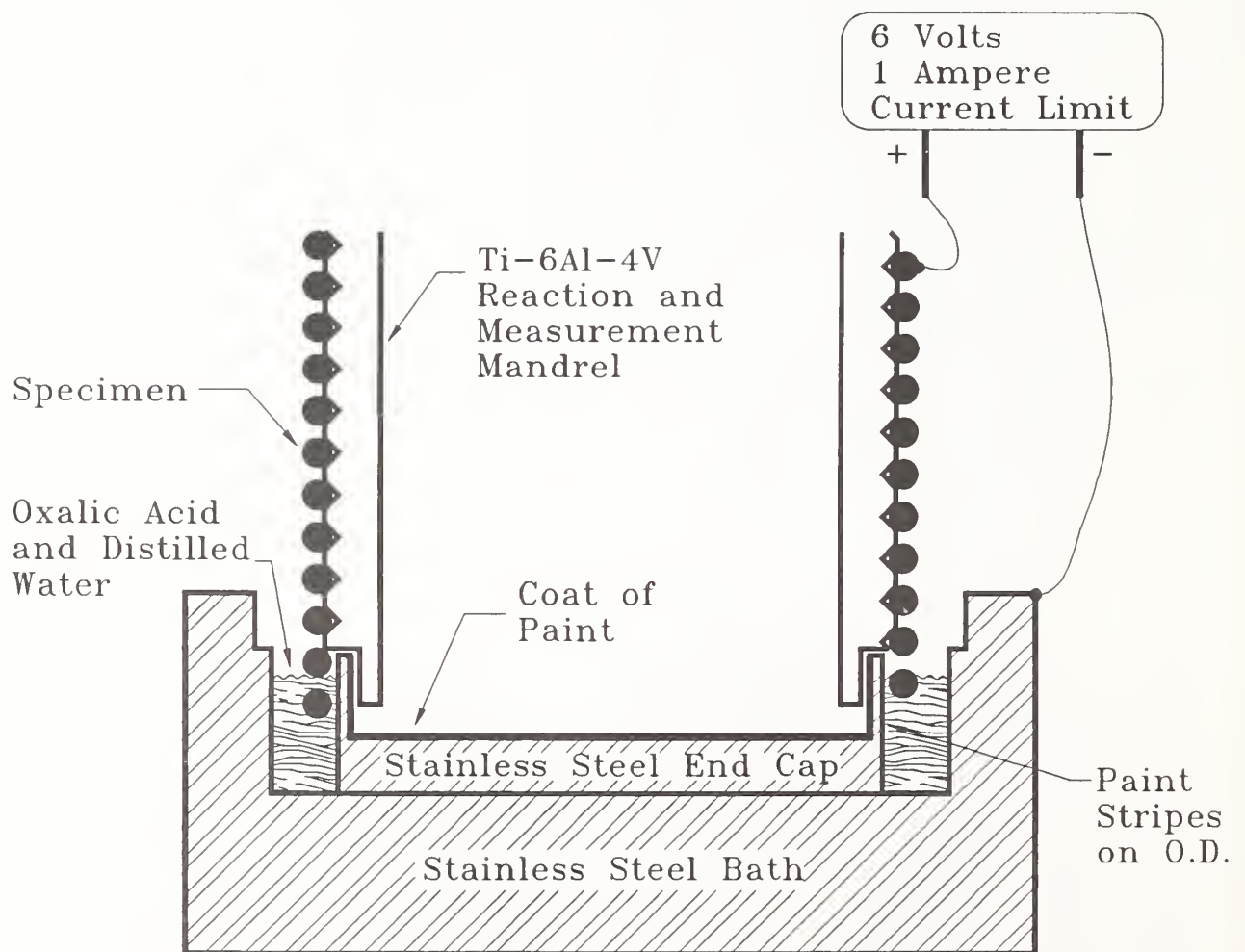


Figure 4-3. Illustration of the electrolytic etch used to remove the chrome plating from the current contact region of the Nb_3Sn wire.

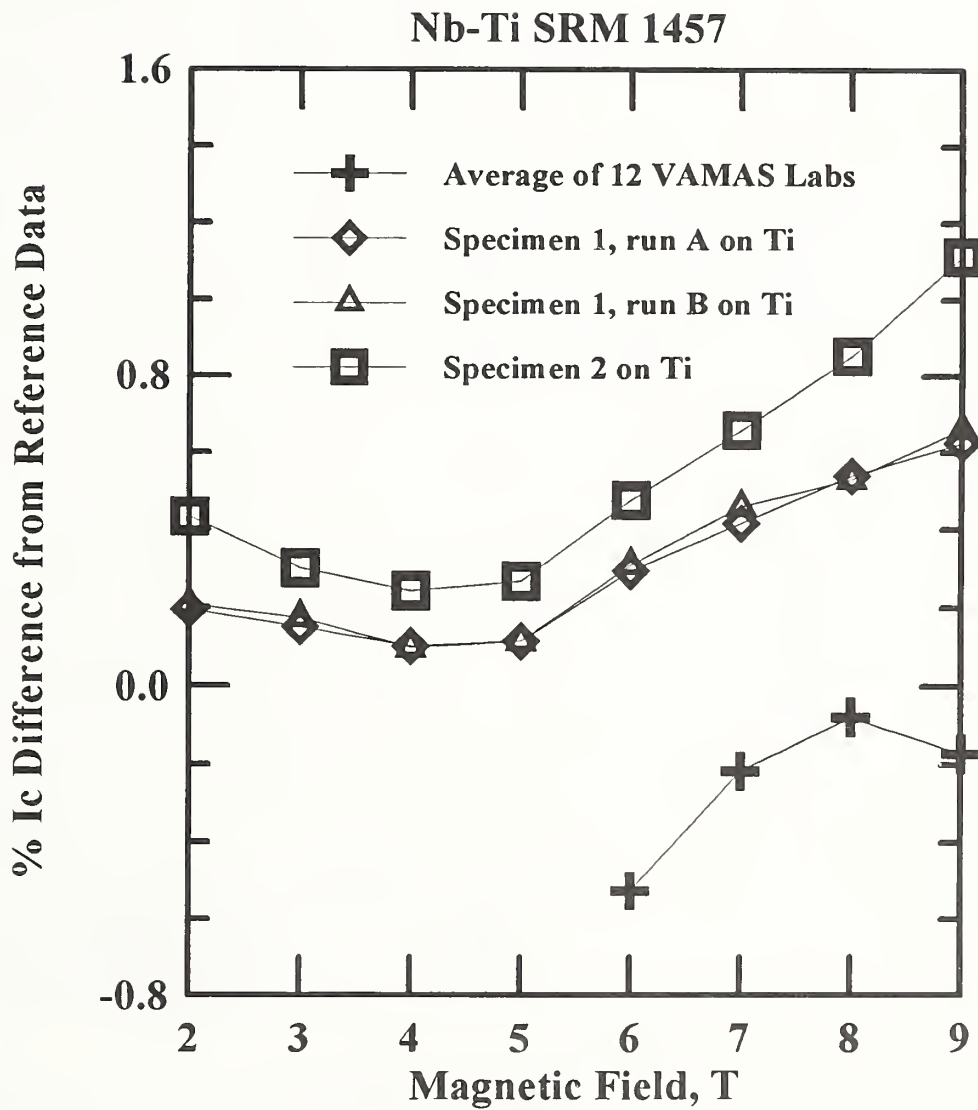


Figure 4-4. Percent difference of critical current from the reference data versus magnetic field for a number of measurements on the Nb-Ti SRM-1457.

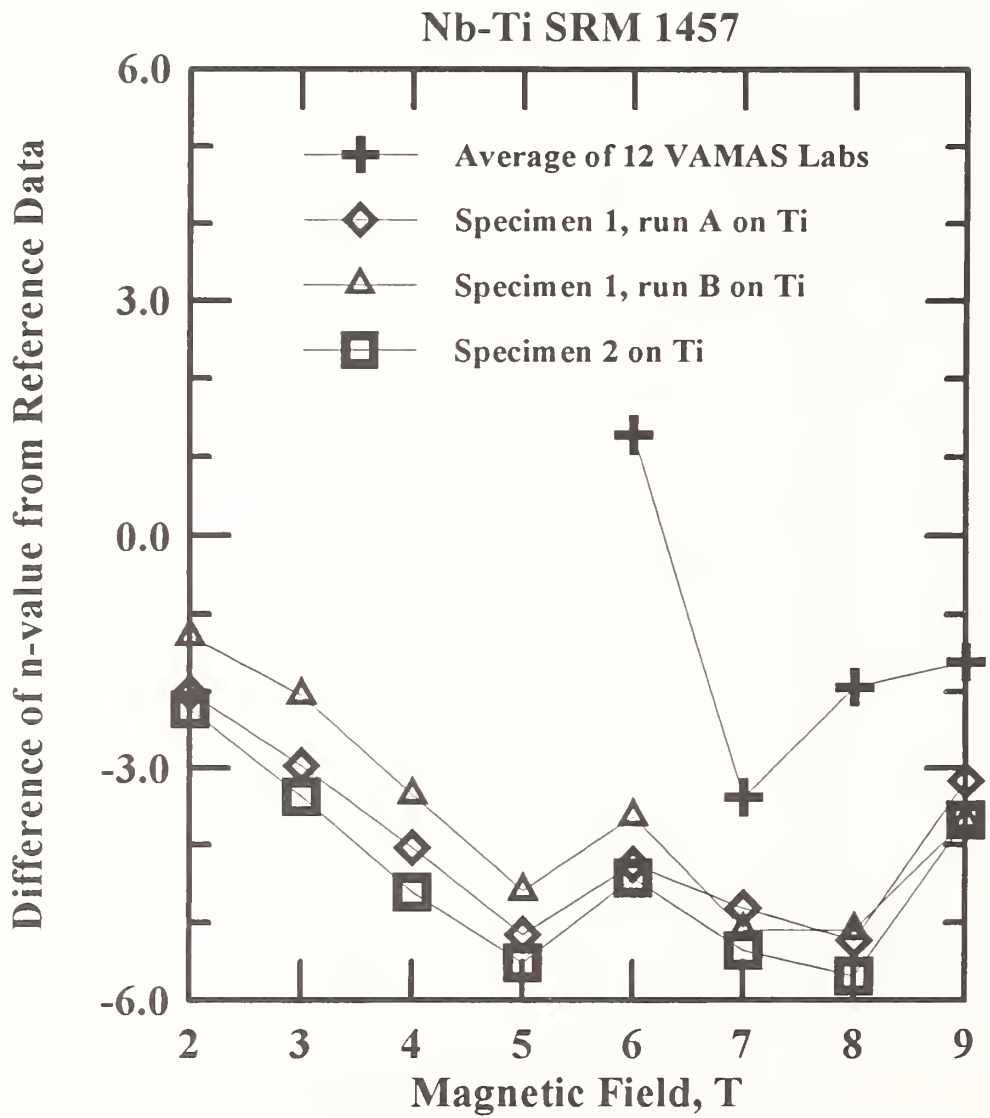


Figure 4-5. Difference of n-value from the reference data versus magnetic field for a number of measurements on the Nb-Ti SRM-1457.

5. COMMENTARY ON A Nb₃Sn REFERENCE WIRE

5.1 Introduction

This is a requested commentary on the advantages and disadvantages of creating a Nb₃Sn Reference Wire (RW) and a recommendation. The timely development of a standardized I_c measurement methodology for Nb₃Sn superconducting wire is essential for acceptance testing and quality assurance of the strand procurement program. The question is, does this include the creation of a Nb₃Sn RW or not? A Nb-Ti Standard Reference Material (SRM) for the measurement of critical current (I_c) exists already; however, there are significant differences between Nb-Ti and Nb₃Sn conductors in sample preparation, performance, and strain sensitivity.

The existing Nb-Ti I_c SRM (SRM-1457) was created at NIST and made available in 1984. This SRM has been well accepted by the superconductivity community: over 200 units have been sold, approximately half to foreign laboratories. It has been used in a number of interlaboratory comparison of I_c measurements. It was used as a control sample in the latest Versailles Project on Advanced Materials and Standards (VAMAS) interlaboratory comparison of I_c on Nb₃Sn wires.

It is helpful to compare the possible use of a Nb₃Sn RW to the present use of the Nb-Ti SRM. The existing Nb-Ti SRM is used to ensure the integrity of the measurement system. For example, one U.S. superconducting wire manufacturer measures a Nb-Ti SRM sample after every 20 measured test samples. A single Nb-Ti SRM unit can be used repeatedly and provides a fairly complete evaluation of the measurement system. In contrast, multiple use of a mounted Nb₃Sn RW would only address a portion of the Nb₃Sn measurement variables. This necessitates an evaluation schedule that includes some re-testing of old units and the incorporation of new units. The envisioned strand test plan for ITER will require testing from several hundred to a thousand samples each year. If a Nb₃Sn RW is used at the same rate as the Nb-Ti SRM, this would consume nearly 50 units per year. A repeatability study of the RW should be performed in order to determine the total number of units and estimated cost.

Although a SRM is the ultimate physical standard, a Nb₃Sn I_c RW may be more appropriate for this application and the cost of development would be lower. The additional complications and sensitivities of the I_c of a Nb₃Sn wire do not favor an attempt to make a fully certified SRM. There is also a lingering question about the ultimate homogeneity of a Nb₃Sn wire.

5.2 Advantages

- The significant differences between Nb₃Sn and Nb-Ti wires require that a new RW for Nb₃Sn I_c measurements be developed in order to verify the precision and accuracy of Nb₃Sn I_c measurement systems. Unlike Nb-Ti, Nb₃Sn superconducting wire requires heat treatment on a reaction mandrel and is extremely sensitive to mechanical strain. Thus the choice of reaction

and measurement mandrels, as well as the measurement technique, is an important factor in reducing measurement variability for the Nb₃Sn RW.

- A Nb₃Sn RW would provide a means for periodic checks of the detailed measurement procedure without conducting a full-scale interlaboratory comparison. A Nb₃Sn RW could also provide a more precise check. During the second VAMAS international interlaboratory comparison of critical-current measurements on Nb₃Sn conductors, a standardized test procedure which specifies the sample geometry, reaction and measurement mandrel geometry, and other details of the measurement yielded results with significantly lower variability than the first comparison. The results of the second study do not preclude other procedures that would yield sufficiently consistent results. A general result of these interlaboratory comparisons was the strong need for a detailed procedure. The results from the first ITER Benchmarking Test on I_c were consistent with this need. The largest difference in the average I_c measurements of two ITER laboratories that did not use a common procedure was 23%. The largest difference in the average I_c measurements of two ITER laboratories that did use a common procedure was 6.5%. There is still room and perhaps a need for improvement in the consistency of I_c measurements.
- The research conducted during the development of a Nb₃Sn RW would also provide an in-depth analysis of the state-of-the-art materials. This could include: short- and long-range inhomogeneity, dependence on magnetic field from 6 to 14 T, dependence on temperature from 4.0 to 4.4 K, dependence on criteria (1 to 10 μV/m), dependence on voltage tap separation (5 to 75 cm), dependence on reaction parameters, dependence on reaction and measurement mandrel materials, dependence on mounting procedure and the level of measurement variability. This would offer insight into reducing the variability and developing a standard measurement methodology for improving the repeatability of the critical-current measurement on Nb₃Sn superconducting wires.

5.3 Disadvantages

- The present state-of-the-art materials may not provide a suitably low variability to serve as a RW.
- If the resources are not available to complete the creation of a Nb₃Sn RW, it should not be started. This will be a fairly large project, so there may be better projects to invest in.
- If the NIST Office of Measurement Services (formerly Office of Standard Reference Materials) is involved in the creation of this RW, they will set the unit price. The cost is the same to everyone; an agency that helped create them pays the same as a foreign laboratory.

5.4 Recommendation

If there is a need for higher accuracy and reliability in Nb_3Sn I_c measurements, then invest in a Nb_3Sn I_c Reference Wire. If this need is less than the benefit of using the limited resources on other projects, then do not start on a Nb_3Sn RW.

Appendix A.

STANDARDIZED LABORATORY REPORTING SHEETS

By request, we drafted a standard reporting sheet, distributed it to a total of nine U.S. measurement laboratories for comments and completion, and compiled the information received from seven laboratories as they were provided to us. This serves to document the present procedures that are being used for Nb₃Sn I_c measurements. This reporting sheet included measurement conditions, calibration method,¹ sample heat treatment, measurement mandrel and mounting details, and measurement results. Possible changes to this sheet were suggested by some of the labs and included are two possible new versions of the last page of the reporting sheet, 4a and 4b. Sheet 4a is designed for reporting measurement results on a number of samples at one magnetic field. Sheet 4b is designed for reporting measurement results on one sample at magnetic fields of 6 to 14 T.

¹Certain commercial products are identified by the participants to adequately describe their experimental procedure completely. In no case does such identification imply recommendation or endorsement by NIST, nor does it imply that the products are necessarily the best available for the purpose.

DATA FORMAT SHEETS

INSTITUTE Francis Bitter National Magnet Laboratory (FBNML)

Sheet-1

1. MEASUREMENT CONDITIONS

1.1 TEST SETUP

a) magnetic field (water cooled bitter magnet, high homogeneity, 2V)

magnet bore diameter 52.5 mm

accuracy of central field ± 0.25 % at 14 T

field measurement method(s)

Integrated coil

field variation over V-V taps (including mis-location of sample) ± 0.05 % at 12 T

rms ripple field ± 0.05 % at 12 T

field range covered 10 T to 14.5 T

b) sample current

current calibration method

Zorn industries, NIST traceable shunt, 300 A-0.001 Ω

accuracy of sample current ± 0.2 % at 100 A

rms ripple current ± 0.05 % at 100 A

current sweep rate : < 4 A/s or _____ seconds to I_c

c) sample voltage

voltage calibration method

EDC millivolt standard model MV 100N

accuracy of sample voltage ± 0.05 % at 10 μ V/m

typical noise level ± 2 μ V/m

response time of voltmeter _____ sec

d) helium bath temperature

temperature measurement method(s)

Pressure MKS Instruments Barytron

accuracy of temperature \pm _____ K at _____ K

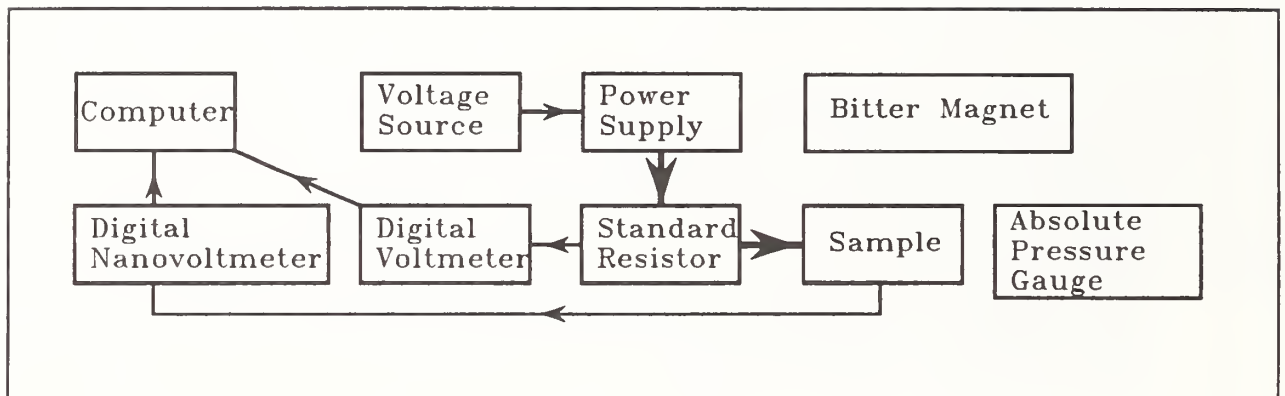
e) critical current measurement

measurement system verification

_____ I_c measurement: estimated uncertainty \pm _____, estimated precision ± 0.5 %

n-value measurement: estimated uncertainty \pm _____, estimated precision ± 5 %

f) measurement circuit diagram



1.2 SAMPLE HEAT TREATMENT

a) reaction mandrel

material Ti 6/4
 surface treatment graphite spray
 groove geometry 60°
 retainer stainless
 pitch length 3.2 mm
 outer diameter 32 mm
 number of wind turns 13 1/2

b) heat treatment furnace (used gettered He gas atmosphere)

temperature determination Chromel Alumel thermocouple
 variation in space ± 3 °C
 variation in time ± 1 °C

1.3 MEASUREMENT MANDREL AND MOUNTING DETAILS

a) measurement mandrel = reaction mandrel

mandrel material Ti 6/4
 outer diameter of mandrel 32 mm
 inner diameter of mandrel 28 mm
 pitch length of spiral groove 3.2
 groove geometry and angle V 60°
 current terminal; material(s) Cu
 geometry cylindrical

b) sample mounting

bonding material not used
 thin layer of bonding material? NA
 mounting procedure after reaction retainer rings are removed and wire is wrapped tight around the mandrel in groove
 solder material In
 flux material stainless steel flux
 soldering temperature ~180°C
 sample well seated in groove? yes

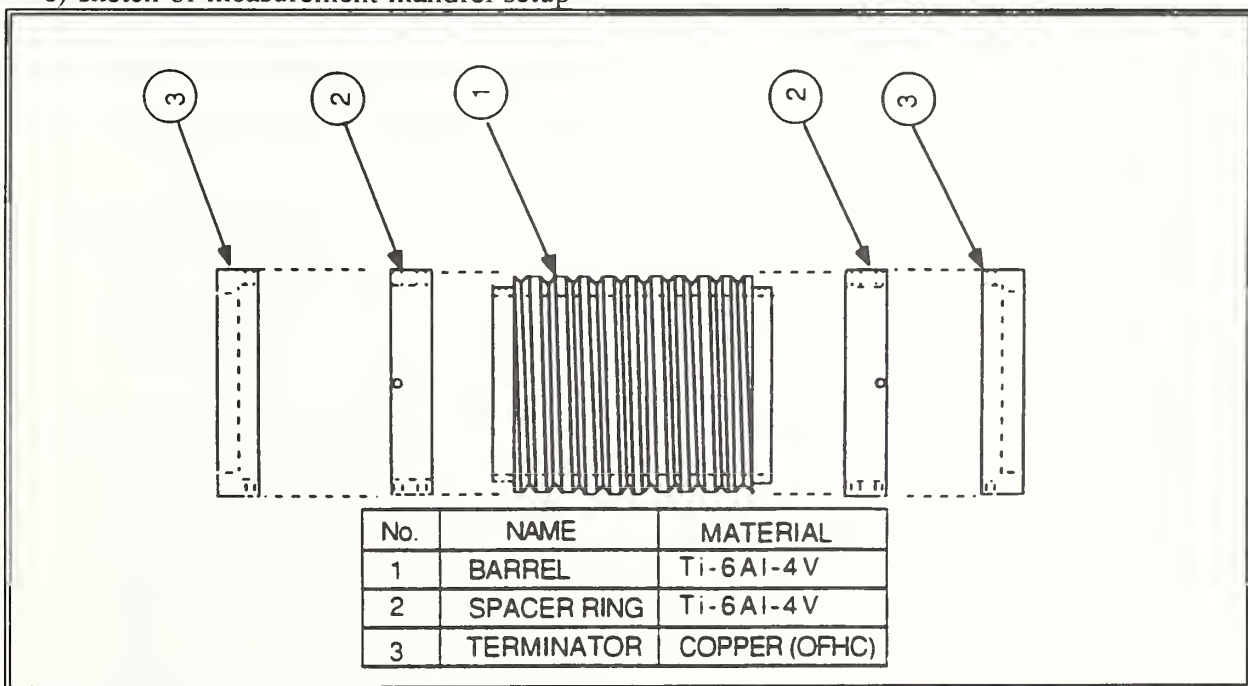
c) sample geometry and dimensions

wire length between V taps (1) 50 cm
 wire length between an current junction and its nearest V tap (2) 20 cm
 length of sample soldered to an current terminal (3) 10-20 cm
 total sample length (1 + 2x (2 + 3)) 135 cm
 winding diameter (outer) 32.3-32.5 mm (depends on wire diameter)
 total number of winding turns 13 1/2

d) sample cooling to 4.2 K

cooling time from room temperature to 4.2 K 5-10 minutes
 precooled with liquid nitrogen? yes
 directly cooled with gas or liquid helium? yes

e) sketch of measurement mandrel setup



DATA FORMAT SHEETS

INSTITUTE MIT Plasma Fusion Center

Sheet-1

1. MEASUREMENT CONDITIONS

1.1 TEST SETUP

a) magnetic field

magnet bore diameter 51 mm

accuracy of central field \pm 0.5 % at 12 T,

field measurement method(s)

Hall sensor

field variation over V-V taps (including mis-location of sample) \pm 0.05 % at 12 T

rms ripple field \pm ___ % at ___ T Superconducting magnet

field range covered .3 T to 12 T

b) sample current

current calibration method

Calibrated resistor

accuracy of sample current \pm 0.1 % at ___ A

rms ripple current \pm ___ % at ___ A

current sweep rate : < 3 A/s or _____ seconds to I_c

c) sample voltage

voltage calibration method

Standard voltage source

accuracy of sample voltage \pm 1 % at 10 μ V/m

typical noise level \pm 0.05 μ V/m

response time 0.3 sec

d) helium bath temperature

temperature measurement method(s)

Capacitance and CGR temperature sensor

accuracy of temperature \pm 0.01 K at 4.22 K

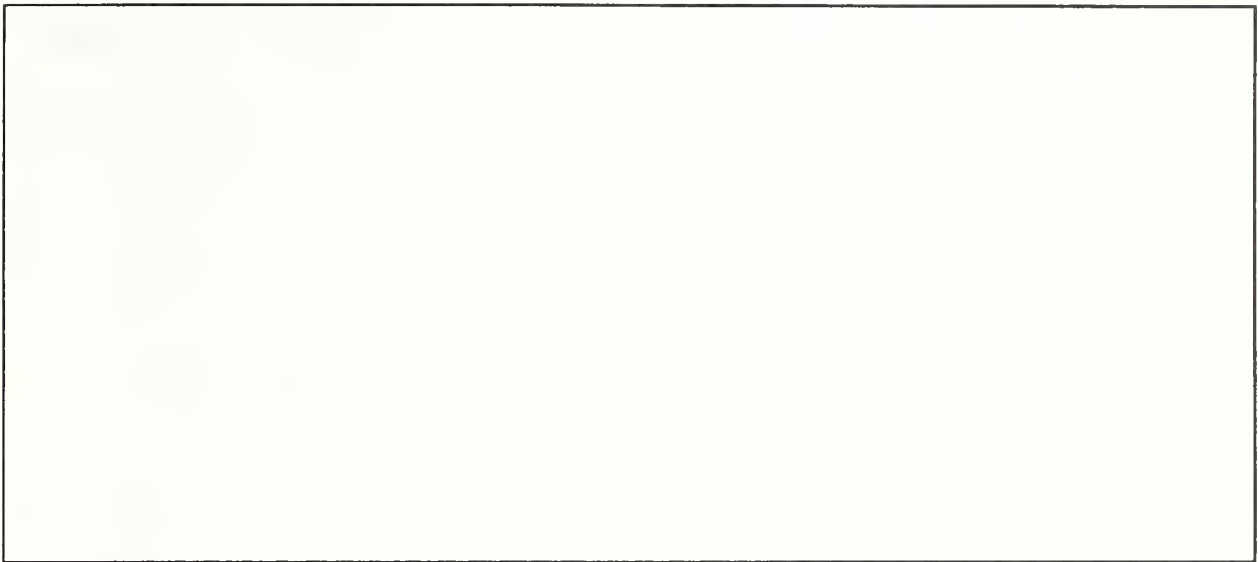
e) critical current measurement

measurement system verification

I_c measurement: estimated uncertainty \pm _____, estimated precision \pm _____

n-value measurement: estimated uncertainty \pm _____, estimated precision \pm _____

f) measurement circuit diagram



1.2 SAMPLE HEAT TREATMENT

a) reaction mandrel

material Ti-6 Al-4 V

surface treatment Graphite

groove geometry 90° "V" groove

retainer stainless steel wires

pitch length 8 per inch

outer diameter 32 mm

number of wind turns 11

b) heat treatment furnace

temperature determination K-type thermocouple

variation in space \pm 2 °C

variation in time \pm 0.5 °C

1.3 MEASUREMENT MANDREL AND MOUNTING DETAILS

a) measurement mandrel

mandrel material Ti-6 Al-4 V

outer diameter of mandrel 32.0 mm

inner diameter of mandrel 27.9 mm

pitch length of spiral groove 3.175 mm

groove geometry and angle 90° "V" groove

current terminal; material(s) Cu

geometry Cylinder

b) sample mounting

bonding material none

thin layer of bonding material? no

mounting procedure Remove Cr mechanically, solder one end and tighten by hand. Clamp and solder other end

solder material 80% In- 15% Pb-5% Ag

flux material Rosin

soldering temperature ~ 200 °C

sample well seated in groove? yes

c) sample geometry and dimensions

wire length between V taps (1) 0.5 m

wire length between an current junction and its nearest V tap (2) 0.2 m

length of sample soldered to an current terminal (3) > 0.1 m

total sample length (1 + 2x (2 + 3)) > 1.1 m

winding diameter (outer) 31 mm

total number of winding turns 11

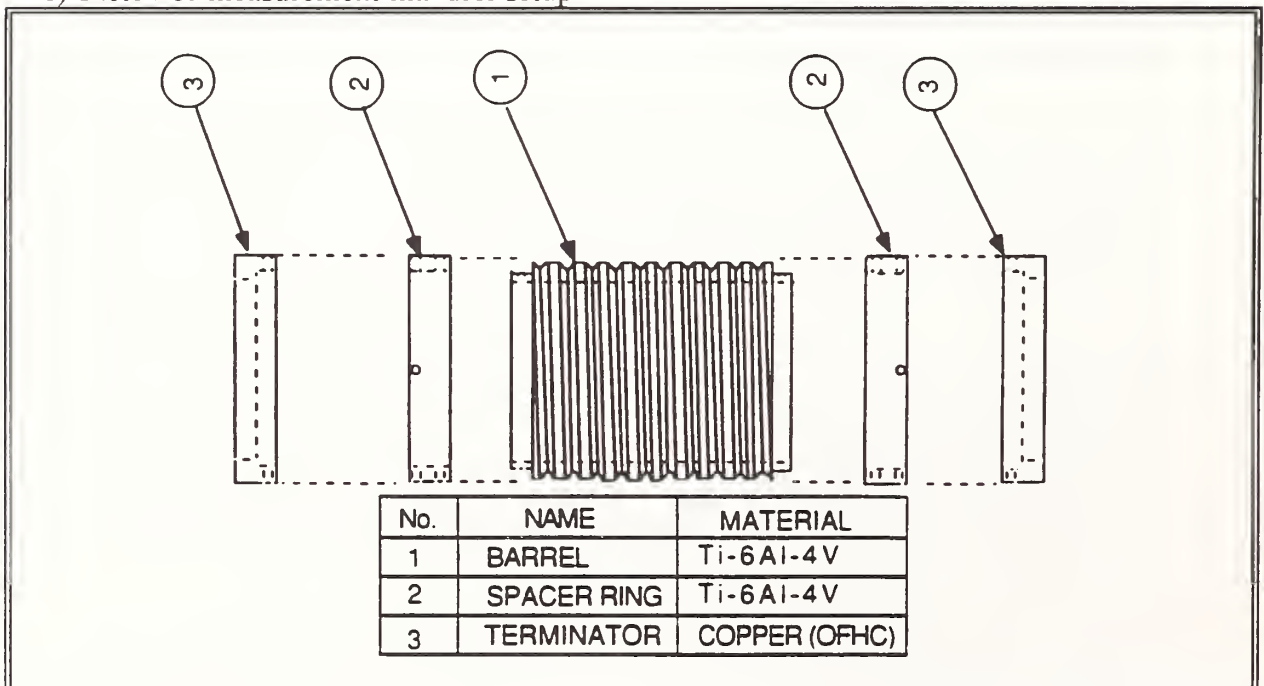
d) sample cooling to 4.2 K

cooling time from room temperature to 4.2 K ~ 30 minutes

precooled with liquid nitrogen? yes

directly cooled with gas or liquid helium? _____

e) sketch of measurement mandrel setup



DATA FORMAT SHEETS

INSTITUTE National Institute of Standards and Technology (NIST)

Sheet-1

1. MEASUREMENT CONDITIONS

1.1 TEST SETUP

a) magnetic field

magnet bore diameter 52 mm

accuracy of central field \pm 0.1 % at 2 T, \pm 0.05 % at 12 T

field measurement method(s)

Nuclear Magnetic Resonance + four wire standard resistor

field variation over V-V taps (including mis-location of sample) \pm 0.1 % at 12 T

rms ripple field \pm 0.01 % at 12 T

field range covered 2 T to 12 T

b) sample current

current calibration method

Cross check with calibrated resistor

accuracy of sample current \pm 0.02 % at 50 A

rms ripple current \pm 0.01 % at 100 A

current sweep rate : \leq 0.1 A/s or _____ seconds to I_c

c) sample voltage

voltage calibration method

Voltage source and precision divider

accuracy of sample voltage \pm 0.5 % at 10 μ V/m

typical noise level \pm 0.3 μ V/m

response time of voltmeter 0.1 sec

d) helium bath temperature

temperature measurement method(s)

Equilibrium vapor pressure, 1958 He⁴ temperature scale, pressure traceable to NIST

accuracy of temperature \pm 0.01 K at 4.20 K

e) critical current measurement

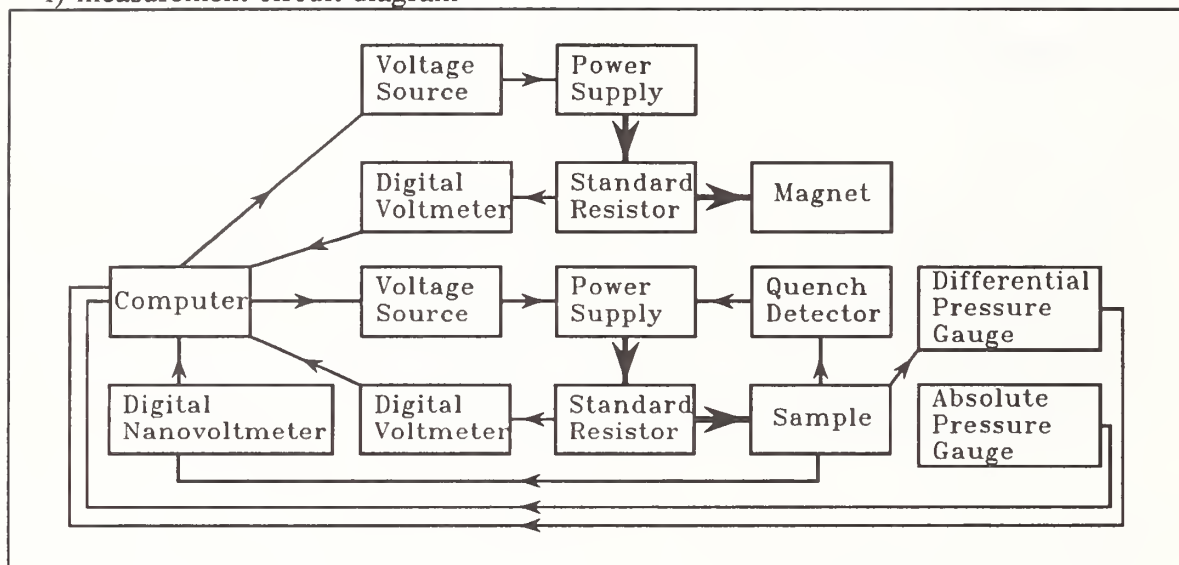
measurement system verification

Periodic measurements made on SRM 1457 and passive critical current simulators

I_c measurement: estimated uncertainty \pm 2%, estimated precision \pm 0.1%

n-value measurement: estimated uncertainty \pm 10%, estimated precision \pm 2%

f) measurement circuit diagram



1.2 SAMPLE HEAT TREATMENT

a) reaction mandrel

- material Ti - 6% Al - 4% V
- surface treatment oxidized with graphite spray
- groove geometry 90° V groove
- retainer stainless steel wires
- pitch length 3.175 mm (8 threads/inch)
- outer diameter 32.0 mm
- number of wind turns 11

b) heat treatment furnace

- temperature determination _____
- variation in space \pm _____ °C
- variation in time \pm _____ °C

1.3 MEASUREMENT MANDREL AND MOUNTING DETAILS

a) measurement mandrel

- mandrel material Ti-6Al-4V same as reaction material
- outer diameter of mandrel 32.0 mm
- inner diameter of mandrel 27.9 mm
- pitch length of spiral groove 3.175 mm
- groove geometry and angle 90° V groove
- current terminal; material(s) copper
- geometry Cylinder

b) sample mounting

bonding material none

thin layer of bonding material? NA

mounting procedure Clamp one end of sample, sample taut, clamp other end of sample, solder current contacts, solder voltage taps.

solder material Pb 40% Sn 60%

flux material Rosin core

soldering temperature 370 °C

sample well seated in groove? yes

c) sample geometry and dimensions

wire length between V taps (1) ~250 mm

wire length between an current junction and its nearest V tap (2) ~320 mm

length of sample soldered to an current terminal (3) ~80 mm

total sample length (1 + 2x (2 + 3)) ~1050 mm

winding diameter (outer) ~31 mm

total number of winding turns ~11

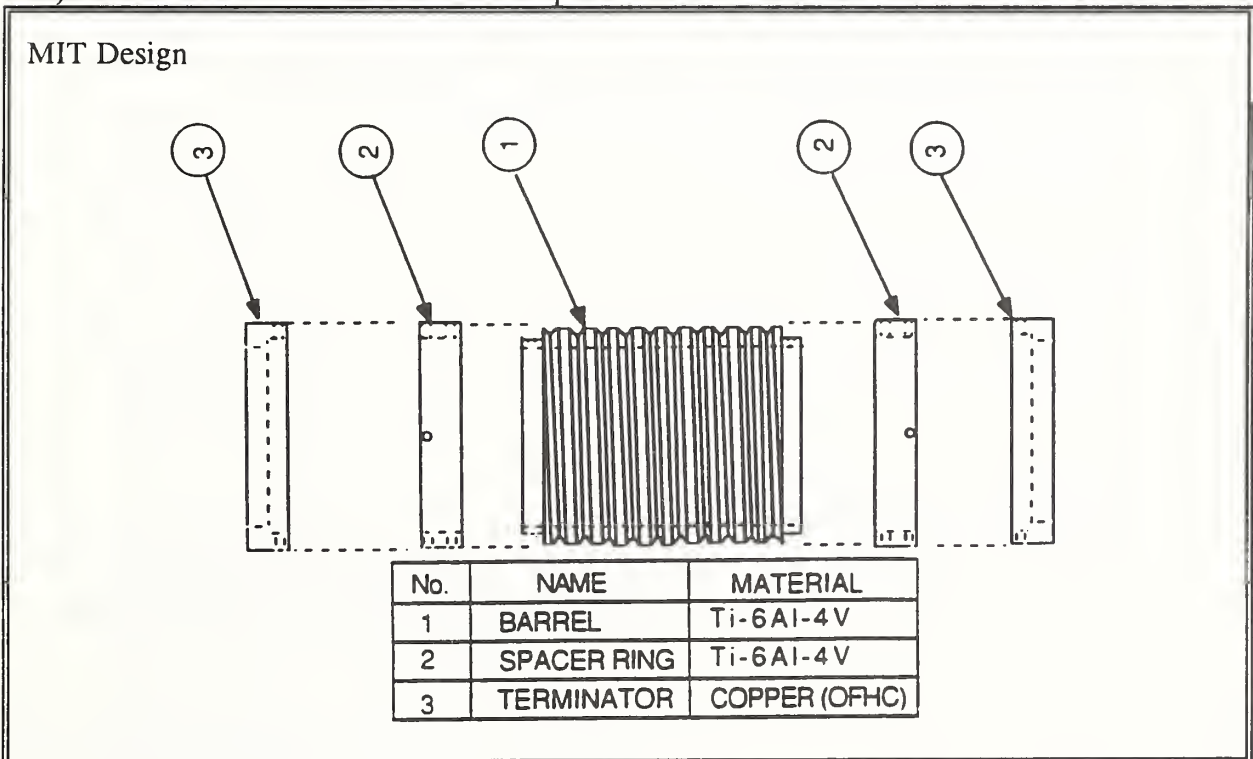
d) sample cooling to 4.2 K

cooling time from room temperature to 4.2 K 3 to 5 minutes

precooled with liquid nitrogen? no

directly cooled with gas or liquid helium? yes

e) sketch of measurement mandrel setup



DATA FORMAT SHEETS

INSTITUTE Oxford Superconducting Technology (OST)

Sheet-1

1. MEASUREMENT CONDITIONS

1.1 TEST SETUP

a) magnetic field

magnet bore diameter 52 mm

accuracy of central field ± 1 % at 12 T

field measurement method(s)

Magnet Current (Current-Field Calibration using calibrated Hall Probe)

field variation over V-V taps (including mis-location of sample) ± 0.5 % at 12 T

rms ripple field ± % at T

field range covered 0 T to 12 T

b) sample current

current calibration method

Standard resistor

accuracy of sample current ± 0.2 % at 500 A

rms ripple current ± % at A

current sweep rate : < 25 A/s or seconds to I_c

c) sample voltage

voltage calibration method

Keithley nV meter calibrated to NIST Tracable Voltage Standard

accuracy of sample voltage ± 0.2 % at 0.1 μ V/m

typical noise level ± 0.5 μ V/m

response time of voltmeter 0.1 sec

d) helium bath temperature

temperature measurement method(s)

None

accuracy of temperature ± K at K

e) critical current measurement

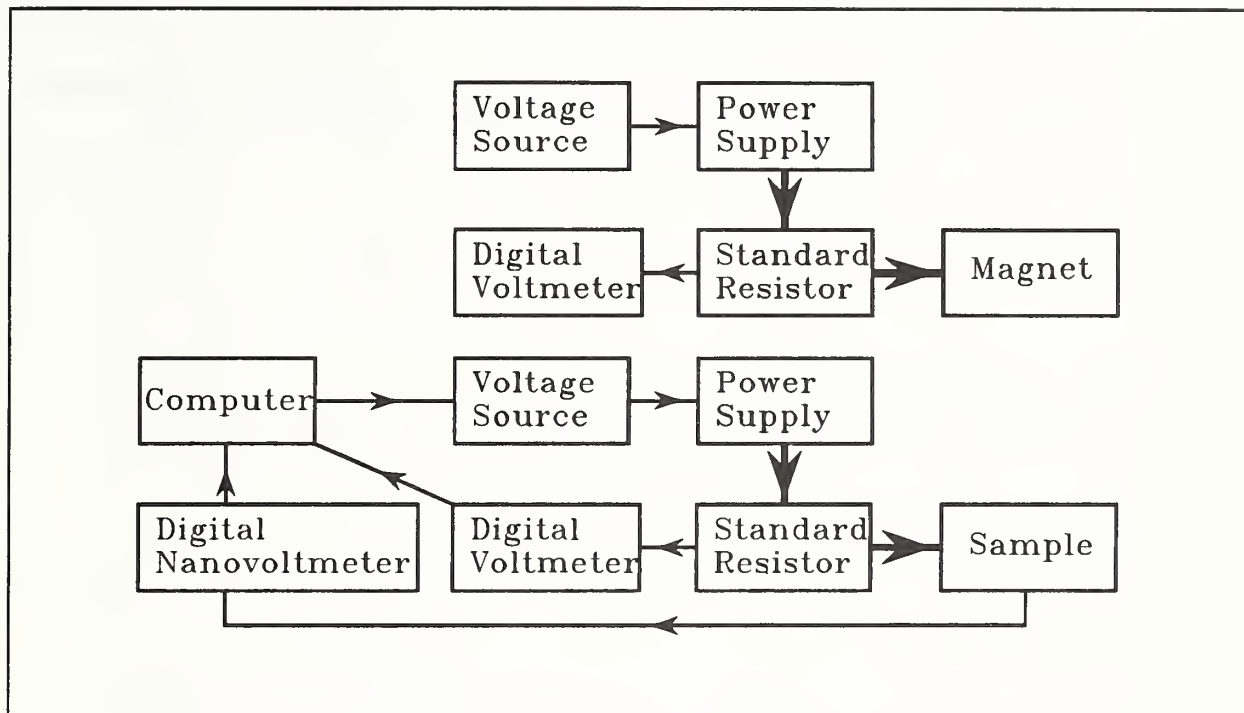
measurement system verification

Nist I_c Standard Wire (SRM 1457)

I_c measurement: estimated uncertainty ± 3%, estimated precision ± 1%

n-value measurement: estimated uncertainty ± 20% estimated precision ± 10%

f) measurement circuit diagram



1.2 SAMPLE HEAT TREATMENT

- a) reaction mandrel
 - material 304 or 316 stainless steel
 - surface treatment oxidized
 - groove geometry 1/32" radius
 - retainer _____
 - pitch length 4.2 mm
 - outer diameter 3.5 cm
 - number of wind turns 12

- b) heat treatment furnace
 - temperature determination Calibrated type K thermocouple
 - variation in space \pm 1 °C
 - variation in time \pm 1 °C

1.3 MEASUREMENT MANDREL AND MOUNTING DETAILS

- a) measurement mandrel
 - mandrel material 304 or 316 stainless steel
 - outer diameter of mandrel 3.5 cm
 - inner diameter of mandrel 3.2 cm
 - pitch length of spiral groove 4.2 mm
 - groove geometry and angle 1/32" radius
 - current terminal; material(s) copper
 - geometry _____

b) sample mounting

bonding material Pb-Sn solder

thin layer of bonding material? yes (may vary)

mounting procedure carefully screw sample onto measurement mandrel, fasten one end with clip, smooth wire into groove, fasten second end with clip, solder

solder material Pb-Sn

flux material Copper-Mate

soldering temperature ~275°C

sample well seated in groove? yes, usually

c) sample geometry and dimensions

wire length between V taps (1) 24 cm

wire length between an current junction and its nearest V tap (2) 24 cm

length of sample soldered to an current terminal (3) 15 cm

total sample length (1 + 2x (2 + 3)) ~1 m

winding diameter (outer) 3.4 cm

total number of winding turns 11 to 12

d) sample cooling to 4.2 K

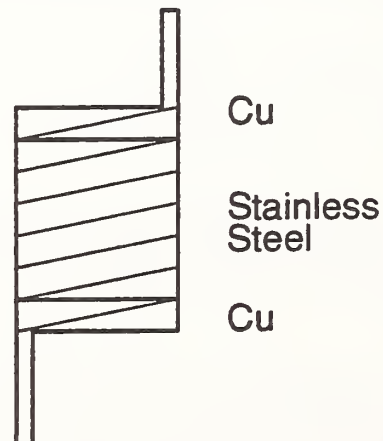
cooling time from room temperature to 4.2 K 2 minutes

precooled with liquid nitrogen? yes

directly cooled with gas or liquid helium? yes

e) sketch of measurement mandrel setup

- Sketch not to scale
- Cu ends are welded to stainless
- Cu ears are integral part of end rings
- Cu ears solder to rig current leads, provide ample current transfer area
- Size and groove details provided in text above.



DATA FORMAT SHEETS

INSTITUTE Supercon Inc.

Sheet-1

1. MEASUREMENT CONDITIONS

1.1 TEST SETUP

a) magnetic field

magnet bore diameter 50.8 mm

accuracy of central field ± 0.5 % at 9 T, ± 3.5 % at 7 T

field measurement method(s)

Based on field to current ratio, which was calibrated using Hall probe (MIT #9250 @ 60 mA)

field variation over V-V taps (including mis-location of sample) ± 0.5 % at 9 T

rms ripple field \pm ___ % at ___ T (not measured)

field range covered 0 T to 9 T

b) sample current

current calibration method

Calibrated standard shunt (resistor)

accuracy of sample current ± 0.25 % at 1000 A

rms ripple current \pm ___ % at ___ A (not measured)

current sweep rate : ___ A/s or 60 seconds to I_c (manual operation)

c) sample voltage

voltage calibration method

Null detector and X-Y plotter were calibrated by ESSCO and traced to NIST

accuracy of sample voltage ± 1 % at 450 μ V/m

typical noise level \pm ___ μ V/m (not measured)

response time of voltmeter 1 sec, rise time (10%-90%)

d) helium bath temperature

temperature measurement method(s)

Absolute pressure gauge

accuracy of temperature ± 0.01 K at 4.2 K

e) critical current measurement

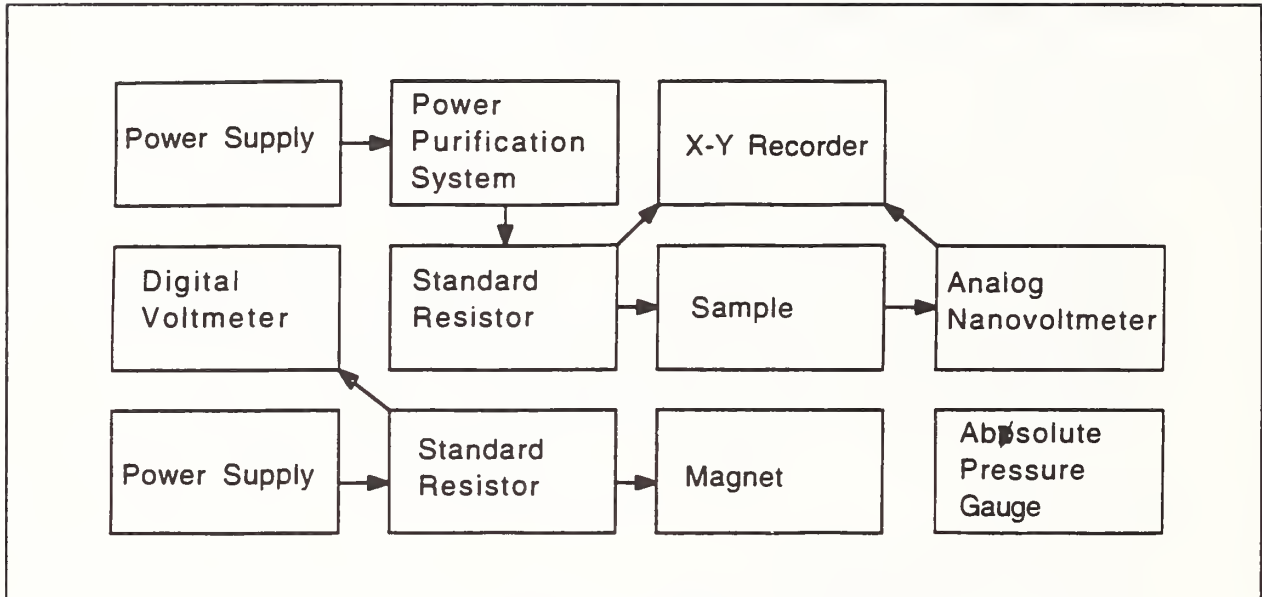
measurement system verification

Verified by two operators in multiple measurements using NIST's SRM 1457

I_c measurement: estimated uncertainty ± 3 % , estimated precision $\pm \leq 2$ %

n-value measurement: estimated uncertainty \pm _____ , estimated precision ± 10 %

f) measurement circuit diagram



1.2 SAMPLE HEAT TREATMENT

a) reaction mandrel

material Ti-6 Al-4V
 surface treatment none
 groove geometry "V" shape
 retainer heat treated in Cu boat
 pitch length 0.125"
 outer diameter 1.260"
 number of wind turns 9

b) heat treatment furnace

temperature determination K type thermocouple/digital thermometer
 variation in space ± 2 °C
 variation in time ± 1 °C

1.3 MEASUREMENT MANDREL AND MOUNTING DETAILS

a) measurement mandrel

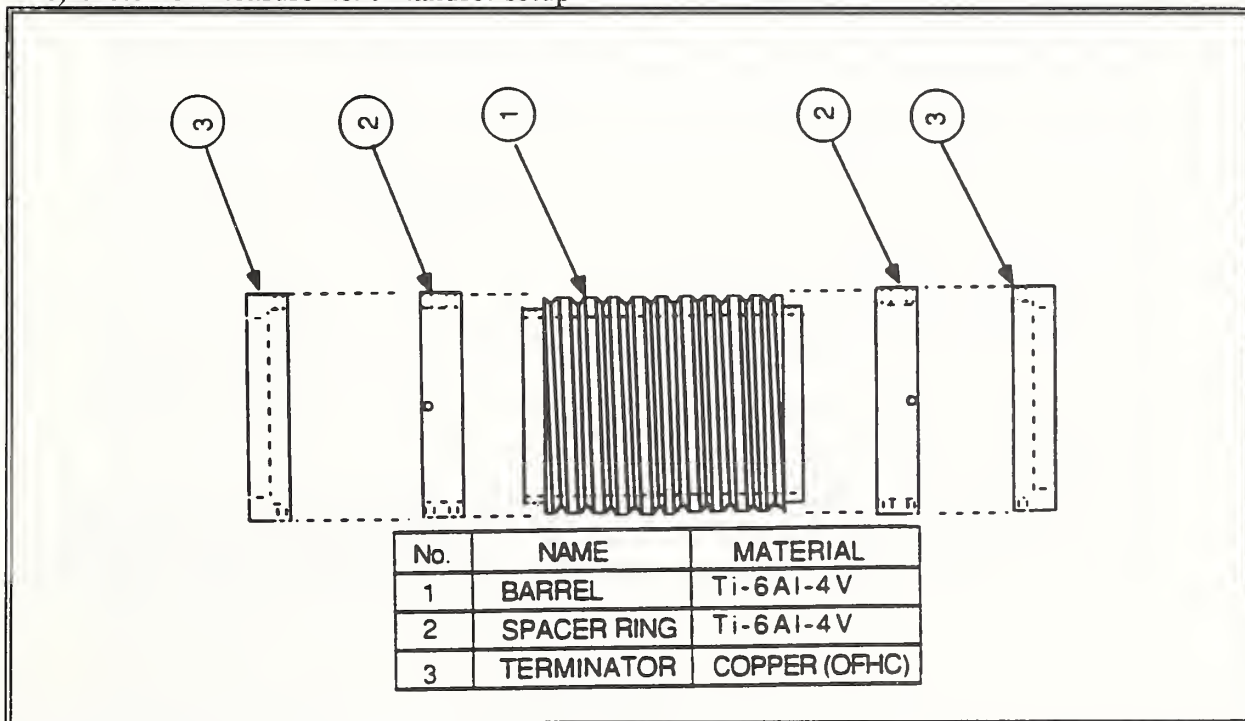
mandrel material Ti-6 Al-4V
 outer diameter of mandrel 1.260"
 inner diameter of mandrel 1.100"
 pitch length of spiral groove 0.125"
 groove geometry and angle "V" shape, 90°
 current terminal; material(s) Cu
 geometry ring

- b) sample mounting
 - bonding material _____
 - thin layer of bonding material? no
 - mounting procedure As specified by Dr. M. Takayasu of MIT's Plasma Fusion Center
 - solder material 50/50 PbSn
 - flux material ZnCl₂ + HCl
 - soldering temperature tip temperature of a 100 W soldering iron
 - sample well seated in groove? yes

- c) sample geometry and dimensions
 - wire length between V taps (1) 70 cm
 - wire length between an current junction and its nearest V tap (2) 10 cm
 - length of sample soldered to an current terminal (3) 20 cm
 - total sample length (1 + 2x (2 + 3)) 130 cm
 - winding diameter (outer) 1.260"
 - total number of winding turns 13

- d) sample cooling to 4.2 K
 - cooling time from room temperature to 4.2 K ~5 minutes
 - precooled with liquid nitrogen? yes
 - directly cooled with gas or liquid helium? yes

e) sketch of measurement mandrel setup



DATA FORMAT SHEETS

INSTITUTE Teledyne Wah Chang Albany(TWCA)

Sheet-1

1. MEASUREMENT CONDITIONS

1.1 TEST SETUP

a) magnetic field

magnet bore diameter 40 mm

accuracy of central field \pm 2 % at 12 T

field measurement method(s)

Magnet current shunt; calibrated with hall probe

field variation over V-V taps (including mis-location of sample) \pm 0.5 % at 12 T

rms ripple field $<$ \pm 0.01 % at 12 T

field range covered 6 T to 14 T

b) sample current

current calibration method

NIST Traceable Shunt and DVM

accuracy of sample current \pm 0.2 % at 100 A

rms ripple current $<$ \pm 0.001 % at 100 A (battery supply)

current sweep rate : 0 A/s or _____ seconds to I_c (step, hold, sample)

c) sample voltage

voltage calibration method

NIST traceable DVM

accuracy of sample voltage \pm 2 % at 100 μ V/m

typical noise level \pm 2 μ V/m

response time of voltmeter $<$ 0.1 sec

d) helium bath temperature

temperature measurement method(s)

Pool boiling helium; open dewar

accuracy of temperature \pm 0.002 K at 4.2 K

e) critical current measurement

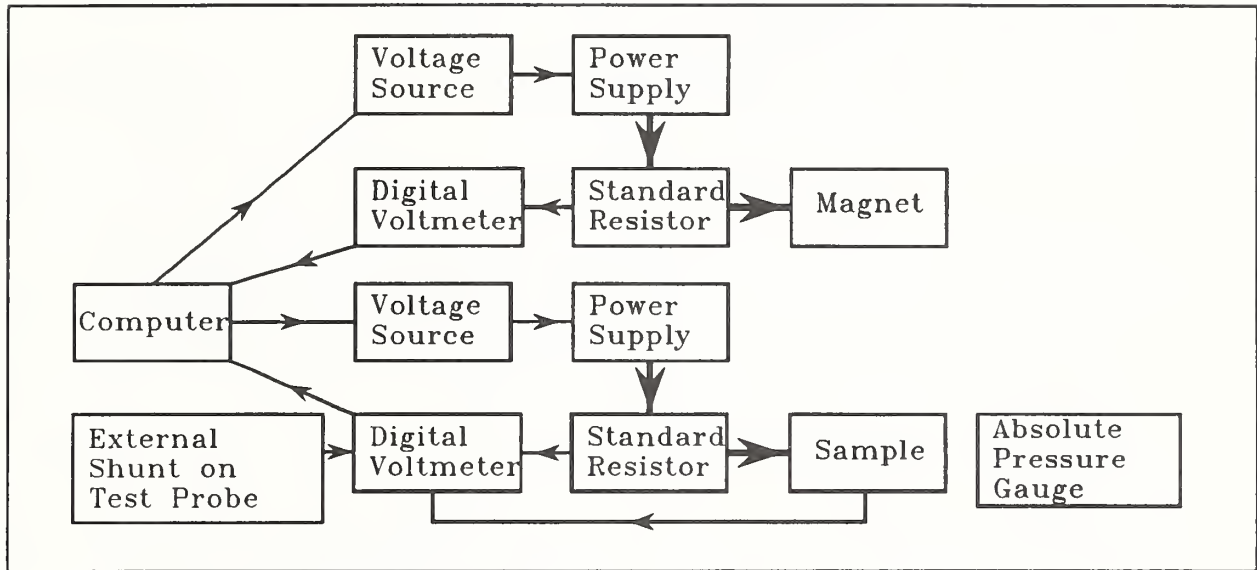
measurement system verification

NIST SRM 1457 on dedicated test probe w/ S.P.C. plot

I_c measurement: estimated uncertainty \pm 2 % ,estimated precision \pm 0.3 %

n-value measurement: estimated uncertainty \pm 10 % ,estimated precision ± 9 % @ 1σ

f) measurement circuit diagram



1.2 SAMPLE HEAT TREATMENT

- a) reaction mandrel
 - material Ti-6 Al-4 V
 - surface treatment Graphite Coat
 - groove geometry per ITER specs
 - retainer per ITER specs
 - pitch length per ITER specs
 - outer diameter per ITER specs
 - number of wind turns 13.6

- b) heat treatment furnace
 - temperature determination Thermocouple, type K
 - variation in space ± 2 °C
 - variation in time ± 2 °C

1.3 MEASUREMENT MANDREL AND MOUNTING DETAILS

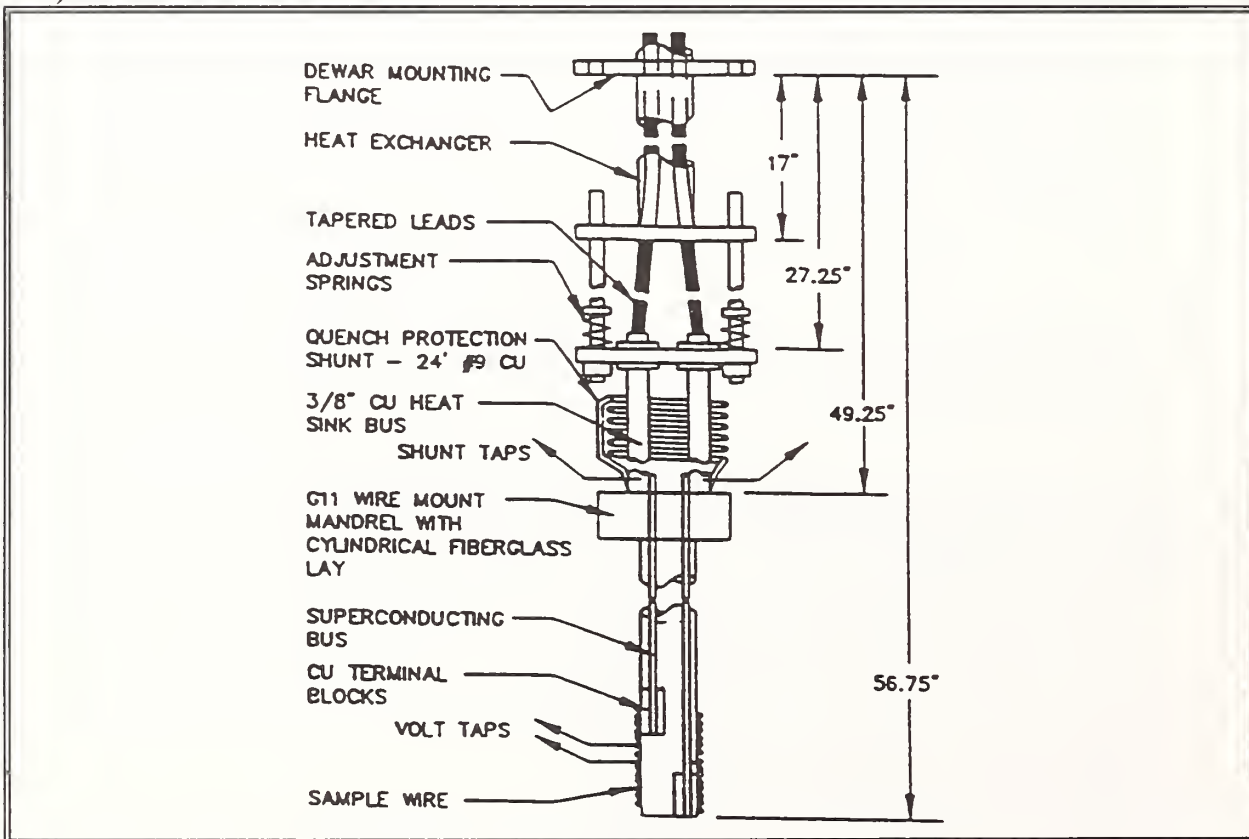
- a) measurement mandrel
 - mandrel material Ti-6 Al-4 V
 - outer diameter of mandrel per ITER specs
 - inner diameter of mandrel per ITER specs
 - pitch length of spiral groove per ITER specs
 - groove geometry and angle per ITER specs
 - current terminal; material(s) copper
 - geometry ring with 5/8" inner diameter

- b) sample mounting
 - bonding material _____
 - thin layer of bonding material? yes
 - mounting procedure Remove retainer ring; insert copper ring; mount on 5/8" mandrel; solder to mandrel; solder wire and taps.
 - solder material 60-40 Sn-Pb
 - flux material 'Nokorrode' soldering paste
 - soldering temperature Just above melting point
 - sample well seated in groove? yes

- c) sample geometry and dimensions
 - wire length between V taps (1) 0.5 m
 - wire length between an current junction and its nearest V tap (2) 0.1 m
 - length of sample soldered to an current terminal (3) 0.09 m
 - total sample length (1 + 2x (2 + 3)) 0.88m
 - winding diameter (outer) ~32 mm
 - total number of winding turns 8.8

- d) sample cooling to 4.2 K
 - cooling time from room temperature to 4.2 K > 15 minutes
 - precooled with liquid nitrogen? yes (N₂ vapors above L N₂ > 10 min)
 - directly cooled with gas or liquid helium? no (He vapors above L He > 5 min)

e) sketch of measurement mandrel set



DATA FORMAT SHEETS

INSTITUTE University of Wisconsin ASC

Sheet-1

1. MEASUREMENT CONDITIONS

1.1 TEST SETUP

a) magnetic field

magnet bore diameter 52 mm

accuracy of central field ± 0.2 % at 12 T,

field measurement method(s)

Axial Hall Probe and power supply control voltage

field variation over V-V taps (including mis-location of sample) ± 0.15 % at 12 T

rms ripple field ± 0.05 % at 12 T

field range covered 0 T to 14 T

b) sample current

current calibration method

Cross check to calibrated resistor

accuracy of sample current ± 0.1 % at 50 A

rms ripple current ± 0.02 % at 100 A

current sweep rate : < 0.2 A/s or _____ seconds to I_c

c) sample voltage

voltage calibration method

Comparison with recently calibrated Keithley 180/2001 DVM

accuracy of sample voltage ± 1 % at 10 μ V/m

typical noise level ± 0.04 μ V/m

response time of voltmeter _____ sec

d) helium bath temperature

temperature measurement method(s)

Absolute pressure, manometer calibration traceable to NIST

accuracy of temperature ± 0.01 K at 4.2 K

e) critical current measurement

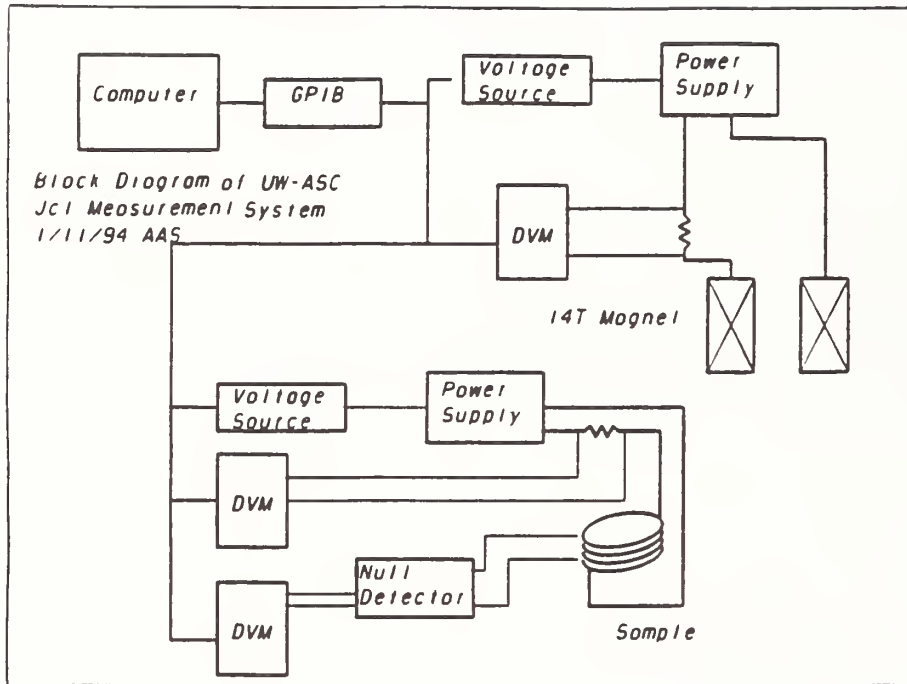
measurement system verification

NIST SRM

I_c measurement: estimated uncertainty $\pm 2\%$, estimated precision $\pm 1\%$

n-value measurement: estimated uncertainty $\pm 10\%$, estimated precision $\pm 5\%$

f) measurement circuit diagram



1.2 SAMPLE HEAT TREATMENT

- a) reaction mandrel
 - material _____
 - surface treatment _____
 - groove geometry _____
 - retainer _____
 - pitch length _____
 - outer diameter _____
 - number of wind turns _____

- b) heat treatment furnace
 - temperature determination _____
 - variation in space \pm _____ °C
 - variation in time \pm _____ °C

1.3 MEASUREMENT MANDREL AND MOUNTING DETAILS

- a) measurement mandrel
 - mandrel material _____
 - outer diameter of mandrel _____
 - inner diameter of mandrel _____
 - pitch length of spiral groove _____
 - groove geometry and angle _____
 - current terminal; material(s) _____
 - geometry _____

2. RESULTS

Magnetic Field _____ T

Sample Name	Barrel #	Temp. (K)	I_c (A) at $10 \mu\text{V/m}$	n-value ¹	Remarks

¹ n-value is defined as an exponent in the V-I relation of $V = bI^n$.

Voltages or voltage range used to estimate n-value _____ $\mu\text{V/m}$

Comments

HEAT TREATMENT

atmosphere _____

temperature and time table:

	Stage 1	Stage 2	Stage 3	Stage 4
Temperature				
Time				
ramp rate				

2. RESULTS

Sample Name _____ Barrel # _____ Helium bath temp. _____

B(T)	I_c at $10 \mu\text{V/m}$ (A)	n-value ¹	Remarks
6			
7			
8			
9			
10			
11			
12			
13			
14			

¹ n-value is defined as an exponent in the V-I relation of $V = bI^n$.

Voltages or voltage range used to estimate n-value _____ $\mu\text{V/m}$

Comments

HEAT TREATMENT

atmosphere _____

temperature and time table:

	Stage 1	Stage 2	Stage 3	Stage 4
Temperature				
Time				
ramp rate				

This paper was presented at the 7th International Workshop on Critical Currents in Superconductors (Alpbach, Tyrol, Austria, January 24-27, 1994). It will be published by World Scientific Publishing CO. PTE. LTD.

A SIMPLE AND REPEATABLE TECHNIQUE FOR MEASURING THE CRITICAL CURRENT OF Nb₃Sn WIRES*

L. F. Goodrich and A. N. Srivastava
National Institute of Standards and Technology
325 Broadway, Boulder CO, 80303, USA.

ABSTRACT

We evaluated an alternate approach for measuring the critical current (I_c) of Nb₃Sn wire which uses a standard mandrel geometry and apparatus interface. Preliminary data indicate that the tension in the conductor before reaction and measurement may affect the repeatability. We show preliminary summary statistics for measurements of conductors performed by five US laboratories. The reaction and measurement mandrel used was fabricated using a Ti-6Al-4V alloy. This high temperature alloy was used to avoid transferring the specimen between mandrels, thus reducing the likelihood of inadvertent mechanical damage of the specimen. Besides this advantage, these holders are inexpensive and nonmagnetic, and have a low thermal expansion and a high electrical resistivity ($147 \mu\Omega \cdot \text{cm}$ at 4 K). Using the same mandrel for reaction and measurement improves the quality assurance of the I_c measurement for data base creation and acceptance testing for large scale applications such as ITER (International Thermonuclear Experimental Reactor). The US ITER Home Team adopted this approach in a recent test because it was expected to be easily implemented and yield consistent results.

1. Introduction

The data presented here are Nb₃Sn superconductor critical current and n-value measurements made during an interlaboratory comparison in which a common holder with standardized design was used for reaction and measurement. Our experience indicates that standardizing experimental variables reduces the uncertainty in the measurement and increases the repeatability of the overall experiment [1].

2. Design of the Titanium Reaction/Measurement Holders

The reaction mandrel consists of three Ti alloy parts: a main tube and two removable end rings. The main tube has a threaded groove (3.15 threads/cm) with a groove angle of 90°. The end rings are held onto the main tube with a stainless steel wire (spring clip) through mating holes in the main tube and end cap. The end rings are not threaded; their outer diameter was machined to hold the specimen at the same coil diameter as when seated in the grooves of the main tube. A small diameter retaining wire is used to tie the specimen to each end ring, thus holding the wire coil on the reaction mandrel.

After reaction the end rings are removed, and Cu current contact rings are put on and

* Publication of NIST, not subject to copyright.

held in place with stainless steel wire. If there is a Cr coating on the wire, it is removed from the region of the current contacts and voltage taps. One end of the specimen is clamped, and the wire is seated into a groove starting from the clamped end and proceeding along the wire to the far end which is then clamped. The specimen is then soldered to the Cu current contact rings and voltage tap wires are soldered to the specimen. We call this fully instrumented unit, an *instrumented specimen*.

We also standardized the attachment of the instrumented specimen to the test fixture. In all cases, the current contacts to the instrumented specimen were made by pressure contacts to each Cu ring, thus making the instrumented specimen interchangeable and allowing for a classical round robin comparison where each specimen is measured by each laboratory. Identifying and separating the effects of specimen mounting from conductor inhomogeneity and different measurement conditions could be facilitated by combining and comparing the classical round robin and the more common method where each laboratory mounts and measures a different specimen.

The thermal contraction of this Ti alloy is 0.17% from 295 to 4 K. This small contraction causes the Nb₃Sn wire to tighten onto the mandrel as it cools to the measurement temperature. This tightened state reduces specimen motion and the need for a binding agent to hold the specimen, when the Lorentz force is directed into the mandrel. Differential contraction also puts the wire into hoop strain, and creates a transverse stress, and a slight bending strain. We expect that tensile hoop strain is the most significant strain effect. It will slightly increase the I_c from the intrinsic value [2]. We have recently discovered that this holder is superconducting at 4.2 K and magnetic fields below 2 T. Thus, reliable I_c measurements can only be obtained at fields higher than 2 T at 4.2 K with this holder material.

3. Experimental Results

We conducted a repeatability study on two fully instrumented Nb₃Sn specimens. The I_c of each specimen was measured as a function of magnetic field two times. The percent difference in I_c of each specimen from Specimen 1, Run A is shown as a function of magnetic field on Figure 1. The experiment consisted of measuring the critical current of a given specimen as a function of field (Run A), followed by thermal cycling, removal from test fixture, replacement on test fixture, and repeating the measurements (Run B). The results shown here are preliminary; however they indicate that high precision and accuracy in the measurement are possible if the standardized procedures are followed.

The curves corresponding to Specimen 2 (also Specimen 1 to a lesser extent) diverge from each other with increasing magnetic field; we suspect that this was caused by slight changes in the Nb₃Sn stress state that occur during thermal cycling. These changes are not to be confused with the larger effects due to hoop strain. Although this cumulative effect is on the order of 0.5%, it has implications in interpreting the results of an interlaboratory comparison. During a thermal cycle, the specimen is constrained by the mandrel. The thermal contraction of the composite wire is about 0.11% more than the Ti-alloy mandrel. The dynamic differential contraction between these two materials may be more than 0.11% in the cooling or warming cycles. Thus, the wire undergoes hoop

stress and elongation as it is cooled to 4 K. We suspect that the elongation has a cumulative effect, since the copper and/or bronze may exceed its elastic limit during the thermal cycle, and that would slightly relieve the precompression of the Nb₃Sn. This would explain the observed effect (see Fig. 1). The fact that the curves diverge with increasing magnetic field also suggests that the underlying effect is due to strain.

We conducted the second experiment to evaluate the effect of mounting a specimen with different initial seating conditions in the mandrel groove. Six I_c measurements were made on Specimen 2 with different initial seating conditions. The seating conditions were changed by incrementally applying positive or negative torsion to the coiled conductor. We designed this experiment to model the effects of different initial seating conditions which may occur during an interlaboratory comparison of I_c.

Figure 2 shows the measured I_c as a function of run number, where each run had a different initial torsion state. The points which are at the zero initial position (stars) fall on an asymptotic progression. The circle was at a position of -0.07%, the square at -0.10%, and the triangle at 0.03%. For example, if the active length of the specimen is 95 cm (contact to contact), a -0.10% change in position would correspond to shifting one end of specimen by 0.95 mm in the direction that makes the wire less tight on the holder. The results were consistent with the expected behavior, except for the enhanced sensitivity to the additional tension from the initial position.

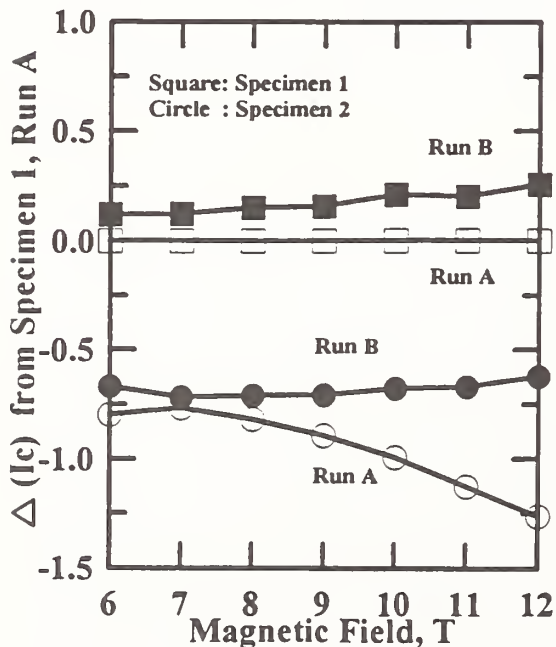


Figure 1. The percent difference in critical current relative to measured values of Specimen 1, Run A versus magnetic field.

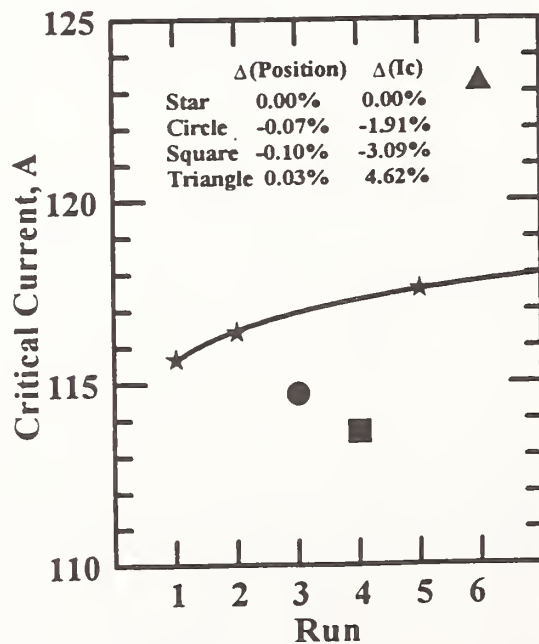


Figure 2. Measured I_c of Specimen 2 versus run number. Symbols refer to the relative position; % differences are calculated relative to the baseline curve.

In the interlaboratory comparison, the measured critical currents agreed. Thus, we suspect that the initial seating conditions of the laboratories were similar. These results are not unique to the Ti-alloy holders; Incoloy or any other mandrel material would exhibit similar effects. To standardize these effects, it might be necessary to develop an apparatus which applies a preset amount of tension to the specimen. We expect tension before reaction to have a smaller effect than tension after reaction since in the former case the main effect is a slight variation in bending strain.

Table 1 shows a statistical summary the results of an interlaboratory comparison of I_c measurements for four conductors from five laboratories. These conductors were not designed to meet a certain specification and had different diameters. Each laboratory prepared two specimens and followed a procedure similar to that described here.

Table 1. Preliminary summary statistics for each sample measured at 4.2 K at 12 T.

	Sample W	Sample X	Sample Y	Sample Z
Mean I_c , A	117.6	212.8	141.5	84.0
σ , A	4.3	6.1	6.4	2.7
σ/mean , %	3.7	2.9	4.6	3.2
Mean n	29.0	29.2	27.8	14.9
σ	3.5	3.1	2.3	1.0
σ/mean , %	12.2	10.6	8.3	6.9

4. Conclusions

This standardization procedure yielded repeatable results during a recent interlaboratory comparison of critical current measurements on Nb_3Sn wires. We also implemented a standardized holder for both reaction and measurement. We believe that the tension of the conductor before reaction and before measurement should be controlled in order to achieve high precision quality assurance. This procedure yields predictable results, as demonstrated in the repeatability and initial seating experiments. ●

5. References

1. H. Wada and K. Itoh, *Cryogenics* 32 ICMC Supplement (1992) 557.
2. J. W. Ekin, *Cryogenics* 20 (1980) 611.

6. Acknowledgements

The authors extend their thanks to M. Takayasu (MIT) for his contribution in the design of the common holder, J. Minervini (MIT) for his organization of the interlaboratory comparison, US ITER Home Team for their cooperation, T. C. Stauffer for assisting in the measurements, and J. A. Wiejaczka for assisting with data analysis. This work was supported by the Office of Fusion Energy (US Department of Energy) and the Plasma Fusion Center (MIT).

